

DISSERTATION

PERCEPTUAL DIFFERENCES AND PERCEPTIVE FIELDS
IN BINOCULAR AND MONOCULAR COLOR VISION

Submitted by

Jamie K. Opper

Department of Psychology

In partial fulfillment of the requirements

For the Degree of Doctor of Philosophy

Colorado State University

Fort Collins, Colorado

Summer 2016

Doctoral Committee:

Advisor: Vicki Volbrecht
Co-Advisor: Deana Davalos

Chuck Anderson
Ed DeLosh

Copyright by Jamie K. Opper 2016

All Rights Reserved

ABSTRACT

PERCEPTUAL DIFFERENCES AND PERCEPTIVE FIELDS IN BINOCULAR AND MONOCULAR COLOR VISION

This study investigated perceptual differences in stimuli viewed with one eye (monocular) or two eyes (binocular) in the central (fovea) and peripheral retina (10° retinal eccentricity). In particular, this study focused on changes in color perception for monochromatic stimuli (450 nm to 670 nm, in 20 nm steps) varying in size (1° , 1.7° , 2.25° , 2.7° , 3.7°). A hue-scaling procedure was utilized to ascertain hue perception. With this procedure, three binocular normal and one strabismic amblyope assigned percentages to each of the four elemental hues (i. e., blue, yellow, red, and green) as well as saturation. Only one to two hue terms were allowed to describe a single stimulus, and the percentages had to sum to 100. Members of opponent-color pairs (red/green and yellow/blue) could not be used simultaneously to describe the same stimulus. Hue-scaling results from normal observers showed that, in general, smaller stimuli (1° , 1.7° , 2.25°) in the peripheral retina resulted in weaker hue perception than a 1° stimulus presented to the fovea, although this reduction was less noticeable for the binocular peripheral conditions than for the monocular peripheral conditions, and more noticeable for the monocular nasal retinal condition than the monocular temporal retinal condition. Differences between peripheral and foveal hue perception abated as stimulus size increased. Additionally, the range of wavelengths where blue (yellow) was perceived was narrower (wider) in the periphery relative to the fovea for all stimulus sizes. No differences were observed between monocular and binocular foveal hue or saturation perception, where only one stimulus size was used (1°).

Peripherally-presented binocular stimuli fell upon the nasal retina of one eye and the temporal retina of the other, and peripheral binocular hue and saturation perceptions for smaller stimuli were more similar to that of the monocular temporal retina, regardless of whether the stimulus fell on the temporal retina of the left or right eye.

Since hue-scaling data were obtained for several stimulus sizes in the peripheral retina it was possible to derive the size of perceptive fields, which are perceptual analogues of receptive fields and indicate the stimulus size at which hue perception stabilizes; i.e., the size at which amount of perceived hue ceases to increase with further increase in stimulus size. Perceptive fields measured in the monocular nasal retina were larger than those measured in the monocular temporal retina for all elemental hues. Overall, monocular perceptive fields were larger than the binocular perceptive fields. Possible physiological reasons for the findings include suppression of chromatic signals by rod photoreceptors, differences in cone photoreceptor distribution and relative ratios of cone types over the surface of the retina, and changes in the nature of the connections of the cone photoreceptors to their associated ganglion cells with increasing retinal eccentricity. The amblyopic observer was found to have abnormal hue and saturation perception relative to the normal observers, particularly for stimuli perceived as red and green, which may be due to abnormalities in the parvocellular pathway, the neural pathway presumed to mediate the perception of red and green.

ACKNOWLEDGEMENTS

This endeavor would not have been possible without the guidance of Dr. Deana Davalos and Dr. Vicki Volbrecht, who provided not only their expertise, but also their invaluable guidance and support during the process. I also owe my gratitude to my committee members, Dr. Charles Anderson and Dr. Edward DeLosh, and Dr. Patrick Monnier, who was willing to take a gamble on me as a graduate student and without whom I likely would not have considered the field of vision science as a career.

I could not have completed this project without the assistance of my colleague, Nate Douda, and some wonderful research assistants: Alexandra Lake, Andrew Wilson, and Katie Youngpeter. Their hard work and unflagging enthusiasm helped ensure I could finish data collection under very tight time constraints, and I could not have asked for a better group of coworkers.

My family also deserves a heartfelt thank you for their moral, emotional, and financial support throughout my graduate school career: my father, Forrest Opper; my mother, Dorothy Bennett; my aunt, Peggy Wilcox; Sarah Smith; and my brother, Fred Opper, sister-in-law, Birte Horn-Hanssen, and my wonderful niece and nephew, Emma and Conrad.

TABLE OF CONTENTS

ABSTRACT.....	ii
ACKNOWLEDGEMENTS.....	iv
LIST OF TABLES.....	vii
LIST OF FIGURES.....	viii
1. CHAPTER 1 – INTRODUCTION.....	1
1.1 PHOTORECEPTOR DISTRIBUTION ACROSS THE RETINA.....	4
1.2 RETINAL LOCATION AND COLOR PERCEPTION.....	5
1.3 BINOCULAR COLOR PERCEPTION.....	8
1.3.1 PHOTORECEPTOR LEVEL.....	10
1.3.2 RETINAL LEVEL.....	14
1.3.3 CORTICAL LEVEL.....	14
1.4 EYE DOMINANCE AND BINOCULAR VISION.....	17
2. CHAPTER 2 - METHOD.....	20
2.1 PARTICIPANTS.....	20
2.2 MATERIALS.....	20
2.2.1 APPARATUS.....	20
2.2.2 STIMULUS.....	22
2.3 CALIBRATION.....	22
2.4 PROCEDURE.....	25
3. CHAPTER 3 - RESULTS.....	27
3.1 HUE PERCEPTION.....	27
3.1.1 EFFECTS OF FIXATION CONDITION.....	28
3.1.2 EFFECTS OF STIMULUS SIZE.....	34
3.1.3 BINOCULAR VS. MEAN MONOCULAR PERCEPTION.....	40
3.1.4 HUE PERCEPTION SUMMARY.....	45
3.2 PERCEPTIVE FIELD SIZES.....	45
3.2.1 PERCEPTIVE FIELD SIZES SUMMARY.....	53
4. CHAPTER 4 – DISCUSSION.....	55
4.1 HUE SCALING.....	55
4.1.1 FOVEA VS. PERIPHERY.....	55
4.1.2 POSSIBLE PHYSIOLOGICAL UNDERPINNINGS.....	59
4.2 PERCEPTIVE FIELD SIZE.....	61
4.3 BINOCULAR VS. MONOCULAR HUE PERCEPTION.....	66
4.4 AMBLYOPIC OBSERVER VS. NORMAL OBSERVERS.....	68
4.5 CONCLUSION.....	78
5. REFERENCES.....	80
6. APPENDIX A: GRAND MEAN HUE-SCALING DATA.....	90
6.1 MONOCULAR LEFT EYE LEFT FIXATION.....	90
6.2 MONOCULAR LEFT EYE RIGHT FIXATION.....	92
6.3 MONOCULAR RIGHT EYE LEFT FIXATION.....	94
6.4 MONOCULAR RIGHT EYE RIGHT FIXATION.....	96
6.5 BINOCULAR LEFT FIXATION.....	98

6.6 BINOCULAR RIGHT FIXATION.....	100
6.7 FOVEAL DATA.....	102
7. APPENDIX B: AMBLYOPIC OBSERVER MEAN HUE-SCALING DATA.....	103
7.1 MONOCULAR LEFT EYE LEFT FIXATION.....	103
7.2 MONOCULAR LEFT EYE RIGHT FIXATION.....	104
7.3 MONOCULAR RIGHT EYE LEFT FIXATION.....	105
7.4 MONOCULAR RIGHT EYE RIGHT FIXATION.....	106
7.5 BINOCULAR LEFT FIXATION.....	107
7.6 BINOCULAR RIGHT FIXATION.....	108
7.7 FOVEAL DATA.....	109

LIST OF TABLES

TABLE 2.1- WAVELENGTH OF PEAK ENERGY CONCENTRATION.....	25
AND HALF-BANDWIDTH OF INTERFERENCE FILTERS	
TABLE 2.2- FOVEAL AND PERIPHERAL FIXATION CONDITIONS.....	26
TABLE 3.1- RETINAL AREA STIMULATED IN EACH FIXATION.....	28
CONDITION	
TABLE 3.2- MEAN <i>K</i> VALUES FOR ALL FIXATION CONDITIONS.....	48
TABLE 3.3- MEAN <i>G</i> VALUES FOR ALL FIXATION CONDITIONS.....	49
TABLE 3.4- RANGE AND MEAN OF <i>R</i> VALUES FOR EACH HUE.....	50
TERM FOR EACH FIXATION CONDITION	

LIST OF FIGURES

FIGURE 1.1- SAMPLE HUE-SCALING DATA.....	3
FIGURE 1.2- DIAGRAM OF RETINAL LOCATION OF PERIPHERAL.....	9
BINOCULAR STIMULUS	
FIGURE 2.1- SCHEMATIC OF STIMULUS PRESENTATION.....	21
APPARATUS	
FIGURE 2.2- DIAGRAM OF FIXATION POINT PLATE.....	23
FIGURE 2.3- SAMPLE PEAK SPECTRAL IRRADIANCE AND.....	24
HALF-BANDWIDTH CALCULATION	
FIGURE 3.1- HUE-SCALING FUNCTIONS FOR BINOCULAR,.....	28
MONOCULAR LEFT, AND MONOCULAR RIGHT	
FOVEAL DATA	
FIGURE 3.2- HUE-SCALING FUNCTIONS FOR MONOCULAR LEFT.....	30
EYE TEMPORAL AND NASAL AS COMPARED TO	
MONOCULAR LEFT FOVEAL DATA	
FIGURE 3.3- HUE-SCALING FUNCTIONS FOR MONOCULAR RIGHT.....	32
EYE TEMPORAL AND NASAL AS COMPARED TO	
MONOCULAR RIGHT FOVEAL DATA	
FIGURE 3.4- HUE-SCALING FUNCTIONS FOR BINOCULAR LEFT.....	34
AND RIGHT FIXATION AS COMPARED TO	
BINOCULAR FOVEAL DATA	
FIGURE 3.5- HUE-SCALING FUNCTIONS FOR BINOCULAR LEFT.....	36
FIXATION AS COMPARED TO MONOCULAR LEFT	
TEMPORAL AND MONOCULAR RIGHT NASAL DATA	
FIGURE 3.6- HUE-SCALING FUNCTIONS FOR BINOCULAR RIGHT.....	39
FIXATION AS COMPARED TO MONOCULAR RIGHT	
TEMPORAL AND MONOCULAR LEFT NASAL DATA	
FIGURE 3.7- HUE-SCALING FUNCTIONS FOR BINOCULAR LEFT.....	42
FIXATION AS COMPARED TO THE MEAN OF	
MONOCULAR LEFT TEMPORAL AND MONOCULAR	
RIGHT NASAL DATA	
FIGURE 3.8- HUE-SCALING FUNCTIONS FOR BINOCULAR RIGHT.....	44
FIXATION AS COMPARED TO THE MEAN OF	
MONOCULAR RIGHT TEMPORAL AND MONOCULAR	
LEFT NASAL DATA	
FIGURE 3.9- HUE-SCALING FUNCTIONS FOR BINOCULAR FOVEAL.....	45
AS COMPARED TO THE MEAN OF MONOCULAR LEFT	
AND RIGHT FOVEAL DATA	
FIGURE 3.10- SAMPLE MICHAELIS-MENTEN FUNCTION.....	47
FIGURE 3.11- MEAN K VALUES AS A FUNCTION OF WAVELENGTH.....	51
FIGURE 3.12- MEAN $3K$ VALUES AS A FUNCTION OF HUE TERM.....	52

FIGURE 4.1- HUE-SCALING FUNCTIONS FOR AMBLYOPIC.....	72
OBSERVER FOR BINOCULAR LEFT AND RIGHT FIXATION CONDITIONS AS COMPARED TO BINOCULAR FOVEAL DATA	
FIGURE 4.2- HUE-SCALING FUNCTIONS FOR AMBLYOPIC.....	74
OBSERVER AS COMPARED TO MEAN NORMAL OBSERVER DATA FOR BINOCULAR LEFT FIXATION, MONOCULAR LEFT TEMPORAL, AND MONOCULAR RIGHT NASAL CONDITIONS FOR A 1.7° STIMULUS	
FIGURE 4.3- HUE-SCALING FUNCTIONS FOR AMBLYOPIC.....	75
OBSERVER AS COMPARED TO MEAN NORMAL OBSERVER DATA FOR BINOCULAR LEFT FIXATION, MONOCULAR LEFT TEMPORAL, AND MONOCULAR RIGHT NASAL CONDITIONS FOR A 3.7° STIMULUS	
FIGURE 4.4- HUE-SCALING FUNCTIONS FOR AMBLYOPIC.....	76
OBSERVER AS COMPARED TO MEAN NORMAL OBSERVER DATA FOR BINOCULAR RIGHT FIXATION, MONOCULAR RIGHT TEMPORAL, AND MONOCULAR LEFT NASAL CONDITIONS FOR A 1.7° STIMULUS	
FIGURE 4.5- HUE-SCALING FUNCTIONS FOR AMBLYOPIC.....	77
OBSERVER AS COMPARED TO MEAN NORMAL OBSERVER DATA FOR BINOCULAR RIGHT FIXATION, MONOCULAR RIGHT TEMPORAL, AND MONOCULAR LEFT NASAL CONDITIONS FOR A 3.7° STIMULUS	

CHAPTER 1

INTRODUCTION

The fact that humans possess two eyes laterally offset from one another affords us the remarkable capacity for binocular vision, enabling us to enjoy a perception of three-dimensional depth, also known as stereopsis. This lateral displacement of the two eyes allows us to investigate the way binocular signals combine in the visual pathway. For example, Sir Isaac Newton and contemporaries in eighteenth century Europe (Wade, 2000; Wade & Ono, 2012) studied dichoptic color processing, where a pair of color-mismatched stimuli are presented one to each eye. Since Newton's time, a substantial body of dichoptic research (e. g., Erkelens & van Ee, 2002; Hecht, 1928; Ikeda & Sagawa, 1979; Kingdom & Libenson, 2015; Lange-Malecki, Creutzfeld, & Hinse, 1985; O'Shea & Williams, 1996) has investigated how competing color signals from individual eyes combine to yield not only binocular color fusion, where different hues presented to the individual eyes "mix" cortically to produce a secondary color, but also binocular rivalry, where the two hues will not "mix", but instead, will alternate in terms of which color dominates visual perception. The majority of research studying colored stimuli with both eyes falls into this category of dichoptic color, and while this can yield a great deal of insight into cortical processes underlying dichoptic viewing and the general manner in which binocular signals combine under dichoptic viewing conditions, it does not necessarily address the question of how binocular color perception occurs under everyday conditions, where the chromatic input to the two eyes is identical (or, allowing for possible variations in lighting due to slight differences in viewing angle for each eye, at least very similar). Seldom do we spontaneously

encounter a scenario in which the input to each individual eye differs so starkly as it does in dichoptic paradigms.

In a similar manner, psychophysical color vision research has historically been conducted monocularly, with observers viewing stimuli with only one eye to control for possible interocular differences in ocular media, eye dominance, and photoreceptor distribution across the retina. This general experimental procedure has yielded a majority of the information regarding the function of the retina and its underlying structures, and has previously shown that there are differences in color perception for stimuli presented to different areas of the retina (e. g., Abramov, Gordon, & Chan, 1991; Buck, Knight, & Bechtold, 2000; Gordon & Abramov, 1977; Nerger, Volbrecht, & Ayde, 1995; Opper, Douda, Volbrecht, & Nerger, 2014; Stabell & Stabell, 1979; Thomas & Buck, 2006; Volbrecht, Nerger, Imhoff, & Ayde, 2000; Volbrecht, Nerger, & Trujillo, 2011).

One of the more common methods for investigating how color perception changes across the retina is a procedure known as hue-scaling, where observers are shown monochromatic stimuli and asked to describe their appearance in terms of a percentage of each of the four elemental hues: red, green, blue, and yellow. Observers are also asked to specify a percent saturation, as well, indicating the degree to which the stimulus appears to contain chromatic, as opposed to achromatic, information. The higher the percent saturation specified, the stronger the chromatic experience.

Figure 1.1 shows hue-scaling data obtained monocularly with the right eye for a 1.0° stimulus presented 10° temporally (dashed lines) and 10° nasally (dotted lines). Notable in the figure is that hue perception is not the same for the two retinal locations, although retinal eccentricity and stimulus size is the same for both locations. In particular, the perception of blue

is greater in the temporal retina than the nasal retina, and the perception of yellow occurs over a narrower range of wavelengths in the temporal as compared to the nasal retina (left panel).

Stimuli presented to the temporal retina were also perceived as containing a lower percentage of yellow for wavelengths from 490-550 nm. Similarly, differences were observed between the two retinal locations for red and green, with stimuli in the temporal retina perceived as containing a greater percentage of both red and green. These differences are most likely attributed to the chromatic signal being stronger in the temporal retina than the nasal retina as indicated by higher saturation values (right panel) and to changes in hue ratio between the two hue terms, where hue percentages exceed the saturation differences.

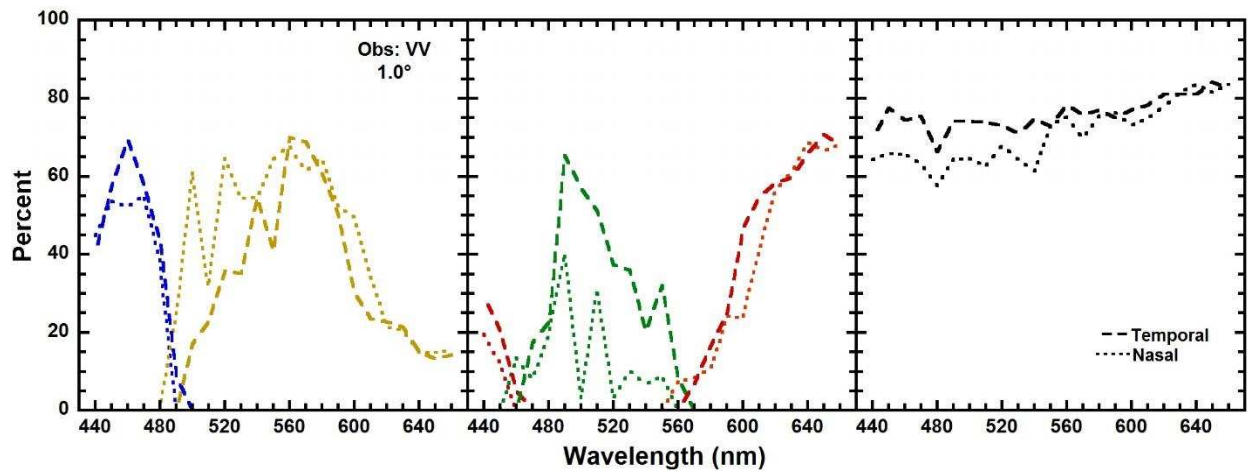


Figure 1.1. Percent hue or saturation is specified as a function of wavelength for stimuli presented to the temporal (dashed lines) and nasal (dotted lines) retina of an observer's right eye. The left panel presents hue-scaling results for blue and yellow, the center panel for green and red, and the right panel for saturation. Within the left two panels, a particular hue is indicated by line color. Hue values for a given wavelength have been scaled to the saturation values for that wavelength.

These differences in hue perception across the retina are not entirely unexpected, as photoreceptor distribution across the retina is neither uniform nor symmetrical within a single eye (Curcio & Allen, 1990; Curcio, Sloan, Kalina, & Hendrickson, 1990). In everyday life, however, we seldom use only one eye to gain an impression of the world around us. Although results obtained with the traditional monocular method have granted us a great deal of insight

about how the eyes function individually, like dichoptic color studies, they may be of questionable ecological validity with respect to color vision as it is regularly experienced. Given the variability in the photoreceptor mosaic underlying different parts of the retina, the differences in hue perception for different retinal areas, and the fact that under some circumstances stimuli viewed binocularly will fall on different areas of the retina for each eye, it remains to be seen how color information from the two retinas combines binocularly.

Photoreceptor Distribution Across the Retina

The human eye possesses two distinct classes of photoreceptor: cone and rod photoreceptors. Rod photoreceptors are primarily responsible for encoding visual information under low luminance conditions, whereas the three types of cone photoreceptors (short-, middle-, and long-wavelength sensitive, referred to as S, M, and L cones, respectively) are those that allow humans to experience color and operate at higher luminance levels than rods. Østerberg (1935) was the first to quantify photoreceptor density in the human eye and to document the variability in the distribution of the photoreceptor types as one moves across the retina. Although his results were based entirely on a single retinal sample, the overall distribution patterns he found, such as the decrease in number of cone photoreceptors and the increase in number of rod photoreceptors as one moves away from the fovea (central retina), have since been corroborated, and refined, by a substantial body of anatomical and psychophysical research (e. g., Ahnelt, Kolb, & Pflug, 1987; Curcio & Allen, 1990; Curcio et al., 1990, 1991; Nerger & Cicerone, 1992; Roorda & Williams, 1999; Williams, MacLeod, & Hayhoe, 1981a, b).

Cones are concentrated primarily in the fovea, a pit occupying the center of the retina, and their numbers decline as one moves from the center of the fovea to the periphery of the retina (Curcio & Allen, 1990). The distribution of cones across the periphery is not uniform;

cones are more numerous on the nasal side of the retina than the temporal side (Curcio & Allen, 1990; Curcio et al., 1990). Additionally, the three types of cones are not equally distributed across the retina. The number of L and M cones exhibit a steep drop as one moves peripherally away from the center of the fovea, whereas S cones show a less pronounced decrease with increasing retinal eccentricity, as well as appearing to be absent from, or at least, very sparse in, the very center of the fovea (Ahnelt et al., 1987; Curcio et al., 1991; Williams et al., 1981a, b). The highest densities of S cones exist between approximately 0.36° and 1.07° eccentricity (Curcio et al., 1991). The ratio of M cones to L cones also varies over the surface of the retina, with the number of M cones to L cones decreasing toward the periphery, which has been documented as occurring from 3.0 mm (approximately 10.71° of retinal angle) retinal eccentricity outward (Brainard et al., 2000; Curcio et al., 1991; Hagstrom, Neitz, & Neitz, 1998; Roorda & Williams, 1999). Besides changes in cone density across the retina, rod distribution differs across the retina, with the number and density of rods, as well as the ratio of rods relative to cones, increasing with increasing retinal eccentricity. The fovea contains no rod photoreceptors, and the highest concentration of rods appears to be in the superior part of the nasal retina, peaking at approximately 15° (Curcio et al., 1990).

Retinal Location and Color Perception

In order to yield perceptual information on chromaticity and luminance, the visual system combines input from the various photoreceptor types. As the ratios of the photoreceptor types to one another vary over the surface of the retina (e. g., Curcio et al., 1990, 1991; Nerger & Cicerone, 1992; Roorda & Williams, 1999), the area of the retina to which a stimulus is presented can influence the perceived hue of that stimulus (e. g., Abramov et al., 1991; McKeefry, Murray, & Parry, 2007; Murray, Parry, & McKeefry, 2006). For example, under

most viewing circumstances, the fovea displays the strongest chromatic response (cf. Opper, et al., 2014). The specific effects of retinal location depend on a number of factors, including the particular wavelength and stimulus size (Abramov et al., 1991; Buck, Knight, & Bechtold, 2000; Volbrecht, Clark, Nerger, & Randell, 2009). In general, the larger the peripherally-presented stimulus, the more fovea-like the color perception (e. g., Abramov et al., 1991; Gordon & Abramov, 1977). Some differences in hue perception between the fovea and the periphery do remain, however, regardless of the size of the peripheral stimulus. Notably, the range of wavelengths perceived as green-yellow tends to be larger in the peripheral retina than the fovea regardless of stimulus size (Opper et al., 2014). Additionally, under some circumstances, peripheral stimuli may also be experienced as more saturated than stimuli presented to the fovea, or “supersaturated” (Moreland & Cruz, 1959; Opper et al., 2014; Stabell & Stabell, 1976).

Although peripheral hue perception approaches that of the fovea as stimulus size increases, there is a point at which the hue perception will stabilize and continuing to increase the stimulus size will cause no further improvement in hue perception (Abramov et al., 1991). This effect is referred to as “filling a perceptive field”, which may be conceived as the perceptual equivalent of a receptive field (Abramov et al., 1991; Pitts, Troup, Volbrecht, & Nerger, 2005). Perceptive field size increases with increasing retinal eccentricity as one moves from the fovea toward the periphery of the retina (Abramov et al., 1991; Nerger et al., 1995; Volbrecht et al., 2009) suggesting that the photoreceptor mosaic underlying a given retinal area influences perceptive field size. For instance, Curcio and colleagues (1990) found monocular differences in the photoreceptor distribution between the temporal and nasal areas of the retina: the temporal retina possesses more cones than the nasal retina up to 2.86° retinal eccentricity. From 3.21° to 7.14° retinal eccentricity, the nasal retina possesses more cones, although at 10.71° retinal

eccentricity, the temporal retina again has a higher average number of cones. Similarly, the temporal retina possesses more rods than the nasal retina up to 3.57° of retinal eccentricity, whereas the number of rods is greater in the nasal retina at 7.14° of retinal eccentricity, although at 10.71° , the number of rods is again greater in the temporal retina (Curcio et al., 1990). The presence of the optic disk in the nasal retina affects the distribution of rods, as well, causing the area of highest rod density in the nasal retina to be at a greater retinal eccentricity than the area of highest rod density in the temporal retina (Curcio et al., 1990). The nasal retina also possesses irregularly-distributed patches of high cone and low rod concentration not seen in the temporal retina (Curcio et al., 1990). Due to these differences in photoreceptor distribution between the nasal and temporal retinas, at 10° retinal eccentricity, perceptive fields tend to be larger in the nasal retina than in the temporal retina (Volbrecht et al., 2009; Volbrecht & Nerger, 2012).

The effects of photoreceptor distribution on perceptive field size appear to be due at least in part to the influence of rod signals: the greater the ratio of rods to cones in a retinal area, the larger the size of the perceptive field (Troup, Pitts, Volbrecht, & Nerger, 2005; Volbrecht et al., 2009). Additionally, data collected after the retina has been bleached (i. e., exposed to a bright light to render rod photoreceptors temporarily desensitized) show that perceptive field sizes are smaller when rod input is minimized (Pitts et al., 2005; Volbrecht et al., 2009). This is not to say, however, that rod input alone determines perceptive field size, as perceptive fields change in response to changing stimulus intensity even under circumstances designed to minimize rod input (Troup et al., 2005). Volbrecht et al. (2009) found that at 10° retinal eccentricity, larger cone-to-ganglion-cell ratios were correlated with increased perceptive field size, indicating that neural convergence of cone signals contributes to determining the size of perceptive fields in a given retinal location under conditions minimizing rod input.

Binocular Color Perception

Although many studies have investigated the relationship between perceptive field size and color perception monocularly, it does not appear that perceptive field size and its influence on perception has been examined for stimuli viewed binocularly. In humans, the placement of the eyes in their sockets is such that when fixating an object, the image of the object will not necessarily fall on the same area of the retina in each eye. This is illustrated in Figure 1.2. A frontally-placed object fixated on with both eyes, for example, will fall on the fovea (F) of both eyes (panel A) whereas if the viewer is looking to the right, an object directly in front of the viewer will yield an image on the temporal side of the right retina and the nasal side of the left retina (panel B). Although not shown, if a viewer is looking to the left, an object directly in front of them will yield an image on the temporal side of the left retina and the nasal side of the right retina.

As discussed in the previous section, photoreceptor distribution is not symmetrical between the nasal and temporal halves of the retina, which may cause hue perception to differ for stimuli presented monocularly to the temporal or the nasal retina (see Figure 1.1). Given these photoreceptor distribution differences, under binocular viewing conditions such as those in Figure 1.2b, color perception will not be identical for both eyes, as the image will fall on the temporal retina of one eye and the nasal retina of the other; however, in spite of this, we experience a chromatically uniform image when viewing stimuli binocularly. Recall that perceptive field size also differs in the periphery for the temporal and nasal retinas, with temporal perceptive fields generally smaller than nasal perceptive fields (Volbrecht et al., 2009; Volbrecht & Nerger, 2012). It is thus currently unclear how differences in perceptive field size for different areas of the retina will affect color perception for stimuli viewed binocularly.

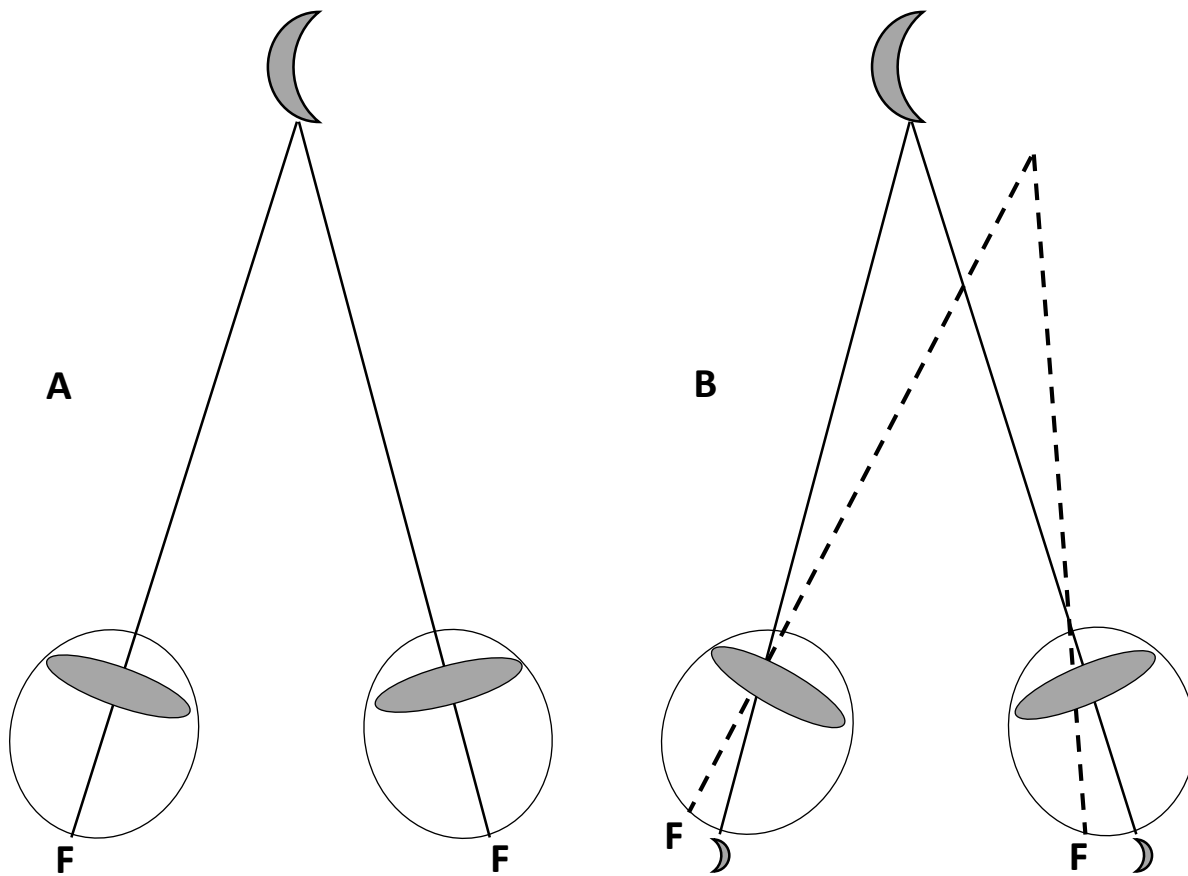


Figure 1.2. Location of the retinal image for a frontally-placed object binocularly fixated (panel A), and a frontally-placed object when binocular fixation is to the right of the object (panel B) Dashed lines indicate the path of fixation, solid lines the position of the object's image, and "F" indicates the location of the fovea.

Previous studies using both binocular and dichoptic presentation of stimuli have provided some insight into the processing of visual information, including color, by the two eyes. In binocular studies, both eyes view the same stimulus, whereas in dichoptic studies, a different stimulus is presented to each eye. Dichoptic paradigms allow for the investigation of such perceptual effects as binocular rivalry, the inability of the two eyes to fuse the differing stimuli into a single percept, resulting in either the suppression of one of the stimuli, or a perceptual alternation between the two stimuli, and binocular fusion, where the two different stimuli are fused into a single uniform percept. As studies are described below, the terms "binocular" and "dichoptic" will refer to the binocular and dichoptic paradigms specified above. Together the

various studies predict potential consequences for color perception when stimuli are viewed with one eye versus when they are viewed with two eyes. Discussion will begin with the most basic level of visual processing, that of the photoreceptors, then move up through the visual pathway to the retinal level and the visual cortex.

Photoreceptor level. While differences in photoreceptor distribution across an individual retina may lead to different hue percepts for stimuli presented to different areas of the same eye, rod and cone photoreceptors may interact differently under conditions using both eyes than under monocular viewing conditions. Additionally, signals from the three types of cone photoreceptors appear to interact differently when stimuli are viewed with both eyes, rather than monocularly.

Rod-cone interactions. A common way to investigate differences in photoreceptor contribution to perception is to vary luminance. Rods are known to respond best to low light levels (scotopic or night conditions), while cones are known to respond best to higher light levels (photopic or daylight conditions). Yet there is a range of light levels referred to as mesopic (similar to light levels at dusk/dawn) where both rods and cones operate, although neither functions optimally. The light levels in this range are approaching luminance levels where the rod response will saturate and the cone response is just barely above its threshold range. Since rods and cones respond differently to different luminance levels, manipulating stimulus luminance for dichoptically-presented stimuli provides some insight into how rod and cone photoreceptor signals interact between the two eyes, especially under mesopic conditions, when both rods and cones respond to stimuli. Early studies (Kakizaki, 1960; Kaplan & Metlay, 1964) found that in a dichoptic rivalry task, the stimulus that had the highest degree of luminance tended to dominate perception, suppressing the less intense stimulus, possibly indicating that cone photoreceptor signals are weighted more heavily than rod photoreceptor signals under

dichoptic viewing conditions. This dominance of cone signals, however, was found only under mesopic conditions, and once stimulus luminance entered the photopic range, further increasing the luminance of a stimulus ceased to increase its degree of dominance. This led Young and Young (1979) to speculate that, because cone responses increase with increasing luminance, but do not saturate, while rod responses both increase with increasing luminance and saturate at photopic levels (e. g., Aguilar & Stiles, 1954; Alpern, Rushton, & Torii, 1970a, 1970b), perhaps rod photoreceptor signals alone determine perception when information from the individual eyes is combined into a single percept. Young and Young tested this hypothesis via a binocular rivalry paradigm, in which observers used a timer to record for what proportion of a 60-s stimulus presentation interval the stimulus presented to the right eye dominated perception, a measurement termed the *prevalence* of the right stimulus. The luminance of the right stimulus was varied relative to that of the left stimulus for each stimulus presentation, and the prevalence of the right stimulus was graphed as a function of the relative luminance for each wavelength (440-650 nm in 10-nm steps) at which the right stimulus was presented. Young and Young calculated the spectral sensitivity of the prevalence response and found that it was not consistent with rod spectral sensitivity, and in fact more closely resembled that of the photopic spectral sensitivity curve; i. e., the spectral sensitivity of cones. Due to the fact that the influence of luminance on prevalence saturates at photopic levels, however, they also concluded that cone photoreceptor signals alone did not determine prevalence, either, as, again, cones do not saturate under constant illumination the way that rods do. Thus it appears that neither rod nor cone photoreceptor signals alone, but rather combined rod and cone signals, determine perception under viewing conditions involving both retinas, yielding a spectral sensitivity function

resembling that of cones, but with the tendency to saturate at high luminance levels in the manner of rods.

Stimulus luminance also affects cortical responses to color presented to both eyes, which may offer information about the consequences of rod-cone interaction between the two eyes beyond the retina. There is some evidence (e. g., Buck & Pulos, 1987; Ciganek, 1970) that the interaction of rod and cone photoreceptor signals differs for stimuli viewed with both eyes relative to stimuli viewed monocularly. For example, for stimulus luminances above cone threshold, visually-evoked potential (VEP) amplitudes for true binocular stimuli (i. e., the same stimulus presented to both eyes) were smaller than VEPs recorded for monocularly-viewed stimuli; whereas for stimuli presented at a luminance below cone threshold, monocular amplitudes appeared to summate to produce a binocular amplitude that was larger than either monocular amplitude alone (Ciganek, 1970). The author interpreted this difference in binocular summation for photopic vs. scotopic stimuli to mean that redundant information from the foveas is discarded along the visual pathway as input from the two eyes combines, leading to a smaller VEP amplitude for the photopic stimuli. Scotopic stimuli, which only stimulate rods, are not of sufficient intensity to activate foveal cones, and thus would generate no such redundant information. Ciganek's (1970) findings, as well as those of Buck and Pulos (1987), who found that scotopic thresholds increased for scotopic test stimuli presented on a photopically bright background only when both the background and test stimulus were presented to the left eye monocularly, and not when presentation was dichoptic (i. e., the background was presented to the left eye and the test stimulus to the right), imply that rod and cone signals interact differently when combining between the two retinas than they do when originating from the same retina.

Interactions between cone types. Combinations of signals originating from the three cone photoreceptor types may also differ for stimuli viewed with both eyes versus stimuli viewed monocularly. At a basic perceptual level, Lange-Malecki, Creutzfeldt, and Hinse (1985) found that proportions of primary hues used to obtain a match to the same chromatic stimulus differed depending on whether presentation of the stimulus was monocular or a result of dichoptic color mixing (i. e., utilizing the principle of binocular fusion to achieve a color mixture across the two eyes, such as presenting a monochromatic red stimulus to one eye and a monochromatic green stimulus to the other to achieve a perception of yellow). This indicates that cone activation differs for monocularly-presented and dichoptically-presented stimuli.

Dichoptic studies have also shown that altering activation of different cone types can differentially affect depth perception (Simmons & Kingdom, 1994). Simmons and Kingdom (1994) tested detection thresholds for stimuli of identical color composition but differing luminance, also known as isochromatic stimuli, and stimuli of identical luminance but differing chromaticity, also known as isoluminant chromatic stimuli at six different retinal disparities. Three of the disparities were crossed, i. e., the stimulus appeared to be in front of the plane of fixation, and three were uncrossed disparities, i. e., the stimulus appeared to be behind the plane of fixation. Although overall chromatic cues did not appear to be as useful for depth detection as luminance cues, increasing the red component, which targeted L cones, of an isoluminant stimulus designed to equally stimulate L and M cones improved observers' accuracy for correctly indicating whether stimuli appeared in front of or behind fixation. Increasing the green component had less of an effect on improving accuracy. These results seem to indicate that signals from L and M cones combine in a unique manner for stimuli viewed with both eyes, with L-cone signals weighted more heavily than M-cone signals.

Regarding S-cone contributions to non-monocular perception, some previous research (e.g., Rogers & Hollins, 1982) indicates that binocular rivalry induced by blue stimuli is either weak or nonexistent, but the stimuli used in these experiments did not necessarily completely isolate S cones, thereby inadvertently allowing input from L and M cones. When O'Shea and Williams (1996) used stimuli designed to selectively target S cones, they found that binocular rivalry does, in fact, occur for stimuli perceived by S cones. O'Shea and Williams suggest that perhaps under everyday viewing conditions, M and L cone signals may mask S-cone contributions to binocular perception in a way that does not occur monocularly.

Retinal level. A series of studies also using the dichoptic paradigm (Crovitz & Lipscomb, 1963; Leat & Woodhouse, 1984; Stanley, Carter, & Forte, 2011) have investigated whether one area of the retina consistently dominates perception when stimuli of short duration (100 to 1000 ms) are presented to different areas of the retina of each eye. While results have been mixed, one study (Crovitz & Lipscomb, 1963) has clearly demonstrated that in a binocular rivalry paradigm, the stimulus falling on the nasal area of the retina tended to dominate perception: the stimulus that fell on the temporal retina was typically not perceived at all. Others (Leat & Woodhouse, 1984; Stanley, Carter, & Forte, 2011) have found similar results, although the effect has been weaker, with participants exhibiting a range of possible dominance patterns (nasal dominates temporal, temporal dominates nasal, or neither location reliably dominates), and for stimuli presented continuously there does not appear to be a clear dominance pattern based on retinal location (Leat & Woodhouse, 1984). This may suggest that retinal location may determine hue perception for stimuli viewed with both eyes, at least for stimuli of short duration.

Cortical level. Studies investigating binocular and dichoptic color perception at the cortical, as opposed to the retinal, level can afford additional information regarding how

information from the two eyes is combined to yield a uniform hue percept, even though the monocular hue percepts underlying it may differ. Although an early study (Perry, Childers, & Dawson, 1969) found evidence that the two eyes make an approximately equal contribution to color perception at the cortical level, in that the amplitude of VEPs for a yellow formed by dichoptically mixing red and green lights fell between the amplitudes of a red and a green light individually, more narrowly-focused research indicates that interaction of chromatic signals between the two eyes may be more complicated than a simple equal contribution. Prior research (Simmons & Kingdom, 1997; Wong & Freeman, 1999) has investigated whether chromatic information can be used to achieve stereopsis, the perception of depth resulting from the lateral offset of the two eyes, which causes each eye to view the same scene from a slightly different angle. Evidence has been found for a neural pathway specifically responsible for integrating chromatic information between the two eyes to achieve a perception of depth (Simmons & Kingdom, 1997). It has been hypothesized that chromatic information pertaining to stereopsis may be carried at least as far as V1 by the parvocellular pathway, the neural pathway thought to be responsible for conveying red-green opponent chromatic information. This may indicate that red and green chromatic signals are processed differently for stimuli viewed with two eyes than for stimuli viewed monocularly, although the exact nature of this difference is as yet unclear. Another study (Wong & Freeman, 1999) has shown additional support for a separate processing pathway for chromatic information presented to both eyes; specifically, that there is a difference in the way binocular chromatic information and binocular luminance information are spatially integrated, with chromatic information “cooperating” (i. e., combining) across the two retinas, and no such cooperation occurring for luminance information. This combining of spatial chromatic information across the two retinas may imply that perceptive field sizes are smaller for

stimuli viewed binocularly, as each eye is contributing to the hue percept from a slightly different angle, perhaps increasing the amount of spatial chromatic information available to the visual pathway.

Although it was long believed that cortical binocular cells were only responsive to luminance, and not chromatic, information, a number of studies (Landisman & Ts'o, 2002; Peirce, Solomon, Forte, & Lennie, 2008; Ts'o, Roe, & Gilbert, 2001) with the macaque have found evidence that there are cells in the binocular pathway that respond to hue, which may imply that binocular hue perception, because it is based in signals from both eyes, has an advantage over monocular color vision. Ts'o, Roe, and Gilbert (2001) found cells in thin stripes of V2 that were both color-selective and responsive to binocular input. This study also showed that color-selective and disparity-selective (i. e., differentially responsive to varying degrees of binocular disparity and thus neurally encoding a perception of depth) pathways are not wholly distinct in macaque visual cortex; instead, there appears to be a gradual transition from solely color-selective to solely disparity-selective areas, with the intermediate areas being both color- and disparity-selective. Cells preferentially responsive to red-green, as opposed to achromatic, stimuli have been found to exist both within the centers of ocular dominance columns and on the borders between them (Landisman & Ts'o, 2002). Peirce, Solomon, Forte, and Lennie (2008) corroborated these results and found that there are color-preferring cells in macaque V1 and V2 that respond to binocular input, implying that there is binocular representation of color in primate visual cortex.

The extent of the implications for these findings on human visual processes is not clear, but there is behavioral evidence from human studies using stimuli designed to induce interocular interference. Interocular interference is an event whereby visual information presented to one

eye affects perception in the contralateral eye, such that after adapting the right eye to a square-wave grating an afterimage appears in the left eye. In order for interocular interference to occur, the stimulus causing the interference must be processed at a point in the visual pathway where information from the two eyes is integrated. van Lier and de Weert (2003) found interocular interference for chromatic patches superimposed on gratings presented dichoptically. As interocular transfer is an effect that occurs at the cortical level, van Lier and de Weert's finding supports the existence of color-selective binocular mechanisms in human visual cortex.

Eye Dominance and Binocular Vision

Complicating matters of binocular summation is the fact that people often have a dominant eye. The distance separating the two eyes in the skull causes each individual eye to perceive the same visual scene from slightly different angles, resulting in a slightly different vantage point for each eye. Research on how eye dominance affects color perception yields mixed results, with some studies finding support for a prevailing influence of the dominant eye (Johansen, 1930; Newman, Wolfe, Stewart, & Lessell, 1991; Peirce et al., 2008) and others finding that eye dominance is not a factor (Costa et al., 2006; Ikeda & Sagawa, 1979; Verriest, Laethem, & Uvijls, 1982). Johanssen's (1930) observers reported greater dominance of a long-wavelength stimulus over a shorter-wavelength stimulus during dichoptic presentation when the long-wavelength stimulus was presented to the right eye. As all observers were right-handed, Johanssen assumed that this meant all observers were right-eye-dominant and interpreted this finding to mean that the dominant eye contributed more strongly to color perception under dichoptic conditions. A major shortcoming of Johanssen's study, however, is that handedness does not necessarily determine eye dominance, as one can be right-handed and left-eye dominant (Miles, 1930). Newman and colleagues (1991) found that patients with optic neuritis were able

to integrate information from their unaffected, dominant eye to yield better binocular than monocular performance on the Farnsworth-Munsell 100 hues test, indicating that viewing color binocularly may convey an advantage over viewing color monocularly, particularly monocularly with the non-dominant eye. Perhaps the most compelling evidence regarding eye dominance and color perception is that although color-preferring cells in V1 and V2 of macaques respond to stimuli presented to either eye, they exhibit a stronger response to stimuli presented to the dominant eye (Peirce et al., 2008).

Ikeda and Sagawa (1979), however, found that the degree of binocular fusion of dichoptically-presented stimuli was more dependent upon how close in wavelength the two stimuli were, rather than to which eye the stimulus was presented; however, they did not appear to control for eye dominance among their observers. The findings of Verriest et al. (1982), who did test for eye dominance, seem to corroborate Ikeda and Sagawa's (1979) conclusions: in comparing monocular performance between observers' two eyes on the FM-100 hues test, they found that which eye performed better seemed to be related to which eye the subject first used for the test rather than which of an observer's eyes actually tested as dominant. Costa et al. (2006) also found no influence of eye dominance on color perception as measured by performance on the Cambridge Colour Test. Their observers exhibited no differences in discrimination between the dominant and non-dominant eyes, nor between binocular vs. monocular conditions.

The current experiment investigated color perception both monocularly and binocularly to determine how information from each individual eye combines to yield a binocular color perception when a stimulus fills or does not fill a perceptive field. Based on previous studies, it was predicted that: 1) binocular peripheral color perception will approach foveal color perception

at smaller stimulus sizes than monocular peripheral color perception, which is to say that 2) binocular peripheral perceptive field sizes will be smaller than monocular peripheral perceptive fields (Landisman & Ts'o, 2002; Pierce et al., 2008; Newman et al., 1991; Simmons & Kingdom, 1997; T'so et al., 2001; Wong & Freeman, 1999); and 3) of the two monocular peripheral conditions, binocular color perception will be most similar to that of a stimulus monocularly presented to the nasal retina of the dominant eye (Crovitz & Lipscomb, 1963; Stanley et al., 2011).

CHAPTER 2

METHOD

Participants

Observers were AL, a 22-year-old female; AW, a 23-year-old male; JO, a 35-year-old female; and VV, a 57-year-old female. All observers had normal color vision in both right and left eyes as assessed with the Farnsworth-Munsell 100-hue panel test, D-15 panel test, desaturated D-15 panel test, and the Neitz anomaloscope (OT-II). Binocular perception was assessed using the Distance Randot Test (Stereo Optical Company, Inc., Chicago, Ill.). All observers except JO were able to correctly perceive the shapes at all retinal disparities. Observer JO is partially stereoblind due to childhood strabismus (left-eye esotropia) and was unable to perceive the shapes for 60 and 100 arcseconds of disparity, but performed normally for the 200 and 400 arcsecond disparities. JO's data were collected only for comparison purposes and were not included in the main analyses. Eye dominance was assessed using the Miles test of ocular dominance (Miles, 1930). All binocular-normal observers were right-eye dominant, as well as the amblyopic observer. All observers except AL were myopic and wore corrective lenses when viewing the stimuli.

Materials

Apparatus. The apparatus setup is depicted in Figure 2.1. Stimuli were presented via a 6-Inch Diameter Integrating Sphere (Gooch & Housego OL IS-670-LED; Figure 2.1 F) connected to a fiber optic light guide (Figure 2.1 I) that was placed in the light path of a Maxwellian-view optical system illuminated by a 300 W (5500 K) xenon arc lamp (Oriental). A

lens (Figure 2.1 C), iris diaphragm (30 mm when fully opened; Figure 2.1 D), and filter box (Figure 2.1 E) were placed between the integrating sphere and the stimulus viewing aperture, for the purposes of magnifying the stimulus, controlling stimulus size, and holding neutral-density filters to achieve constant luminance, respectively.

Observers used a table-mounted chin and forehead rest (Figure 2.1 A) to stabilize the head inside a hood constructed of black cardboard that prevented light leakage. The stimulus was visible through a 30-mm opening created in the cardboard hood located in front of the observer. Observers were seated 1 m from the cardboard aperture. This distance was selected because it is the distance at which all observers were able to achieve binocular fusion of all stimulus sizes. Fixation points stabilized the observer's gaze and were created via optical fibers inserted in the cardboard around the aperture where the stimulus was displayed (Figure 2.1 B and Figure 2.2).

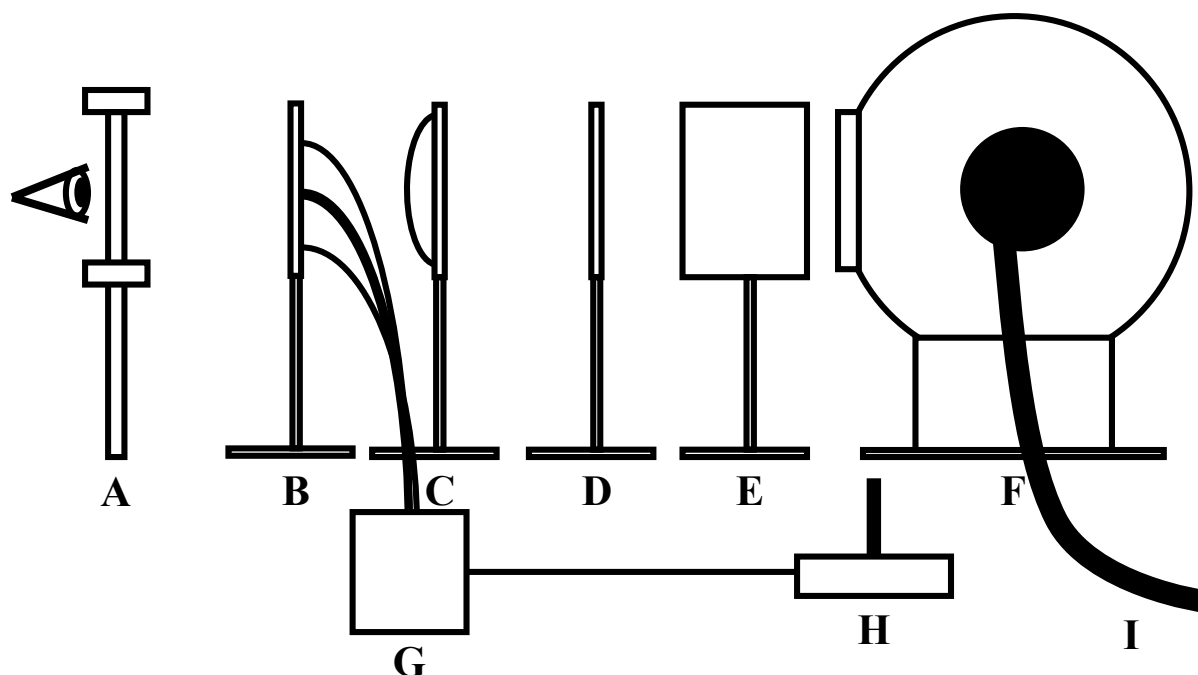


Figure 2.1. Schematic of the experimental apparatus. A: Chin/forehead rest; B: Fixation-point plate; C: Magnifying lens; D: Iris diaphragm; E: Neutral-density filter box; F: Integrating sphere; G: Light source for fixation points; H: Fixation point potentiometer; I: Fiber optic light guide placed in the path of light emitted by a xenon arc lamp.

The optical fibers for the fixation points transmitted light from an LED light source (Figure 2.1 G) regulated by a potentiometer (Figure 2.1 H).

Stimulus. Figure 2.2 depicts the stimulus arrangement. Observers viewed circular monochromatic stimuli ranging from 450 nm to 670 nm in 20-nm steps at approximately 15 trolands (td; range: 13.78-17.00 td). Interference filters (Ditric Optics) with peak transmission from 450 – 670 nm, in 20 nm steps, controlled stimulus hue. Stimulus presentation duration was 500 ms, and was controlled by a shutter (Uniblitz) placed in the Maxwellian-view optical system. The experimenter used the iris diaphragm to adjust the stimulus size so that stimuli subtended 1° of visual angle for the central visual field presentation conditions, or 1° , 1.7° , 2.25° , 2.7° , or 3.7° of visual angle for the peripheral presentation conditions. Stimuli were presented through a 30-mm aperture cut into the cardboard hood that protected the observer from light leakage. As shown in Figure 2.2, two vertical fixation points (Figure 2.2 B) were placed 2.35° above and below the center of the cardboard aperture, half a degree outside the diameter of the largest stimulus size. Two horizontal fixation points (Figure 2.2 C) were oriented on either side of the stimulus, calculated to be 10° from the center of the aperture when viewed from a distance of 1 m.

Calibration

Neutral-density filter calibrations were performed with a UDT S370 radiometer, whereby energy measurements were obtained for each interference filter with and without the presence of the neutral density filter to determine the amount by which each neutral-density filter reduced energy transmission. Photometric calibrations were then made with a Minolta Chroma Meter CS-100 photometer for each interference filter without the presence of neutral density filters.

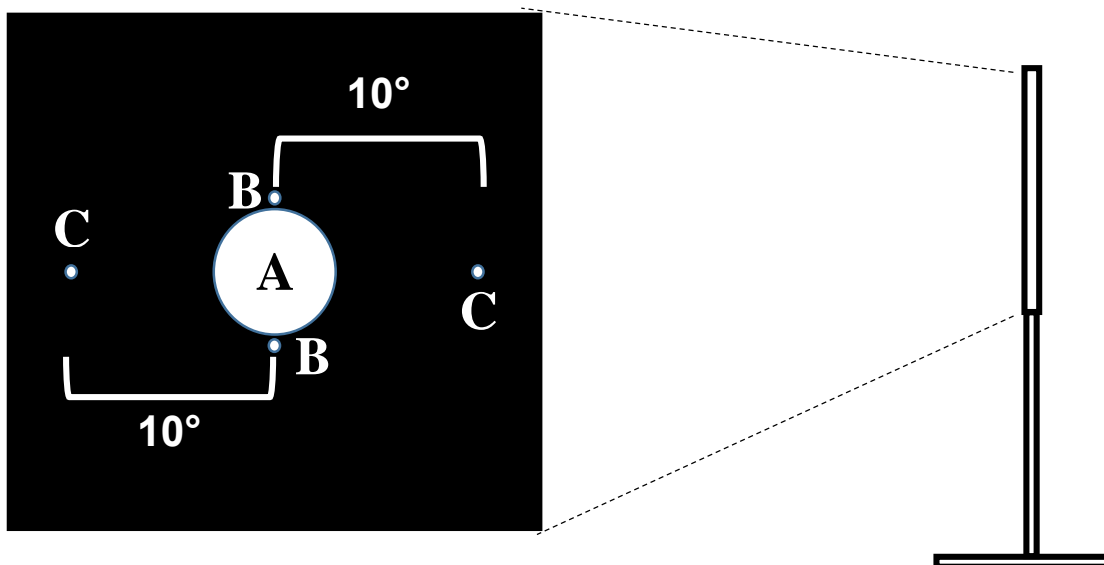


Figure 2.2. Diagram of fixation point plate through which observers viewed the stimuli (detail of Figure 1 B). A: Aperture through which observers viewed the stimulus; B: Vertical fixation points to enable observer to align to the center of the aperture during the central visual field presentation conditions; C: Horizontal fixation points, which observers fixated to obtain peripheral presentation of the stimulus in the peripheral visual field conditions.

This determined the total luminance (cd/m^2) output of each interference filter. Luminance values were then converted to retinal illuminance (trolands) to approximately equate stimuli to values from previous studies conducted in the laboratory (Oppen et al., 2014; Volbrecht et al., 2009; Volbrecht & Nerger, 2012). Since retinal illuminance varies with pupil size, and pupil size varies with not only stimulus luminance, but also observer's age, calculations were performed using Watson and Yellott's (2012) unified formula to determine the age appropriate pupil size for each observer when converting luminance values to retinal illuminance. Although stimuli were viewed both monocularly and binocularly, the monocular coefficient was used for all pupil diameter calculations in order to ensure stimuli were physically identical for all conditions. Following from these measurements and calculations, neutral density filters were selected for each observer to yield a retinal illuminance of approximately 15 td at each stimulus wavelength.

Interference filter spectral irradiance calibrations were performed with a Photo Research SpectraScan PR650 spectral radiometer, which measures energy output at wavelengths ranging

from 380-780 nm in 4-nm steps. Figure 2.3 illustrates the energy output across wavelength for the interference filter with a nominal value of 550 nm. Because this instrument only measures in 4-nm steps, the wavelength for peak energy transmission of each interference filter was estimated by taking the mean of the two highest irradiance levels. The spectral range of transmission was specified by half-bandwidth. The two values at which energy transmission was half that of the peak transmission was determined and the absolute value of the difference between these two wavelengths defined half-bandwidth (see Figure 2.3). Wavelengths of peak

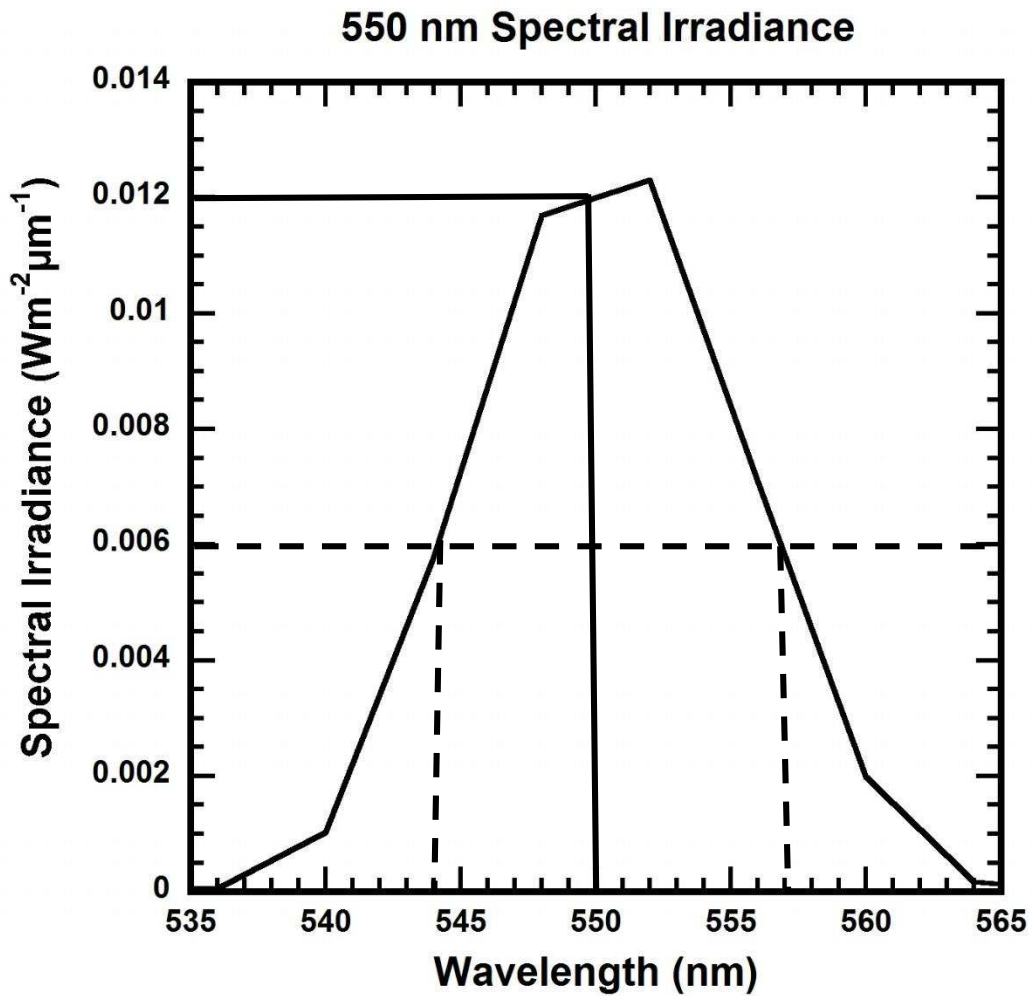


Figure 2.3. Example of energy output across wavelength for the 550 nm interference filter. The solid horizontal and vertical lines indicate the wavelength computed to be at peak energy transmission, and the dashed line shows the wavelengths at half-bandwidth.

energy and half-bandwidths for each interference filter are listed in Table 2.1. In general, the measured wavelengths at peak transmission matched the manufacture’s nominal wavelength values, so the nominal values are used when referring to the wavelength values in this study.

Table 2.1

Wavelength of Peak Energy Concentration and Half-Bandwidth of Interference Filters

Filter	Peak (nm)	Half-Bandwidth (nm)	Filter	Peak (nm)	Half-Bandwidth (nm)
450	450	5.3	570	570	6.4
470	470	5.3	590	590	6.8
490	490	5.5	610	609	6.4
510	510	5.8	630	630	7.0
530	530	6.5	650	650	7.1
550	550	6.5	670	670	7.0

Procedure

Dark adaptation time was 10 minutes for the foveal conditions and 30 minutes for the peripheral conditions to ensure maximal rod input. Each observer viewed each stimulus condition monocularly with his/her right and left eye, and then binocularly, for a total of nine viewing conditions, listed in Table 2.2. Observers utilized the “4+1” hue-scaling procedure (Gordon & Abramov, 1977) to describe the hue of each stimulus while the experimenter recorded their responses. In this procedure, observers are instructed to specify the percent of each of the elemental hues—blue, green, yellow, and red—with a percentage between 0 and 100. The total hue percentages must sum to 100, and observers cannot use opponent color pairs (i. e. red/green or blue/yellow) simultaneously to describe a stimulus (Abramov et al., 1991). Observers also specify the saturation of the stimulus with a percentage between 0 and 100, where 0 is a completely achromatic experience, and 100 is a completely chromatic experience. Three separate data collection sessions were run for each experimental condition and stimulus size,

with a fourth session added for conditions where the data were highly variable. Between four and seven conditions were run per session, with the length of a session ranging from one to two hours. The conditions run in a given session were chosen pseudorandomly by the experimenter.

Table 2.2

Foveal and Peripheral Fixation Conditions

	Fovea	Peripheral Retina
Monocular	Left Eye	Left Eye Left Fixation
		Left Eye Right Fixation
	Right Eye	Right Eye Left Fixation
		Right Eye Right Fixation
Binocular	Binocular	Binocular Left Fixation
		Binocular Right Fixation

CHAPTER 3

RESULTS

Hue Perception

For data analysis, hue percentages specified for each wavelength at each stimulus size and viewing condition underwent an arcsine transformation to reduce unequal variance (Gordon et al., 1994). These transformed values were then scaled to the saturation percentage so that the sum of the hue percentages of all hue terms at a given wavelength equaled the saturation percentage (Abramov et al., 1991). Means of the transformed and scaled hue percentages were computed across experimental sessions for each condition and observer, and then the grand mean and the standard error of the means (SEM) across all three observers with normal stereovision were calculated.

To assist in interpreting the results of this study, Table 3.1 specifies where the stimulus projected on the retina (temporal, nasal) for each eye during peripheral viewing. In presentation of data, each fixation condition will be referred to by the corresponding retinal location (e. g., “left eye, left fixation” will be referred to as “left eye temporal”; “binocular right fixation” will be referred to as “left eye nasal, right eye temporal”).

Table 3.1

Retinal Area Stimulated in Each Fixation Condition

Fixation Condition	Eye	Retinal Area
Left fixation	Left eye	Temporal
	Right eye	Nasal
Right fixation	Left eye	Nasal
	Right eye	Temporal

Note: With binocular viewing the stimulus is simultaneously falling on the temporal retina of one eye and the nasal retina of the other eye.

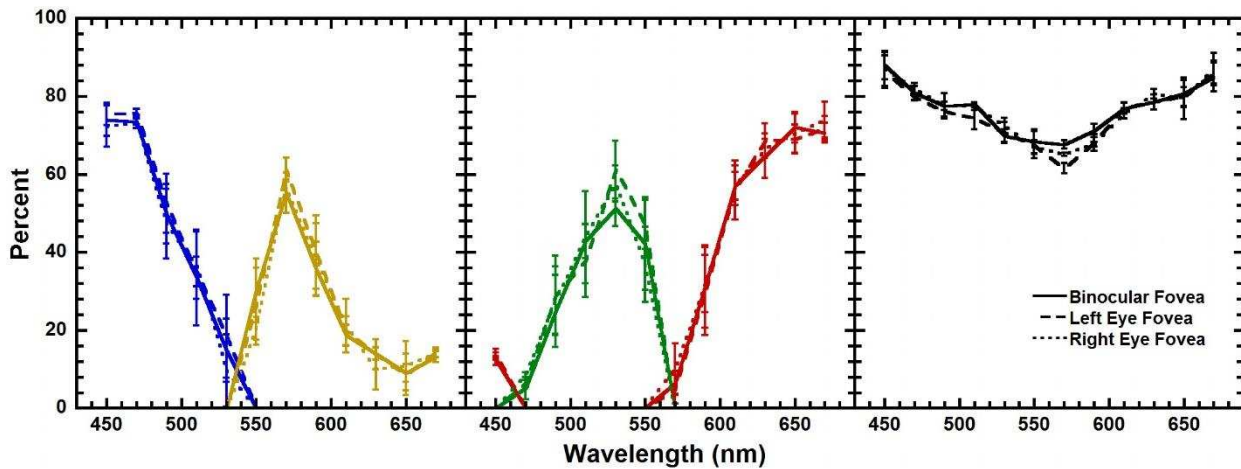


Figure 3.1. Mean percent hue or saturation is specified as a function of wavelength for binocular (solid lines), left eye monocular (dashed line), and right eye monocular (dotted line) foveal viewing conditions. The left panel presents hue-scaling results for blue and yellow, the center panel for green and red, and the right panel for saturation. Within the left two panels, a particular hue is indicated by line color. Error bars denote ± 1 standard error of the mean (SEM).

Effects of Fixation Condition. Figure 3.1 presents mean percent blue and yellow (left panel), green and red (center panel) and saturation (right panel) for the binocular (solid lines), left eye monocular (dashed lines), and right eye monocular (dotted lines) foveal conditions. As illustrated in this figure, there is little difference in mean percents between the binocular and two monocular viewing conditions in the fovea.

One objective of this study was to investigate differences in hue perception between the peripheral fixation conditions and the foveal fixation condition under both monocular and binocular viewing, and how these perceptual differences change as stimulus size in the periphery increases. Recall in the foveal fixation condition observers are viewing the stimulus in the center of the visual field, and the stimulus size is always 1° . Figure 3.2 depicts hue-naming data for conditions viewed monocularly with the left eye; each column represents a different stimulus size presented peripherally and each row percentages of different opponent-hue terms (blue/yellow, red/green) or saturation. Solid lines represent the left eye foveal condition, dashed lines the left eye temporal peripheral condition and dotted lines the left eye nasal peripheral condition. In the peripheral conditions, regardless of stimulus size, stimuli appear less blue and more yellow from approximately 510-530 nm than they do in the fovea; i. e., the yellow function begins at shorter wavelengths with peripheral viewing than with foveal viewing. The green hue-naming functions for the temporal and nasal retinas are shifted relative to the foveal green function, with the peak of the green function occurring around 510 nm for the peripheral conditions and 530 nm for the foveal condition. For the 1.0° and 1.7° stimulus sizes (center row, left two panels), less green and red were perceived in the nasal retina than in the temporal retina. Stimuli were perceived as less saturated in the nasal retina with the 1.0° and 1.7° stimuli (bottom row, left two panels) than in the temporal retina or the fovea. Although for the larger stimulus sizes, saturation for stimuli presented to the left nasal retina is quite similar to that for stimuli presented to the left fovea and left temporal retina, the minimum of the saturation function for the left eye nasal stimulus is also lower (i. e., appeared less saturated) relative to the minima for the other monocular left eye viewing conditions (bottom row, right three panels).

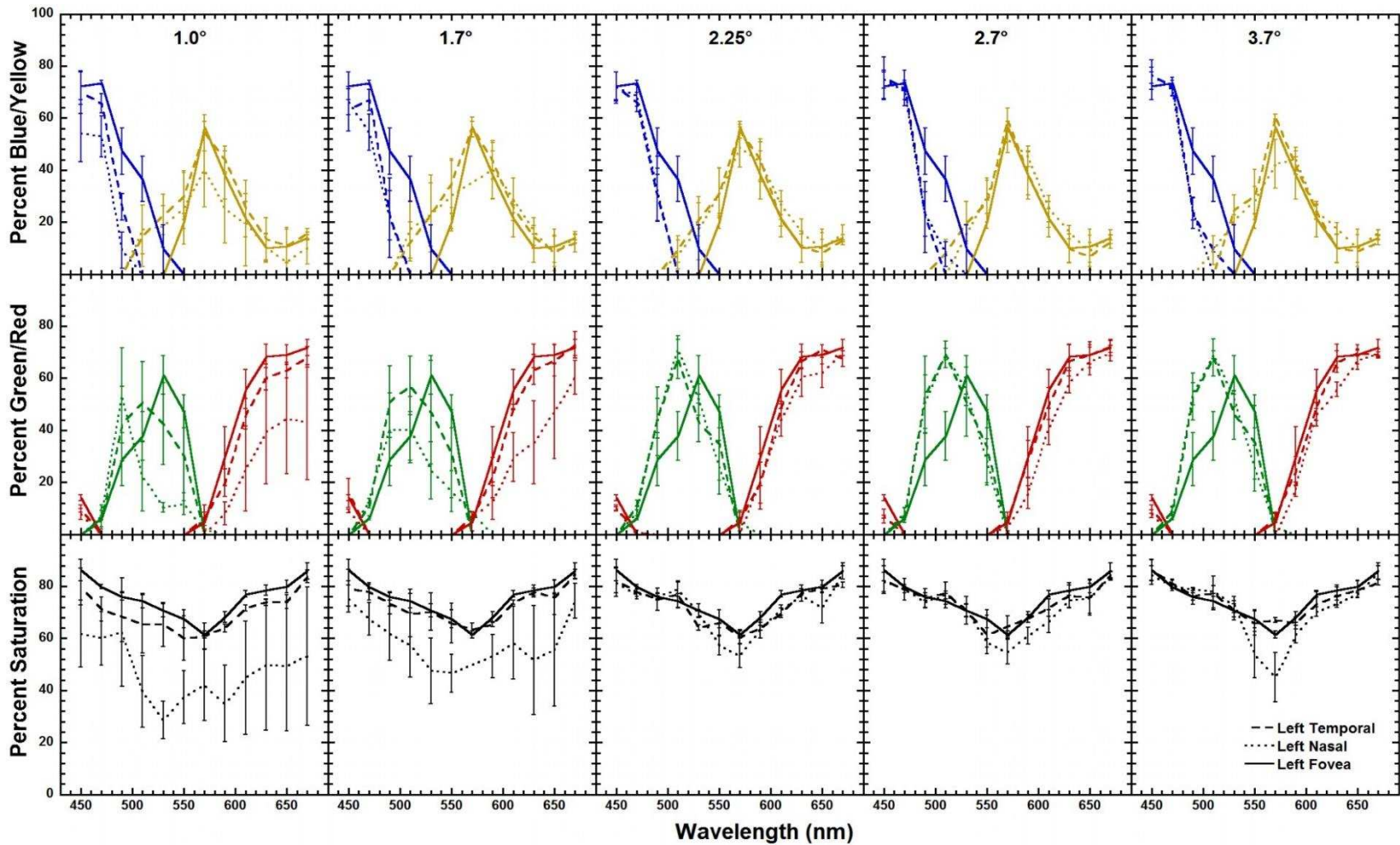


Figure 3.2. Mean percent blue or yellow (top row), green or red (middle row), and saturation (bottom row) are plotted as a function of wavelength for the monocular, left eye viewing conditions. Dashed lines represent the left eye left fixation condition, with the stimulus falling on the temporal retina, and dotted lines depict the left eye right fixation condition, with the stimulus falling on the nasal retina. Solid lines denote the left eye monocular fovea condition. Columns present results for peripheral stimuli of different sizes. The foveal stimulus size is always 1°.

One can observe a similar pattern of results for the right eye monocular conditions in Figure 3.3. Here, the solid lines again represent stimuli falling on the fovea, the dashed lines stimuli falling on the temporal retina, and the dotted lines stimuli falling on the nasal retina. Again, regardless of stimulus size, the percent of blue is reduced and the percent of yellow is enhanced around 510-530 nm in the periphery relative to the fovea (top row). The peaks of the peripheral green function are shifted toward shorter wavelengths compared to the fovea (middle row). In the right eye, the differences in amount of green perceived between the temporal and nasal retina are more persistent across stimulus size, with the nasal retina perceiving less green for all but the largest stimulus size (center row, rightmost panel). This indicates that the stimulus needs to be larger in the right eye nasal condition than it does in the left eye nasal condition before perception of green approaches that for stimuli presented to the right temporal retina or the right fovea. Stimuli presented nasally appear less saturated than those presented temporally or foveally for the 2.25° stimulus (bottom row, center panel) as well as the 1.0° and 1.7° stimuli (bottom row, left two panels). Interestingly, hue and saturation perception in the right eye appear to stabilize at larger stimulus sizes than they do for the left eye (see Figure 3.2). This may be related to the fact that all participants were right-eye dominant; however, one might expect perception to have higher acuity in the dominant than the non-dominant eye, so the fact that the dominant eye appears to require larger stimuli to achieve a stable hue perception seems to warrant further investigation.

Figure 3.4 presents the results for the binocular viewing conditions, comparing the foveal responses obtained with a 1° stimulus to the peripheral responses obtained with four different stimulus sizes. As seen in this figure, regardless of stimulus size, percent blue, yellow, and green in the peripheral conditions resemble each other more than they do with the fovea. The

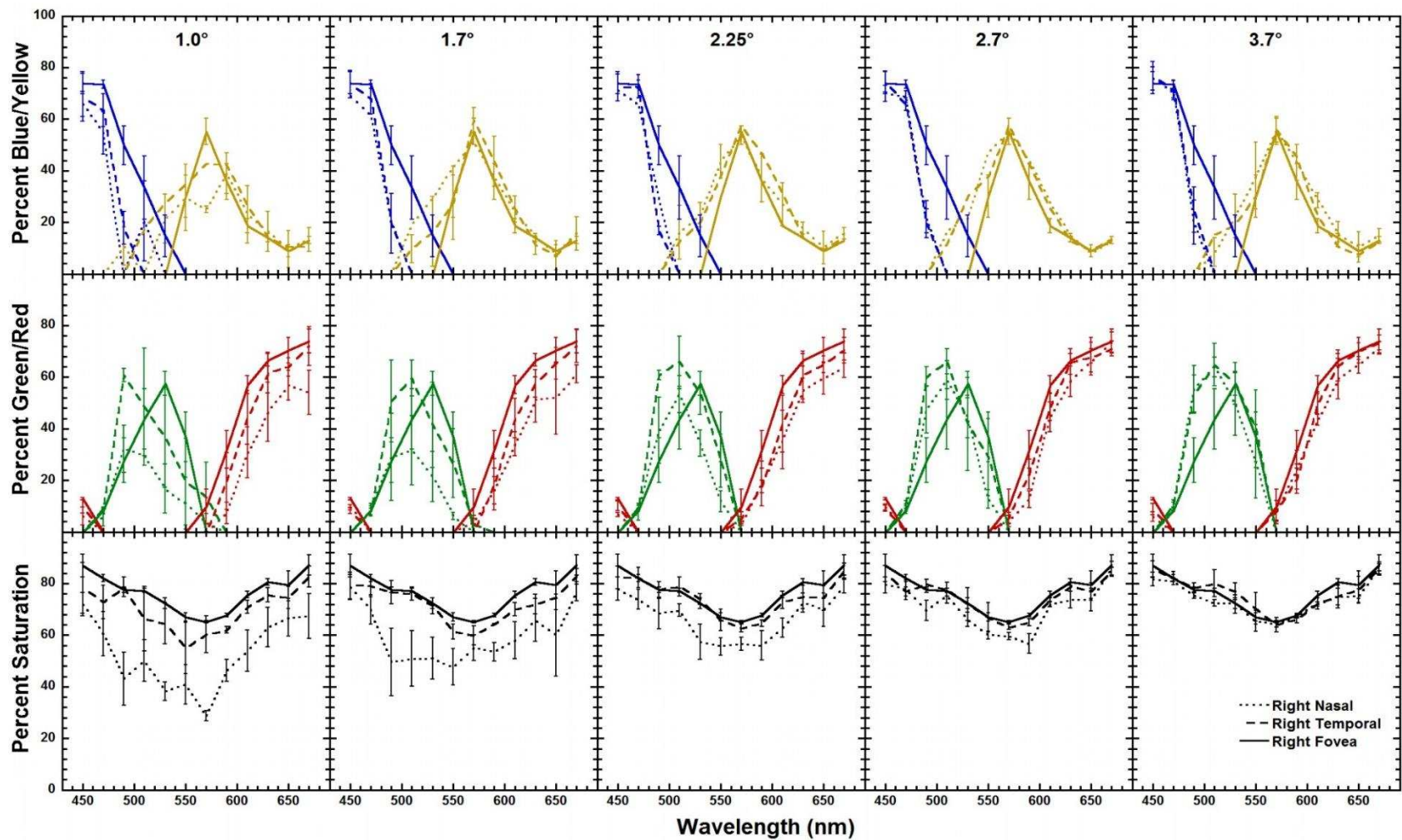


Figure 3.3. Mean percent blue or yellow (top row), green or red (middle row), and saturation (bottom row) is plotted as a function of wavelength for the monocular, right eye viewing conditions. Dashed lines represent the right eye right fixation condition, with the stimulus falling on the temporal retina, and dotted lines depict the right eye left fixation condition, with the stimulus falling on the nasal retina. Solid lines denote the right eye monocular fovea condition. Columns present results for peripheral stimuli of different sizes. The foveal stimulus size is always 1°.

peripheral blue functions are narrower and the peripheral yellow functions are wider than the foveal functions (top row). The green function for the peripheral conditions peak at a higher percentage than the foveal function for stimuli larger than 1.0° (center row).

There are, however some important differences between the binocular (Figure 3.4) and monocular (Figures 3.2 and 3.3) functions. For the 1.0° stimulus, the percentage of green perceived in the two peripheral binocular conditions is quite similar (center row, left panel), whereas, referring back to the first two columns of Figure 3.2 and 3.3, percentages of green in the monocular temporal conditions are greater than those in the monocular nasal conditions. This suggests that in the binocular peripheral conditions, perception of green may be more heavily influenced by the eye for which the stimulus is falling on the temporal retina. The peripheral binocular red functions, similarly, show that for all stimulus sizes, the binocular peripheral conditions are quite similar to one another. Additionally, for smaller stimuli, the binocular red functions resemble the corresponding monocular temporal, rather than monocular nasal, red functions, again indicating that the temporal retina may dominate in binocular perception. Also noteworthy are the binocular saturation functions for the 1.0° stimulus (bottom row, left panel). They do not exhibit the differences in saturation that are seen between the monocular peripheral conditions (Figures 3.2 and 3.3, bottom rows); in fact, the saturation functions for the peripheral binocular condition are quite similar to those for the monocular temporal conditions in Figures 3.2 and 3.3 (bottom rows). Taken as a whole, the binocular hue-scaling data appear to indicate that the perception corresponding to that of the temporal retina is dominating peripheral hue perception.

Also interesting in Figures 3.2-3.4 is the stimulus size at which hue and saturation perceptions appear to stabilize: for the left monocular condition, perception seems to be largely

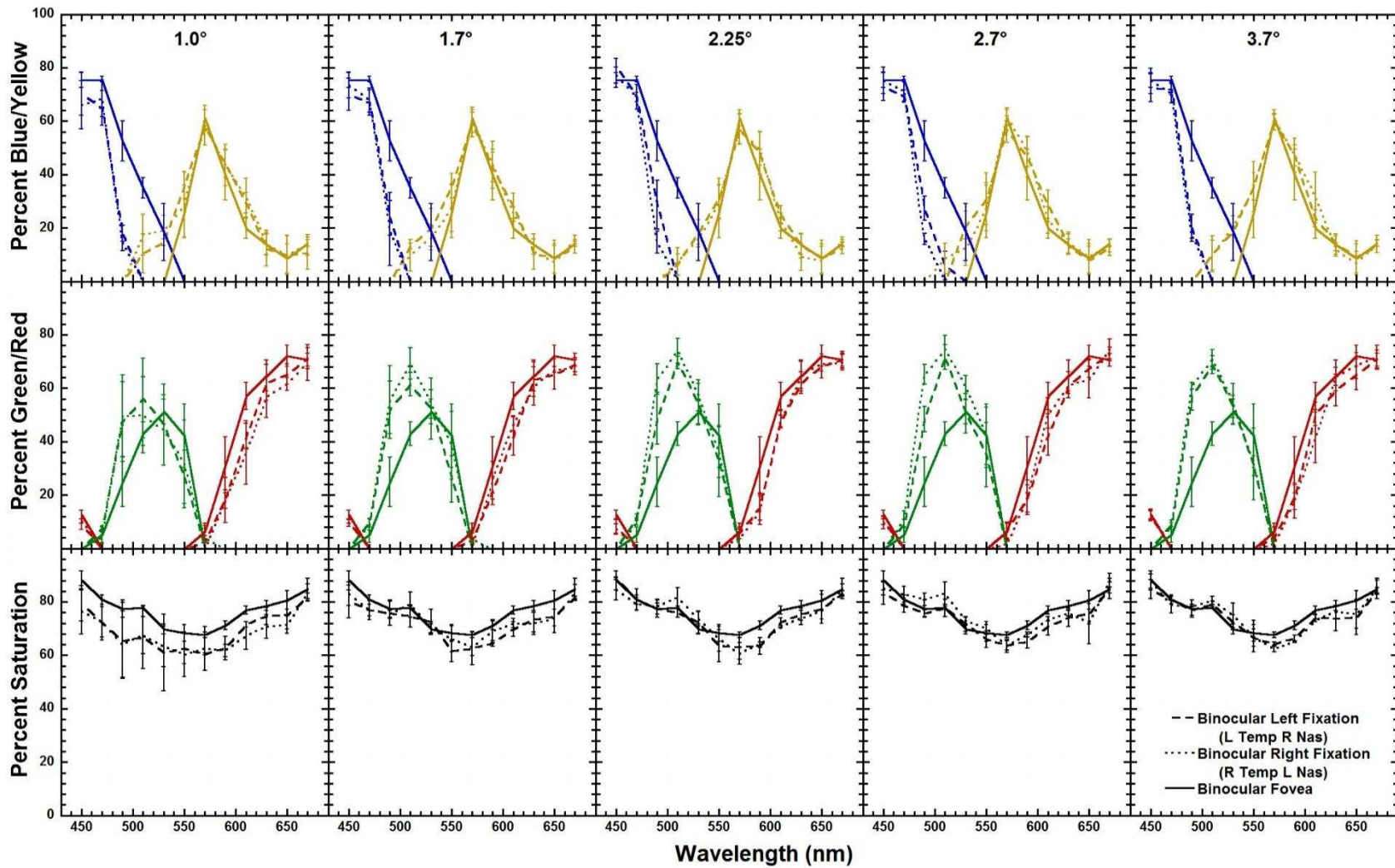


Figure 3.4. Mean percent blue or yellow (top row), green or red (middle row), and saturation (bottom row) are plotted as a function of wavelength for the binocular viewing conditions. Dashed lines depict the binocular left fixation condition (stimulus falling on the temporal retina of the left and nasal retina of the right eye) and dotted lines depict the binocular right fixation condition (stimulus falling on the temporal retina of the right and nasal retina of the left eye). Solid lines depict the binocular fovea condition. Columns present results for peripheral stimuli of different sizes. The foveal stimulus size is always 1°.

invariant by 2.25° , whereas for the right monocular condition, it seems to take until the 2.7° stimulus for perception to become less variable between the right nasal and right temporal conditions. The binocular condition appears only to require a 1.7° stimulus to yield relatively invariant hue and saturation percepts, which seems to indicate that binocular vision conveys an advantage in hue perception for small stimuli as compared to monocular vision.

Effects of Stimulus Size. In order to more directly compare the differential effects of increasing stimulus size on hue perception, Figures 3.5 and 3.6 compare hue-naming functions obtained for different stimulus sizes with the two peripheral fixation conditions. Figure 3.5 depicts hue-scaling functions obtained with the 1.0° (solid lines), 2.25° (dotted lines), and 3.7° (dashed lines) stimuli from the binocular left fixation condition (left column), left monocular temporal condition (center column), and right monocular nasal condition (right column). The monocular left temporal and monocular right nasal conditions are shown with the binocular left fixation condition because the binocular left fixation condition resulted in stimuli falling on the *left* temporal and *right* nasal retinas. Juxtaposing these specific conditions in this way allows for investigation of which monocular peripheral condition resulted in hue and saturation perceptions similar to that of the binocular fixation condition.

The upper left panel of Figure 3.5 shows that for the binocular left fixation condition, a lower percentage of blue was perceived from 450-470 nm for the 1.0° stimulus (solid line) than for the 2.25° (dotted line) and 3.7° (dashed line) stimuli. The binocular left fixation green function shows a similar pattern: a lower percentage of green was perceived for the 1.0° stimulus for wavelengths from 480-520 nm, but the green functions for the 2.25° and 3.7° stimuli are virtually the same (center left panel). Likewise, for saturation, the 1.0° stimulus was

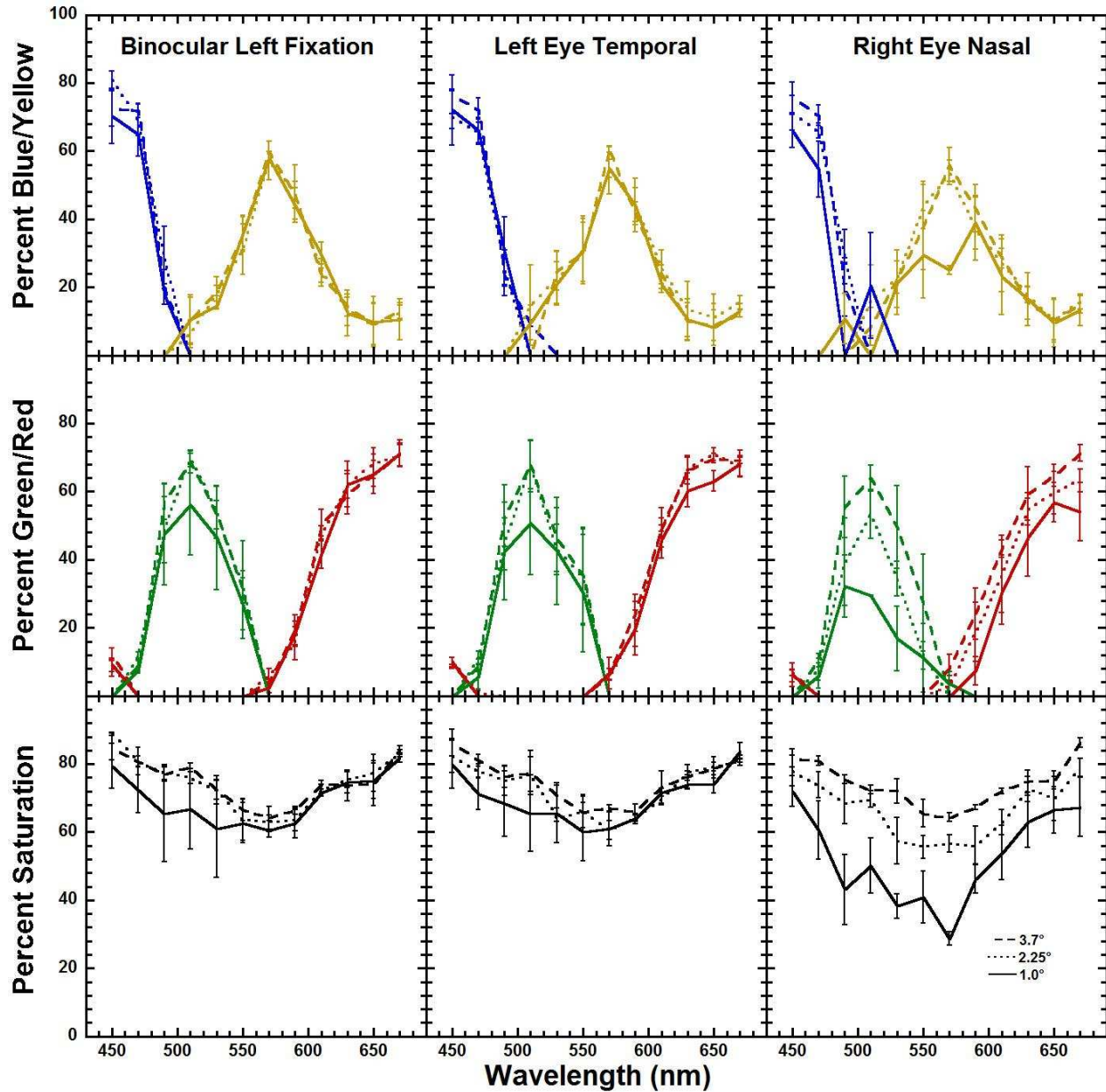


Figure 3.5. Mean percent blue or yellow (top row), green or red (middle row), and saturation (bottom row) are plotted as a function of wavelength for the binocular left fixation (temporal retina of the left eye, nasal retina of the right eye; left column), monocular left temporal (center column), and monocular right nasal (right column) viewing conditions. Solid, dotted, and dashed lines indicate the 1.0°, 2.25°, and 3.7° stimulus sizes, respectively.

perceived as less saturated for wavelengths between 450 and 550 nm, but percentage of saturation shows little change after the stimulus reaches 2.25° (lower left panel). Results for the left eye monocular temporal condition (center column) are nearly identical to those of the binocular left fixation condition, with the 1.0° stimulus showing a lower percentage of blue

(upper center panel), green (center panel), and saturation (lower center panel) than the 2.25° and the 3.7° stimuli at the same wavelengths as in the binocular left fixation condition. The only difference between the left monocular temporal condition and the binocular left fixation condition appears to be in the red function: for the left monocular temporal condition, the 1.0° red function shows a smaller percentage of red for wavelengths from 630-670 nm (center panel), whereas no such difference appears in the binocular left fixation condition.

As the right column of Figure 3.5 shows, the hue and saturation functions for the right nasal retina indicate that the 1.0° and 2.25° stimuli were perceived as having a lower percentage of saturation, and having smaller percentages of each hue, than the 3.7° stimuli. This is not seen for the binocular left fixation or left monocular temporal condition. A lower percentage of blue was perceived at all wavelengths in the right eye nasal condition (upper right panel) for the 1.0°, and from approximately 450-470 nm for the 2.25°, as compared to the 3.7° stimulus. The peak of the yellow function for the 1.0° stimulus is also much lower, with the percentage of yellow for the 1.0° stimulus less than that for the other two stimulus sizes from approximately 500-590 nm. A smaller percentage of green was perceived in the left nasal retina from 490-570 nm, and a smaller percentage of red from 570-670 nm, for the 1.0° and 2.25° stimuli relative to the 3.7° stimulus (center right panel), with the percent hues for the 1.0° stimulus being even smaller than those for the 2.25° stimulus. The 1.0° and 2.25° stimuli appeared less saturated in the right nasal retina for all wavelengths compared to the binocular left fixation and left monocular temporal conditions. The implication is that hue and saturation perception for small stimuli suffer more in the right nasal retina than the left temporal retina, or when viewed binocularly with both eyes looking to the left. Additionally, the strong resemblance between the binocular left fixation and

the left monocular temporal functions indicate that binocular peripheral hue and saturation perception is dominated by the temporal retina, at least for small stimuli.

Figure 3.6 presents the same comparisons between stimulus sizes, but for the binocular right fixation condition (left column), the right monocular temporal condition (center column), and the left monocular nasal condition (right column). Again, the right monocular temporal and left monocular nasal conditions are compared to the binocular right fixation condition as in the binocular right fixation condition, the stimulus falls on the *right* temporal, *left* nasal retinas. For the right binocular fixation condition, the findings are nearly identical to the left binocular fixation condition: the 1.0° stimulus was perceived as a lower percentage of blue for wavelengths from 450-470 nm (upper left panel), a lower percentage of green for wavelengths from 480-520 nm (left center panel), and a lower percentage of saturation for wavelengths from 450-550 nm (lower left panel). One difference for the binocular right fixation condition is that the 1.0° stimulus was also perceived as having a smaller percentage of red than the 2.25° or 3.7° stimuli for wavelengths from 630-670 nm (left center panel). The right monocular temporal retina shows similar results to the right binocular fixation condition, except that the 1.0° stimulus appeared to have a lower percentage of yellow for wavelengths from 550-590 nm, as compared to the 2.25° and 3.7° stimuli presented to the right monocular temporal retina (top center panel), and also to the 1.0° stimulus for the binocular right fixation condition (upper left panel). A lower percentage of green was perceived for the right monocular temporal retina with the 2.25° and 3.7° stimulus sizes from 490-550nm than the corresponding stimulus sizes for the binocular right fixation condition, but a higher percentage of green was perceived for the 1.0° stimulus relative to the binocular right fixation 1.0° stimulus for wavelengths from 480-510 nm (compare the center panel to the left center panel).

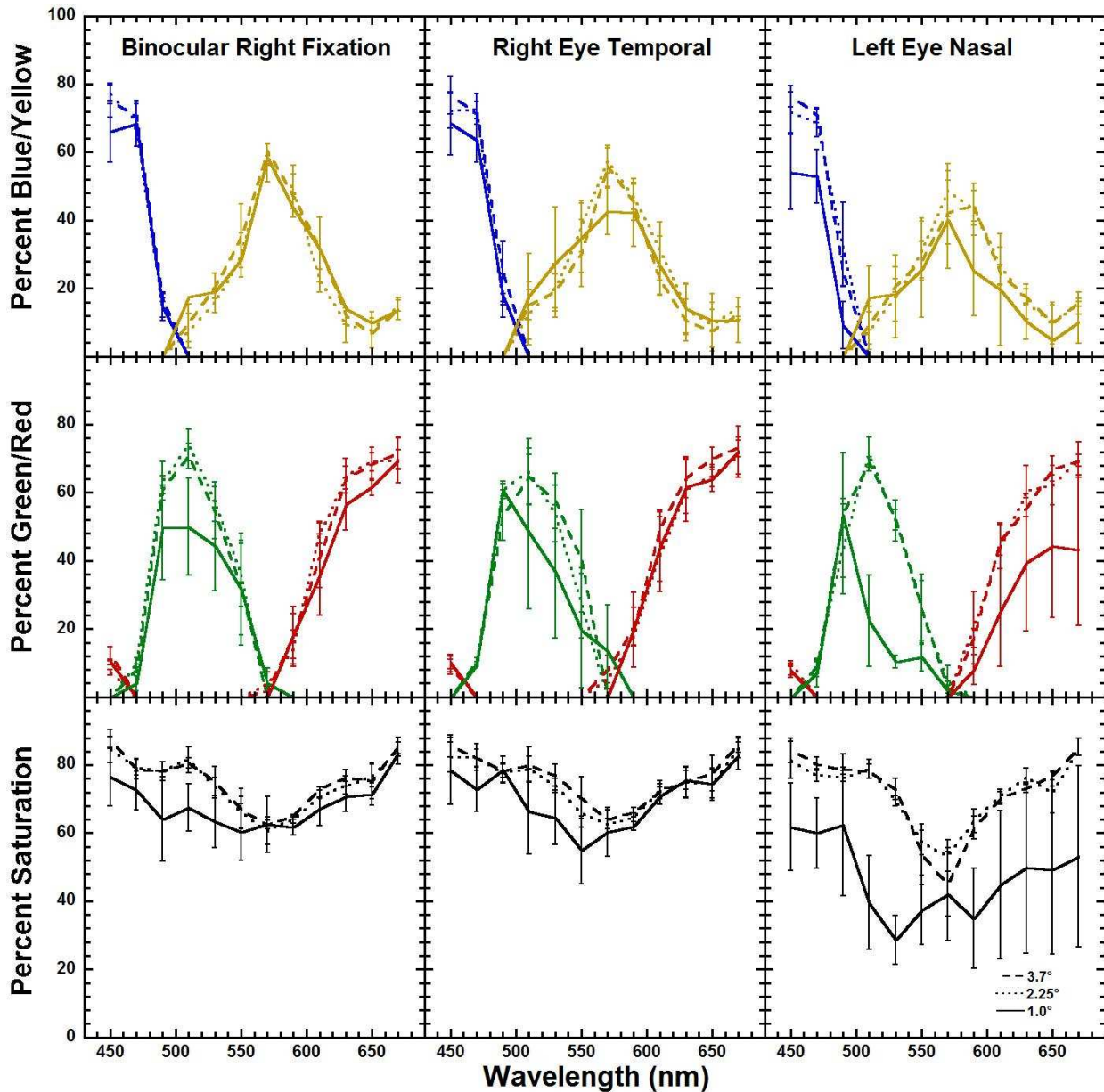


Figure 3.6. Mean percent blue or yellow (top row), green or red (middle row), and saturation (bottom row) is plotted as a function of wavelength for the binocular right fixation (temporal retina of the **right** eye, **nasal** retina of the **left** eye; left column), monocular right temporal (center column), and monocular left nasal (right column) viewing conditions. Solid, dotted, and dashed lines indicate the 1.0°, 2.25°, and 3.7° stimulus sizes, respectively.

The 1.0° stimulus functions for the left monocular nasal retina (Figure 3.6, left column) are similar to those for the right monocular nasal retina (Figure 3.5, right column): hue and saturation perception are compromised with the smallest stimulus size. For the left monocular nasal condition, however, the yellow function shows that a lower percentage of yellow was

perceived in the left nasal retina for wavelengths between 570 and 670 nm (although a greater percentage of yellow was perceived at 510 nm; upper right panel) for the 1° stimulus, which is not seen for the other stimulus sizes. Notable here is that for the left monocular nasal retina, although percentages of green, red, and saturation for the 1° stimulus are smaller than those for the 3.7° stimulus, by the time the stimulus reaches 2.25°, all hue-scaling functions are nearly equivalent to those for the 3.7° stimulus. This was not seen in the hue response functions for the right nasal retina, where smaller percentages of green, red, and saturation were perceived for the 2.25° relative to the 3.7° stimulus [refer back to Figure 3.5 (center right and lower right panels)]. It is possible that this is a result of the observers' right-eye dominance.

We can also see in Figure 3.6 that the right monocular temporal functions are more similar to the binocular right fixation functions, as the left monocular temporal functions are more similar to the binocular left fixation functions (Figure 3.5, left and center columns). This again seems to imply that binocular peripheral perception for smaller stimuli is dominated by the temporal retina; however, as noted above, there are differences between the binocular right fixation and right temporal condition that are not evident in the analogous left conditions. For example, the 1.0° stimulus was perceived as having a higher percentage of green for wavelengths from approximately 480-510 nm in the monocular right temporal condition than in the binocular right fixation condition (Figure 3.6, middle row, center and left panels), whereas in the analogous left conditions, there is little to no difference between the percentage of green perceived in this range (Figure 3.5, middle row, center and left panels). In the monocular right temporal condition, the 1.0° stimulus was perceived as more saturated than in the binocular right fixation condition for wavelengths from 470-510 nm, but less saturated for wavelengths from 550-600 nm (Figure 3.6, bottom row, center and left panels), which is also not seen for the binocular left

fixation and monocular left temporal conditions (Figure 3.5, bottom row, center and left panels). This may imply that there is an interaction between the location of the retina to which a stimulus is presented and eye dominance, as it appears monocular signals are combined differently based on whether the temporal retina is that of the dominant or non-dominant eye.

Binocular vs. Mean Monocular Perception. There are a number of possible ways that input to each individual eye might combine to yield a binocular percept. One of these possibilities is that the signals from each of the individual retinas could average together in the visual pathway, thus each contributing equally to binocular perception. For example, in the binocular left fixation condition, the stimulus falls on the temporal retina of the left eye and the nasal retina of the right eye. In order to test whether hue perception for the binocular left fixation condition is simply the average of the two monocular perceptions, the mean of the left monocular temporal and the right monocular nasal hue-scaling data for each stimulus size was calculated. The resulting mean monocular hue and saturation functions were then compared with the corresponding hue and saturation functions from the binocular left fixation condition for each stimulus size. The same procedure was conducted with the monocular right eye temporal and left eye nasal hue-scaling data to investigate whether the mean of these two conditions would resemble the hue-scaling data for the binocular right fixation condition.

Figure 3.7 compares the mean hue-naming function (dashed line) computed from the appropriate monocular conditions (left-temporal monocular, right-nasal monocular) to the binocular left fixation hue-naming functions (solid lines) for each stimulus size (columns). The two functions for the 1.0° stimulus differ from each other in each of the three panels. In general, percent blue, yellow, green, red, and saturation were less in the monocular conditions from 450-490 nm, 550-600 nm, 490-550 nm, 630-670 nm and 450 to 670, respectively. By 1.7°, the mean

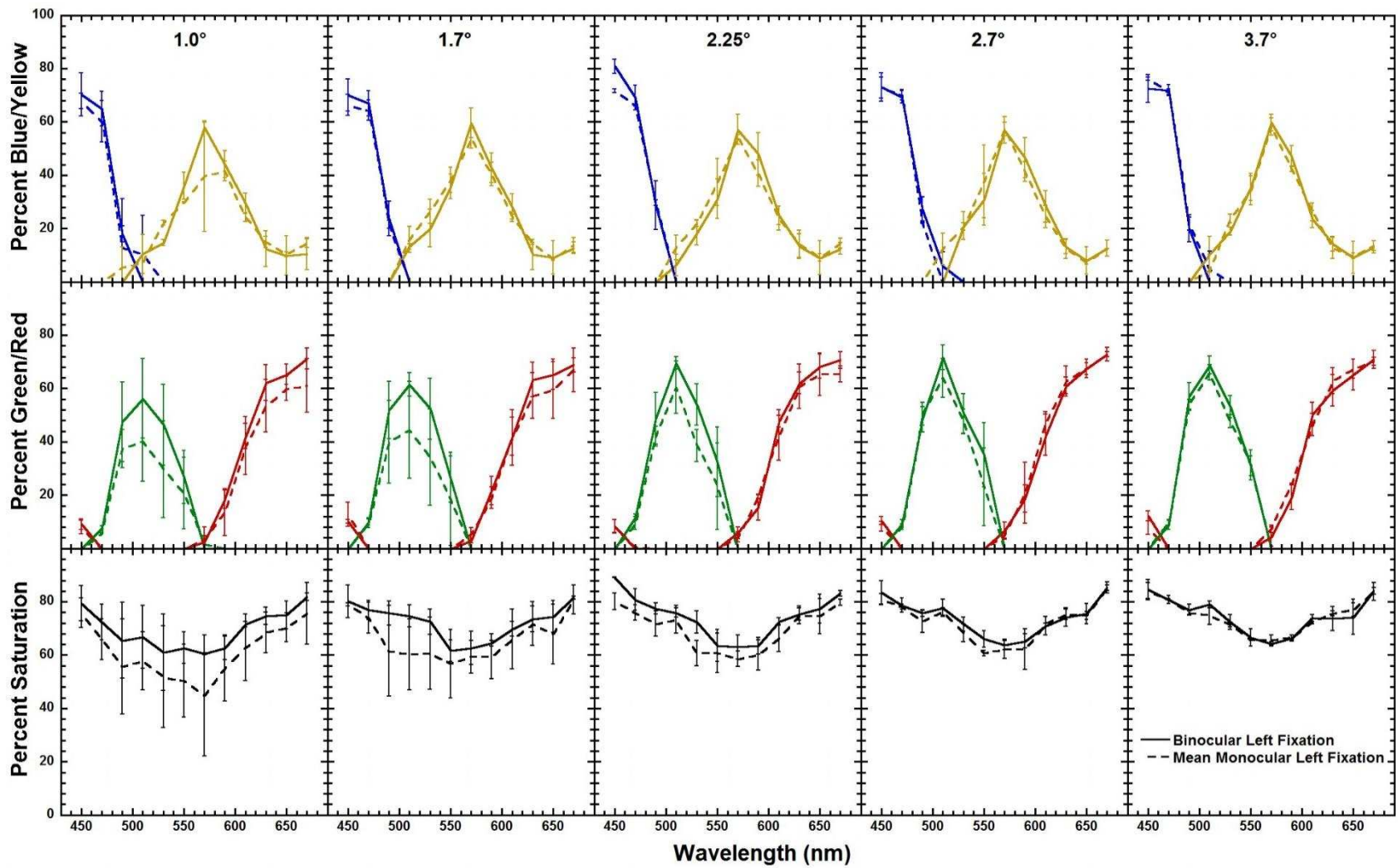


Figure 3.7. Mean percent blue or yellow (top row), green or red (middle row), and saturation (bottom row) is plotted as a function of wavelength for the binocular left fixation condition (stimulus falling on the **temporal** retina of the **left** and **nasal** retina of the **right** eye), and the mean of the data for the monocular left temporal and right nasal conditions. Solid lines represent the binocular left fixation condition and dashed lines depict the mean of the left temporal and right nasal conditions. Columns present results for stimuli of different sizes.

left monocular blue, yellow, and red functions are similar to their respective binocular functions (second column, top and center panels). Differences between the green and saturation functions abate with the 2.25° stimulus (third column, center and bottom panels), and by 3.7° little difference remains between the two functions (last column).

Depicted in Figure 3.8 is the comparison between the binocular right fixation condition (solid lines) and the mean monocular function (right-temporal monocular and left-nasal monocular conditions; dashed lines). A similar trend to that in Figure 3.7 is visible: mean monocular percentages for the 1.0° stimulus are less for each hue and saturation relative to the binocular right fixation functions (first column), but these differences abate as stimulus size increases. For the mean monocular and the binocular right fixation data, however, there remain some differences even at the largest stimulus size that were not observed in Figure 3.7. In Figure 3.8, the peak of the mean monocular yellow function is lower than that of the binocular right fixation function (top row), there is a smaller percent green perceived from 490-510 nm for the mean monocular data (center row), and the mean monocular data show less saturation from 530-600 nm than the binocular right fixation data (bottom row).

The mean monocular foveal hue-scaling functions are compared to the binocular foveal functions in Figure 3.9. Although the two functions in each panel are quite similar, there are some differences; namely, the peak of the mean monocular green function is higher, and the saturation minimum for the mean monocular condition is slightly lower and slightly shifted toward longer wavelengths. Thus it appears that although averaging across monocular retinal locations cannot be ruled out for the larger stimulus sizes, binocular color vision for smaller stimuli in the peripheral retina is not determined by simply averaging across the two individual retinal locations.

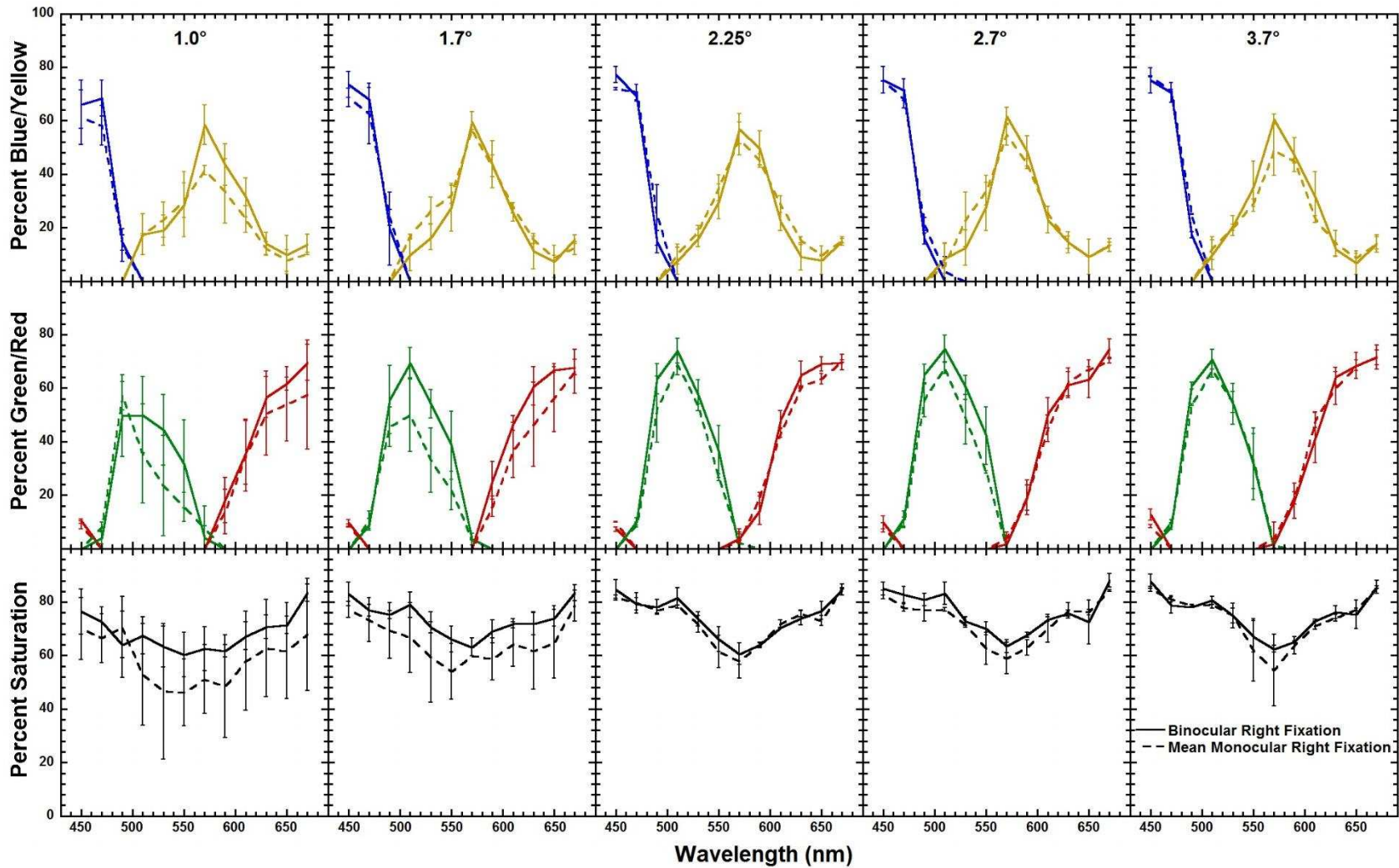


Figure 3.8. Mean percent blue or yellow (top row), green or red (middle row), and saturation (bottom row) is plotted as a function of wavelength for the binocular right fixation condition (stimulus falling on the temporal retina of the right and nasal retina of the left eye), and the mean of the data for the monocular right temporal and left nasal conditions. Solid lines represent the binocular right fixation condition and dashed lines depict the mean of the right temporal and left nasal conditions. Columns present results for stimuli of different sizes.

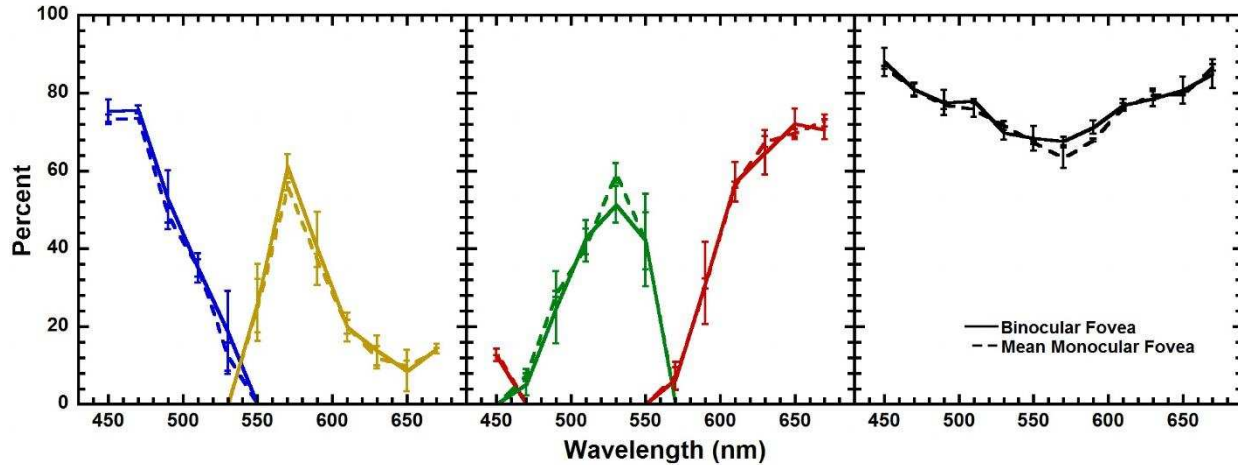


Figure 3.9. Mean percent hue or saturation is specified as a function of wavelength for binocular foveal (solid lines), and mean monocular left and right foveal (dashed lines) viewing conditions. The left panel presents hue-scaling results for blue and yellow, the center panel for green and red, and the right panel for saturation. Within the left two panels, a particular hue is indicated by line color.

Hue Perception Summary. Generally, the results are in keeping with previous color-perception research (e. g., Abramov et al., 1991; Gordon & Abramov, 1977; Parry, McKeefry, & Murray, 2006; Volbrecht et al., 2009), indicating that both monocular and binocular peripheral hue and saturation perception become more “fovealike” (i. e., percent hue increases) as stimulus size in the periphery increases, although differences between the periphery and fovea remain for blue, yellow, and green (see Figures 3.1-3.4). The results also indicate that there are differences between monocular peripheral and binocular peripheral color perception at smaller stimulus sizes that cannot be explained by simply averaging the monocular responses. It seems that, rather than averaging monocular hue percepts, peripheral binocular hue perception for smaller stimulus sizes is dominated by the temporal retina, regardless of eye dominance. Eye dominance does not appear to play a significant role in binocular color perception, although it may have some subtle influence on hue and saturation perception for smaller stimuli.

Perceptive Field Sizes

In order to determine the stimulus size at which hue perception stabilized, perceptive field sizes were determined. The grand means across observers for each scaled and transformed hue term were plotted as a function of stimulus size for each fixation condition and wavelength, provided that they met three criteria: 1) data for a given hue term were available at each wavelength from at least two of the three observers; 2) the grand mean across observers was greater than the standard error of the mean computed across stimulus sizes; and 3) each observer specified a percentage greater than zero for that hue term at all stimulus sizes (Abramov et al., 1991; Pitts et al., 2005; Troup et al., 2005; Volbrecht et al., 2009). As shown in Figure 3.10, a Michaelis-Menten growth function was then fitted to the data using two parameters defined as k and g . The percent value associated with g defines the value associated with the asymptote of the function and k is the stimulus size associated with 50% of the asymptotic percent value. In accordance with Abramov et al. (1991), the perceptive field size was defined as the stimulus size ($3k$) associated with 75% of the asymptotic value of the growth function. Values for the two parameters were determined for each hue term used at each wavelength and for each fixation condition that met the criteria listed above. Values for k , g , and R are listed in Tables 3.2, 3.3, and 3.4, respectively. Note that some k values were negative, which simply indicates an inverse growth, or decay, function. Negative k values have also been reported by others (e. g., Abramov et al., 1991; Pitts et al., 2005; Volbrecht et al., 2009).

Figure 3.11 depicts mean k values as a function of wavelength for each fixation condition for each hue term. Similar to Abramov et al. (1991), the results of the current study indicate that k varies with wavelength to some degree for all hues in all fixation conditions, but variability with wavelength is highest for green (Figure 3.11, second row). For the remaining hue terms,

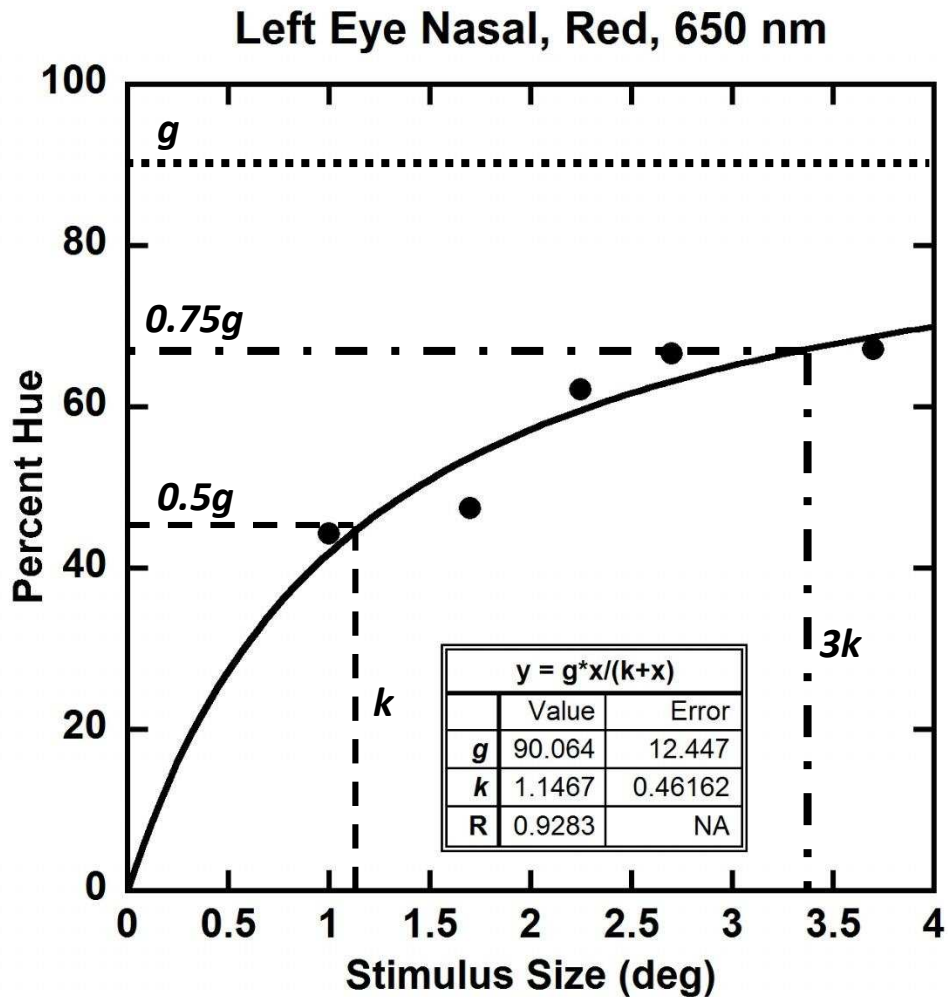


Figure 3.10. Percent red is plotted as a function of stimulus size for a 650-nm stimulus from the monocular left eye, right fixation viewing condition. The solid curve is the Michaelis-Menten function fitted to the data points. The two parameters used to fit the function to the data are k and g (equation specified in the table). The inset table lists the equation for the function, as well as the g , k , and R values for this particular function.

variability appears comparable across viewing conditions, although in some instances there is a single wavelength whose k value differed notably from the others (e. g., blue at 500 nm for the right eye nasal condition, top row, fourth panel).

Both monocular nasal viewing conditions (Figure 3.11, fourth and fifth columns) exhibit the largest variability of k with wavelength relative to the other viewing conditions. The two monocular nasal conditions are, in fact, more similar to one another than they are to any of the other viewing conditions. The two binocular (Figure 3.11, first two columns) and the two

Table 3.2
Mean k Values for All Fixation Conditions

λ	Blue	Green	Yellow	Red
Binocular Left Fixation				
450	0.089			0.397
470	0.147	0.291		
490	0.382	0.182		
510		0.412	-0.183	
530		0.191	0.448	
550		0.419	-0.117	
570			0.004	1.238
590			0.122	-0.030
610			-0.193	0.234
630			0.276	-0.047
650			-0.172	0.031
670			0.329	0.010

Left Eye Left Fixation				
450	0.169			-0.164
470	0.137	0.519		
490	-0.079	0.341		
510		0.621	-0.643	
530		0.155	-0.021	
550		0.264	-0.030	
570			0.148	-0.143
590			-0.100	0.496
610			-0.163	0.107
630			-0.352	0.195
650			-0.363	0.165
670			-0.278	0.026

Right Eye Left Fixation				
450	0.184			0.140
470	0.466	1.303		
490	3.315	2.623		
510		4.487	-0.954	
530		16.635	0.002	
550		**	0.538	
570			1.693	**
590			0.176	4.953
610			0.393	0.818
630			-0.055	0.459
650			0.023	0.281
670			0.077	0.570

λ	Blue	Green	Yellow	Red
Binocular Right Fixation				
450	0.211			0.126
470	0.054	1.375		
490	0.142	0.432		
510		0.648	-0.621	
530		0.404	-0.135	
550		0.151	0.249	
570			0.049	
590			0.175	-0.087
610			-0.213	0.336
630			-0.185	0.186
650			-0.286	0.126
670			0.007	0.067

Left Eye Right Fixation				
450	0.647			-0.008
470	0.581	0.233		
490	0.174	1.662		
510		4.542	-0.661	
530		10.268	-0.345	
550		2.958	0.118	
570			0.189	
590			0.849	1.478
610			0.289	1.874
630			0.954	1.109
650			0.756	1.147
670			0.852	1.009

Right Eye Right Fixation				
450	0.168			-0.091
470	0.141	0.276		
490	0.278	-0.078		
510		0.551	-0.322	
530		0.883	-0.232	
550		2.391	-0.045	
570			0.290	
590			0.081	0.100
610			-0.094	0.158
630			-0.189	0.087
650			-0.261	0.116
670			0.432	0.002

** Indicates the software was not able to generate a value as the function did not reach an asymptote.

Table 3.3
Mean g Values for All Fixation Conditions

λ	Blue	Green	Yellow	Red
Binocular Left Fixation				
450	76.80			12.08
470	73.76	10.87		
490	28.25	55.56		
510		79.44	9.00	
530		56.42	23.00	
550		36.74	31.72	
570			58.46	7.55
590			48.68	18.36
610			23.98	50.45
630			14.51	60.65
650			8.18	67.42
670			14.41	71.28

λ	Blue	Green	Yellow	Red
Binocular Right Fixation				
450	81.56			10.56
470	71.48	14.41		
490	17.62	72.11		
510		90.00	6.57	
530		65.29	15.76	
550		38.94	33.78	
570			61.01	
590			50.84	18.07
610			23.46	52.47
630			10.95	67.58
650			6.88	70.26
670			14.41	73.23

Left Eye Temporal				
450	77.91			9.57
470	73.51	11.24		
490	23.80	57.55		
510		82.27	5.48	
530		49.58	22.15	
550		37.49	30.44	
570			61.56	5.75
590			40.16	28.76
610			21.23	51.57
630			9.213	71.76
650			6.985	73.89
670			11.04	70.90

Left Eye Nasal				
450	91.82			8.34
470	83.93	10.19		
490	27.51	78.94		
510		171.20	6.07	
530		223.96	16.47	
550		51.47	32.67	
570			51.13	
590			58.81	26.47
610			28.54	71.26
630			22.61	77.31
650			11.96	90.06
670			20.00	93.89

Right Eye Nasal				
450	77.16			8.15
470	79.64	13.60		
490	48.28	91.02		
510		146.61	8.79	
530		282.93	23.69	
550		**	51.09	
570			88.41	**
590			43.87	52.16
610			31.22	53.28
630			15.41	66.96
650			9.40	68.52
670			15.06	83.37

Right Eye Temporal				
450	79.01			8.81
470	73.93	11.26		
490	24.07	54.79		
510		78.22	12.05	
530		66.70	22.23	
550		61.08	34.47	
570			61.97	
590			46.54	20.83
610			24.91	49.61
630			11.83	64.94
650			7.89	70.43
670			15.15	71.86

** Indicates the software was not able to generate a value as the function did not reach an asymptote.

Table 3.4

Range and Mean of R Values for Each Hue Term for Each Fixation Condition

<u>Binocular L Fix</u>	Blue	Green	Yellow	Red
Range	0.399 – 0.958	0.465 – 0.915	0.050 – 0.939	0.074 – 0.642
Mean	0.611	0.697	0.564	0.397
<u>Binocular R Fix</u>				
Range	0.292 – 0.897	0.325 – 0.885	0.034 – 0.946	0.132 – 0.877
Mean	0.621	0.729	0.473	0.490
<u>L Eye Temporal</u>				
Range	0.173 – 0.802	0.447 – 0.942	0.070 – 0.863	0.195 – 0.979
Mean	0.513	0.709	0.586	0.614
<u>L Eye Nasal</u>				
Range	0.121 – 0.983	0.293 – 0.962	0.223 – 0.920	0.016 – 0.942
Mean	0.694	0.777	0.671	0.724
<u>R Eye Nasal</u>				
Range	0.667 – 0.995	0.807 – 0.968	0.005 – 0.925	0.169 – 0.976
Mean	0.849	0.905	0.481	0.756
<u>R Eye Temporal</u>				
Range	0.332 – 0.944	0.279 – 0.939	0.152 – 0.836	0.035 – 0.811
Mean	0.639	0.706	0.544	0.402

monocular temporal conditions (Figure 3.11, third and last columns) are fairly similar to one another with k values remaining relatively stable across wavelength.

Perceptive field sizes for a particular hue term were determined by taking the mean of the non-negative $3k$ values across the wavelengths where a given hue term was used (Abramov et al., 1991; Volbrecht et al., 2009). In Figure 3.12, perceptive field sizes are shown for each hue term within a fixation condition. Please note that the y-axis scale for both monocular nasal conditions (Figure 3.12, bottom row) differs from the other panels. It is quite evident from this set of graphs that the perceptive fields for both right and left nasal retina are notably larger than those for the other fixation conditions, whereas perceptive field sizes for both binocular (Figure 3.12, top row) and monocular temporal viewing conditions (Figure 3.12, middle row) more closely resemble one another. Of particular interest is the fact that the perceptive field for green

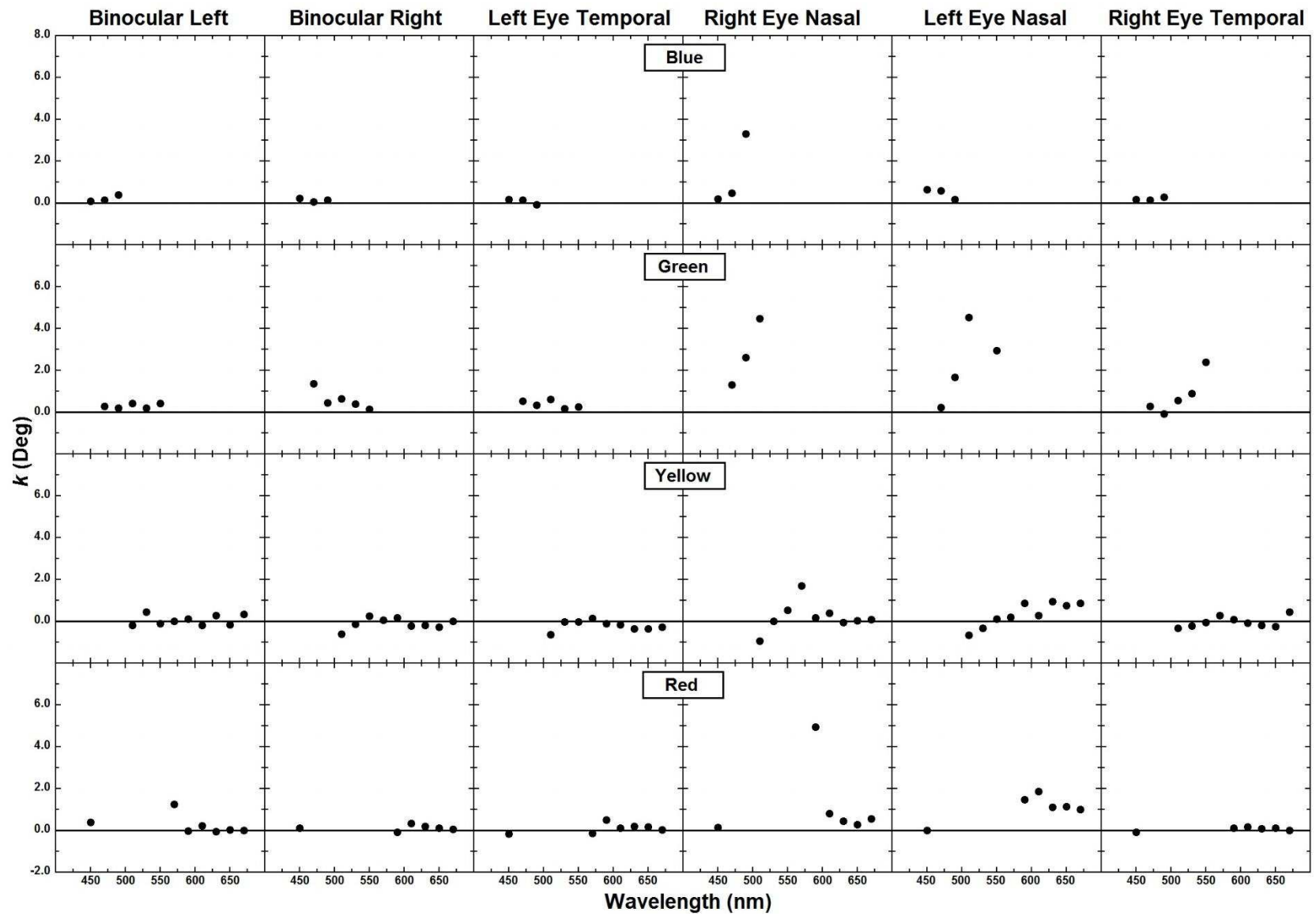


Figure 3.11. k values derived from mean hue-scaling data are graphed as a function of wavelength for each fixation condition (columns) for each hue term (rows).

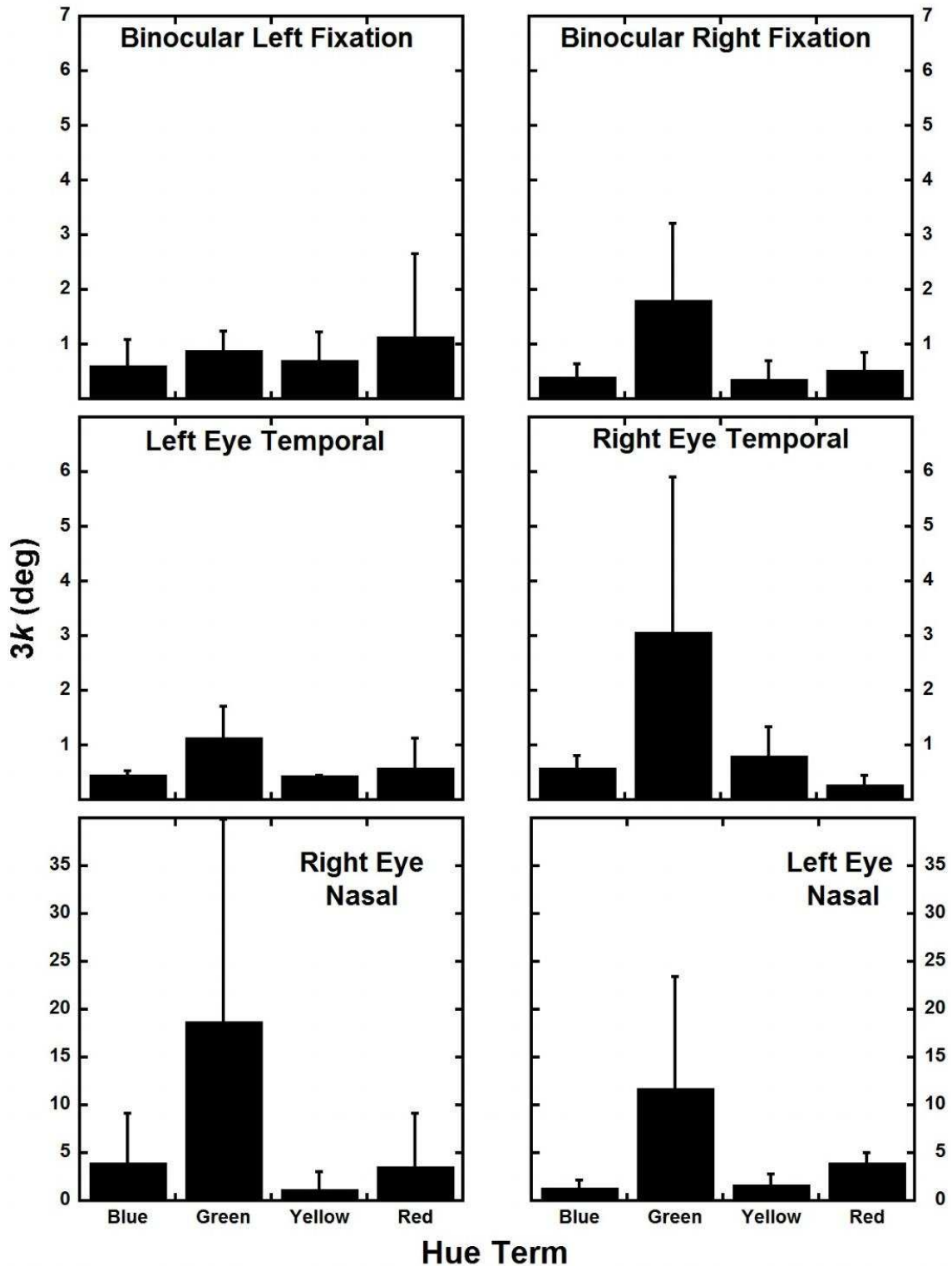


Figure 3.12. $3k$ values specified as a function of hue term for each peripheral fixation condition. $3k$ values were derived from taking the mean of the non-negative $3k$ values across all wavelengths where a given hue term was used. Note that the y-axis scale for the nasal conditions differs from the binocular and temporal conditions. Error bars depict 1 standard error of the mean (SEM).

in the monocular right temporal condition (Figure 3.12, right column, middle panel) is larger than that for the monocular left temporal condition (Figure 3.12, left column, middle panel), and this difference is reflected in the binocular functions: correspondingly, the perceptive field for green in the binocular right fixation condition (Figure 3.12, right column, top panel) is larger than that for the binocular left fixation condition (Figure 3.12, left column, top panel). In general, perceptive fields for green are larger than those for any other hue.

Also visible in Figure 3.12 is that, although there are some hue terms whose perceptive fields are more similar in size to one another than they are to those of other hues (e. g., blue and yellow in the left eye temporal condition; Figure 3.12, left column, center panel), overall the perceptive field sizes differ for all four elemental hue terms. In particular, perceptive field sizes for red and green are quite different for nearly all viewing conditions. This is interesting in light of the fact that perception of red and green are generally considered to be governed by a single opponent-color process. Gordon and Abramov (1977) suggest that hue perceptions governed by a single underlying process should have relatively similar perceptive field sizes. That this does not appear to be the case with red and green raises the possibility that each is governed by a separate process.

Perceptive Field Sizes Summary. The results indicate that perceptive field sizes are largest for green, which is in accordance with previous findings (e. g., Abramov et al., 1991; Volbrecht et al., 2009). For the monocular conditions, perceptive fields in the nasal retina tend to be larger than those in the temporal retina, whereas the monocular temporal perceptive fields tend to be more similar in size to one another. As with the hue-scaling data, it again appears that peripheral binocular hue perception is influenced more heavily by the temporal retina, as

perceptive field sizes for the binocular fixation conditions are similar to those for the monocular temporal conditions, whereas the monocular nasal perceptive fields are, in general, much larger.

CHAPTER 4

DISCUSSION

Hue Scaling

Fovea vs. Periphery. In general, the results regarding differences in hue perception between the foveal and peripheral retina are fairly consistent with previous findings (e. g., Gordon & Abramov, 1977; McKeefry et al., 2007; Moreland & Cruz, 1959; Nerger et al., 1995; Parry et al., 2006; Volbrecht et al., 2009), with some differences noted below.

Blue. Contrary to the current study, where the blue response function narrowed with retinal eccentricity, Buck, Knight, Fowler, and Hunt (1998) and Gordon and Abramov (1977) found that the range of wavelengths associated with the perception of blue expands with increasing retinal eccentricity. The difference may be related to differences in stimulus parameters between these experiments and the current study. Buck et al. (1998) used an 8°-diameter stimulus, more than twice the size of the largest stimulus used in the current experiment, at different luminance levels: 1.0 and 3.5 log scotopic td. The relationship of scotopic to photopic td varies with wavelength, so stimuli for the current study ranged from 2.65 log scotopic td for 450-nm stimuli to -0.76 log scotopic td for 670-nm stimuli. Gordon and Abramov (1977) not only used a larger peripheral stimulus (6.5°, as compared to the current study's largest peripheral stimulus at 3.7°), they sampled the fovea and 45° retinal eccentricity, whereas the current study investigated only the fovea and 10° retina eccentricity. Gordon and Abramov also used a substantially higher luminance level, 1200 photopic td. Differing stimulus size, retinal eccentricity, and retinal illuminance may contribute to these differences.

Yellow. As the range of wavelengths spanned by the blue function narrowed in the peripheral viewing conditions, the range of wavelengths spanned by the yellow function increased, with the yellow function expanding to shorter wavelengths in the peripheral viewing conditions (top row, Figures 3.2-3.4). The peaks of the yellow functions for the peripheral and foveal conditions appear to be at 570 nm for both left and right monocular (Figures 3.2 and 3.3) and binocular (Figure 3.4) viewing conditions, which differs from Buck, Knight, and Bechtold's (2000) findings that peripheral yellow should shift toward longer wavelengths to compensate for blueness added by rod contributions. Again, however, Buck et al.'s stimulus parameters differed from those used in the current experiment: with a 2°-diameter stimulus, their foveal stimulus was twice the size of that used in the current experiment, and their large extrafoveal stimulus was twice as large (7.4° vs. 3.7°) as that in the current experiment). As noted above, their retinal illuminance levels were again different than those of the current study.

Green. The hue for which there were notable differences between the peripheral and foveal viewing conditions, and which exhibited the most variation with increasing stimulus size, was green. The peaks of the monocular temporal and nasal green functions were shifted toward shorter wavelengths relative to the fovea, and smaller stimuli presented to the nasal retina were reported as having a lower percentage of green than those presented to the temporal retina or the fovea (center row, Figures 3.2 and 3.3). Gordon and Abramov (1977) also found that observers reported a reduction in the percent green in the peripheral retina relative to the fovea. It is worth noting in the current study this latter observation is present only for the smaller stimulus sizes in the monocular conditions (Figures 3.2 and 3.3), and not the binocular conditions (Figure 3.4). The percentage at the peak of the peripheral green functions with the larger stimuli is higher than the percentage at the peak of the green function in the fovea, indicating that stimulus size has an

effect on the perception of green in the peripheral retina. As the peak of the green function may represent a unique green, i. e., a green that appears neither bluish nor yellowish and is therefore the purest perceptual green, the fact that the current study found the peaks of the peripheral monocular green functions to be shifted toward shorter wavelengths may relate to findings by Moreland and Cruz (1959) that at 10° retinal eccentricity, unique green shifts toward green-blue (i. e., toward shorter wavelengths). Nerger et al. (1995) also found that unique green shifted toward shorter wavelengths in the periphery relative to the fovea. Others (e. g., Buck et al., 2000; Parry et al., 2006; Stabell & Stabell, 1979), however, have shown the opposite, whereby the green function is shifted toward longer wavelengths.

Buck et al. attributed this shift toward longer wavelengths to an additive influence of rod signals on the perception of peripheral blue: in order to compensate for the blueness added by the rods, the locus of unique green shifts toward yellow. It is possible that differences in stimulus size and retinal eccentricity may also explain this discrepancy; the studies that found green shifted toward longer wavelengths tended to use larger stimuli (Buck et al., 2000; Parry et al., 2006), greater retinal eccentricities (Parry et al., 2006; Stabell & Stabell, 1979), and/or a different range of stimulus luminances from those used in the present study (Buck et al., 2000; Stabell & Stabell, 1979).

Red. The perception of red has been found to remain relatively steady across the retina (Gordon & Abramov, 1977). The current study did find a decrease in the perception of red in the periphery relative to the fovea for the smaller stimuli (center row, Figures 3.2-3.4), which is similar to Abramov et al.'s (1991) findings. There appears to be less information regarding how, and why, red changes with retinal eccentricity and stimulus size in the literature, perhaps because the changes for red are less consistent and of a smaller magnitude than those seen for the other

elemental hues. Volbrecht et al. (2011) found that observers' ability to discriminate long-wavelength stimuli decreased as they dark adapted and rod input to the retina increased, which implies that rod signals are inhibiting cone signals. Rod inhibition of cone signals has been previously demonstrated by others (e. g., Frumkes & Eysteinnsson, 1988; Lange, Denny, & Frumkes, 1997), and could explain why, in the current experiment, the stimuli presented to the peripheral retina, which has a greater population of rods compared to the fovea (Curcio et al., 1990), were reported as having lower percentages of red than those presented to the fovea. Additionally, rod inhibition of chromatic signals is greater for smaller stimuli (Stabell & Stabell, 1999), which is consistent with the reduced hue perception for smaller stimuli found in the current study (see Figures 3.2-3.4)

Saturation. The current study found that small stimuli presented to the periphery were perceived as less saturated than larger stimuli in the periphery or stimuli presented to the fovea (bottom row, Figures 3.2-3.4). This was particularly pronounced in the nasal retina for the monocular conditions. The relative desaturation of peripheral stimuli, particularly at smaller stimulus sizes, is consistent with findings from previous studies (e. g., Abramov et al., 1991; Gordon & Abramov, 1977; McKeefry et al., 2007). Moreland and Cruz (1959) found that the degree to which perceived saturation decreased in the periphery varied with wavelength, with wavelengths in the short-to-medium range (approximately 420-550 nm) exhibiting a greater degree of desaturation, and peripherally-presented wavelengths longer than 550 nm actually appearing more saturated than in the fovea. Opper et al. (2014) reported similar findings for a hue-scaling study, showing that stimuli reported as green-yellow, and occasionally stimuli described as yellow-red, were perceived as being more saturated in the periphery than the fovea, although other studies have not found this supersaturation in the periphery (e. g., Abramov et al.,

1991; Gordon & Abramov, 1977; McKeefry et al., 2007). In the binocular conditions, the difference in saturation between the fovea and the periphery was much smaller (bottom row, Figure 3.4), and the current study did find some supersaturation in the left temporal retina between 560 and 580 nm for the largest stimulus size (see Figure 3.2, bottom right panel).

As previously mentioned, in the binocular peripheral conditions, the stimulus fell on the temporal retina of one eye and the nasal retina of the other. Because perceived saturation was greater for smaller stimuli in the monocular temporal conditions as compared to the monocular nasal conditions, and previous research has shown differences in saturation for stimuli viewed temporally vs. nasally (e. g., Abramov et al., 1991; Volbrecht & Nerger, 2012), it is unknown how the two individual retinal areas contribute to binocular saturation perception. Saturation in the binocular peripheral fixation conditions more closely resembled that of the corresponding monocular temporal retina (see bottom rows of Figures 3.5 and 3.6). The temporal retina thus appears to make a larger contribution toward binocular perception of saturation for smaller stimuli in the periphery than does the nasal retina (bottom row, Figures 3.5-3.6).

Possible physiological underpinnings. A number of previous studies (e. g., Buck et al., 2006; McKeefry et al., 2007; Nerger et al., 1995; Stabell & Stabell, 1999) propose that changes in hue and saturation perception with retinal eccentricity are due to rod influences on chromatic pathways. As previously noted, the central fovea contains no rod photoreceptors, and the number of rods, and the proportion of rods to cones, increases with increasing retinal eccentricity once outside the foveal area (Curcio et al., 1990). Volbrecht et al. (2011) found that as observers dark adapted, thus increasing the strength of rod input to the retina, their ability to discriminate between hues suffered, implying that rod signals act to suppress the response of the chromatic system. As decreased saturation is indicative of a reduced chromatic response and hue

percentages in the current study were scaled to saturation, it is possible that this increased rod influence is responsible for the decreased hue and saturation perception reported for the smallest peripheral stimuli as compared to the foveal stimuli. How, then, does increasing the size of a peripheral stimulus result in hue perception more similar to that seen in the fovea, in particular given that increasing the size of a peripheral stimulus would also increase the area of the retina stimulating rods? Stabell and Stabell (1999) and Volbrecht and Nerger (2012) suggest that the reason increasing stimulus size in the periphery yields a more “fovea-like” hue percept, despite the fact that there are more rods underlying a larger peripheral stimulus than a smaller one, is that there are also more cones underlying a larger peripheral stimulus. Increasing the chromatic input by stimulating more cones suppresses rod signals, resulting in a stronger hue perception. This increase in cone stimulation underlying larger-diameter stimuli may thus be the reason differences in saturation between peripheral stimuli and foveal stimuli abate as the size of the peripheral stimulus is increased (Figures 3.2-3.4).

Also relevant to hue perception differences between the fovea and the peripheral retina are changes in cone photoreceptor distribution and ratios of cone types to one another over the surface of the retina. Of particular relevance are the changes in the L- and M-cone photoreceptor mosaic: L and M cone densities decrease as one moves outward from the fovea (Curcio et al., 1991). McKeefry et al. (2007) suggested shifts in hue and saturation could relate to reduced activity in the L – M channel, the channel responsible for the red-green opponent color response, caused by variations in L- to M-cone distribution over the retina. It is possible that increasing the size of stimuli presented to the peripheral retina compensates for the decreased L and M cone density in the periphery, since a larger stimulus subtends more retinal area and would thus cover more L and M cones than a smaller stimulus. The blue-yellow opponent channel, which

combines input from S-, M-, and L-cones, appears to be better preserved in the periphery (McKeefry et al., 2007; Mullen & Kingdom, 2002; Murray et al., 2006) than the red-green opponent channel. This may be due not only to changes in photoreceptor distribution, but also to changes in connections between the cone types and their associated ganglion cells, as S-cone connections to ganglion cells are fairly constant across the retina, but L- and M-cone connections exhibit increasing randomness as one moves away from the fovea (Derrington, Krauskopf, & Lennie, 1984; Mullen & Kingdom, 2002; Solomon, Lee, White, Rüttiger, & Martin, 2005). Again, in the periphery, a larger stimulus might be required to activate the number of L- and M-cone-associated ganglion cells necessary to approach a “fovea-like” percept.

Aside from the general pattern of differences in hue perception between the periphery and the fovea, there were also individual hues that showed specific differences according to whether they were viewed peripherally or foveally; for example, the shift of green toward shorter wavelengths in the periphery (Figures 3.2-3.4, middle rows). Nerger et al. (1995) hypothesized that such a shift of green toward shorter wavelengths could be due to rod inhibition of S-cone input to the blue-yellow and red-green opponent hue channels. Volbrecht et al. (2000) later proposed that S-cone input may vary to the red-green and blue-yellow opponent systems, in which case rod inhibition of S-cone signals may have differential effects on perceptions of the hues associated with the channels. This in turn could explain why, as the model discussed by Nerger et al. (1995) would predict, green shifts toward shorter wavelengths in the periphery relative to the fovea, but yellow fails to shift toward longer wavelengths.

Perceptive Field Size

As Figure 3.12 showed, perceptive field sizes for blue, yellow, and red were quite similar to one another, except in the right monocular nasal condition, where the perceptive fields for

both blue and red were larger than those for yellow, and for the left monocular nasal condition, where the perceptive field for red was larger than that for yellow. Yellow, red, and blue k -values were relatively invariant across wavelengths within a given fixation condition, as well as across fixation conditions (see Figure 3.11). Although the k -values for yellow, red, and blue do exhibit some variability across wavelength in the monocular nasal conditions, often this variability was small.

Like the current study, Abramov et al. (1991) found that red is fairly invariant across wavelengths; however, the findings of the current study regarding blue perceptive fields conflict with those of Abramov et al. (1991). While Abramov et al. (1991) found that perceptive fields for blue were relatively small, as did the current study, when fitting Michaelis-Menten functions to their hue-scaling results for blue, they found positive k values for wavelengths from 440-480 nm, indicating growth functions (i. e., increasing percent blue with increasing stimulus size), but negative k values for wavelengths from 490-530 nm, indicative of decay functions (i. e., decreasing percent blue with increasing stimulus size). They interpreted this to mean that there were two different visual processes, or submechanisms, underlying the perception of blue: 1) the B (“blue”) submechanism associated with the growth function and 2) the tritan-B mechanism associated with the decay function. Pitts et al. (2005), though, found fewer, less consistent negative k values for blue than those found by Abramov et al., thereby casting doubt on the existence of the tritan-B mechanism. The present study did not find evidence for the tritan-B mechanism, nor did Volbrecht et al. (2009).

Yellow was unique among the other elemental hues in that k values for yellow were negative more often than were k values for the other elemental hues (Figure 3.11, third row), indicating that yellow was more likely to exhibit a decay, rather than a growth function. This

decrease in percent yellow with increasing stimulus size is also evident in Table 3.2, which shows a higher proportion of negative k values for the yellow functions than for the other hues. Pitts et al. (2005) and Volbrecht et al. (2009) found the same tendency toward decay functions rather than growth functions for yellow in their experiments, as well. These researchers suggested that this tendency of yellow to exhibit negative k values may reflect a limitation on the utility of Michaelis-Menten functions for modeling perceptive field size rather than reflecting an underlying physiological mechanism.

As shown in Figure 3.12, perceptive fields were larger overall for the left and right monocular nasal conditions than for the monocular temporal conditions or the binocular fixation conditions. A difference in perceptive field size between the nasal and temporal retinas has been shown previously; in particular, k values were found to be larger in the nasal retina than the temporal retina under dark-adaptation conditions maximizing rod input (Abramov et al., 1991; Volbrecht et al., 2009). Although the current experiment supports previous findings that nasal perceptive fields were largest, the actual sizes of the nasal perceptive fields in the current experiment are larger than any reported previously; for example, Abramov et al. (1991) found that perceptive field sizes for green presented at 10° nasally were 1.89° , and Volbrecht et al. (2009) calculated perceptive field sizes for green in the same retinal location as 6.84° . The current study found a green perceptive field value of 18.79° at 10° nasally in the right eye, and a value of 11.80° at 10° nasally in the left eye.

It is possible that the reason Abramov et al.'s (1991) nasal perceptive fields are comparatively small is that while Volbrecht et al. (2009) and the current study required observers to dark-adapt for 30 minutes for the peripheral stimulus presentation conditions, Abramov et al. only required 10 minutes of dark adaptation and thus may not have allowed enough time for rod

photopigment to fully regenerate. As for the differences in nasal perceptive field sizes found by the current study versus those found by Volbrecht et al., it is worth noting that in the current study, the standard deviation for the nasal perceptive field sizes for green was quite large: 21.11° for the right nasal condition, and 11.65° for the left nasal condition. Thus the perceptive field sizes found by Volbrecht et al. fall within the range of values corresponding to the mean nasal perceptive field size for green found by the current study ± 1 standard deviation of the mean.

Researchers (Volbrecht et al., 2009; Volbrecht & Nerger, 2012) have proposed that differences in rod-cone ratios may explain differences in perceptive field size. While the density of cones in the temporal retina is larger than that in the nasal retina at approximately 10° retinal eccentricity, so is the density of rods (Curcio et al., 1990), resulting in similar rod-cone ratios for the temporal (15:1) and nasal (16:1) retinas (Volbrecht et al., 2009). Buck et al. (1998) proposed that the absolute, rather than relative, level of rod excitation underlying a stimulus determines the effect of rods upon perception, which would seem to imply that it is the absolute number of rods, rather than the rod-to-cone ratio, underlying a stimulus that yields the difference in hue perception for different retinal areas. As rod photoreceptor density is greater in the temporal retina than the nasal retina (Curcio et al., 1990), one might expect the rod effect upon perception to be stronger in the temporal retina, causing perceptive fields in the temporal retina to be larger than those in the nasal retina. Although this is in keeping with Pitts et al.'s (2005) findings that perceptive field sizes decrease with increasing retinal illuminance, indicating that decreasing rod contribution decreases perceptive field size, Buck et al.'s hypothesis is inconsistent with findings from the current experiment, as well as those of others (Troup et al., 2005; Volbrecht et al., 2009). Thus, although it is possible, and even likely, that rod photoreceptor signals contribute to

changes in hue perception across the retina, the situation appears to be more complicated than the absolute number of rods, or even the rod-to-cone ratio, in determining perceptive field size.

Of the unique hues, perceptive field sizes were found to be the largest overall for green. McKeefry et al. (2007) have suggested that changes in red, green, and saturation perception with increasing retinal eccentricity are connected to changes in the L – M-cone opponent pathway, which is proposed to mediate perception of red and green and underlie the parvocellular pathway. Previous research has found that the L – M cone pathway becomes less sensitive (Martin, Lee, White, Solomon, & Rüttiger, 2001) and less active (Solomon et al., 2005) as retinal eccentricity increases. McKeefry et al. (2007) speculated that a possible cause for this decreasing L – M channel activity may be a decrease in L- and M-cone densities as one moves away from the fovea (Curcio et al., 1991; Roorda & Williams, 1999), while Mullen and Kingdom (2002) proposed that the decrease in L – M channel signals with eccentricity may be related to the fact that L- and M-cone connections to ganglion cells become more erratic as retinal eccentricity increases (Dacey, 1993; Dacey & Peterson, 1992; Mullen & Kingdom, 1996, 2002; Solomon & Lennie, 2007; cf. Solomon et al., 2005). It is possible that the loss of sensitivity in the L – M-cone opponent mechanism, whatever its cause, requires larger stimuli peripherally to achieve a stable hue percept, thereby resulting in larger perceptive fields; however, this cannot explain the difference in perceptive field sizes for red and green. It is possible that the reason perceptive field sizes for green, the perception of which is mediated by M cones, are large, but perceptive field sizes for red, mediated by L cones, are comparable to those for blue and yellow, may be related to findings that indicate L cones tend to outnumber M cones, although the precise ratio does vary between individuals (Cicerone & Nerger, 1989; Nerger & Cicerone, 1992; Roorda & Williams, 1999). Another possible explanation is an

increase in the number of L-cone-mediated, relative to M-cone-mediated, parvocellular cells with hidden color opponency as one moves from the fovea to the peripheral retina (e. g., DeMonasterio, Gouras, & Tolhurst, 1975; Shapley & Perry, 1986). Color-opponent cells are cells whose response may be inhibitory or excitatory depending on the wavelength of the light stimulating the cell. Cells with hidden color-opponency are those that demonstrate color opponency only after chromatic adaptation suppresses one of the cone mechanisms contributing to the cell response (DeMonasterio et al., 1975). This increase in the ratio of L- to M-cone-mediated cells with hidden color-opponency could result in L-cone signals suppressing M-cone signals, which may explain why the decrease in R/G opponent channel sensitivity with increasing retinal eccentricity has a particularly detrimental effect on the perception of green, while perception of red is largely preserved. Shapley and Perry (1986) also proposed the “hit-or-miss hypothesis”: as one moves out toward the periphery, ganglion cell responses are no longer driven by a single cone as they are in the fovea, and peripheral L cones have more connections to bipolar cells as compared to M cones. This results in L-cone input having greater influence upon the parvocellular pathway than M-cone input. In turn, this results in a decreased neural response to green while simultaneously preserving neural responses to red and leading to differential perceptive field sizes for red and green.

Binocular vs. Monocular Hue Perception

As mentioned previously, for both hue-scaling data and perceptive field data, binocular perception for a given fixation condition appears to be determined by the temporal retina, rather than the nasal retina or an averaging of the signals between the two individual retinas. This was quite surprising, as all observers for the current study exhibited right-eye dominance. Even more unexpected was that previous research (Crovitz & Lipscomb, 1963; Stanley et al., 2011)

involving binocular rivalry for chromatic stimuli found that a stimulus presented to the temporal visual field, and thus falling on the nasal side of the retina, appeared to dominate, regardless of actual ocular dominance. Both studies found that observers' most commonly reported response tended to correspond to the stimulus that occupied the temporal visual field and thus fell on the nasal side of the retina, whereas for the stimulus occupying the nasal visual field, thus falling on the temporal side of the retina, perception either briefly occurred but was quickly dominated by the stimulus occupying the temporal visual field (Stanley et al., 2011), or did not occur until after a delay of several minutes or was not perceived at all (Crovitz & Lipscomb, 1963).

There appears to be some variance between individuals, however, regarding which part of the retina will dominate binocular perception for a peripherally-presented stimulus. Leat and Woodhouse (1984) compared responses to dichoptic stimuli presented both continuously and flashed for 250 ms. They found that for the continuously-presented stimuli, the percept resulting from rivalry was consistent with the observers' dominant eyes, but for the 250-ms stimuli, whether the percept resembled the stimulus presented to the dominant or non-dominant eye varied across observers. While some observers did perceive the flashed stimulus presented to the dominant eye to consistently prevail over the stimulus presented to the other eye, others reported that the stimulus presented to the non-dominant eye typically suppressed that presented to the dominant eye, and still others showed no consistent pattern at all (Leat & Woodhouse, 1984). These differences between individuals could explain the discrepancy of the findings of the current study with those of Crovitz and Lipscomb (1963) and Stanley et al. (2011), as well as the reason that the eye that dominates during sustained binocular viewing, such as occurs as in everyday life and in the circumstances under which eye dominance is traditionally tested, may

not actually be the eye that dominates during binocular perceptual tasks involving briefly-flashed stimuli.

Another possible explanation for the temporal retina determining binocular perception may be that the optic disk, or “blind spot”, the area of the retina with no photoreceptors where the optic nerve leaves the eye, is situated in the nasal retina. Because there are no photoreceptors at the optic disk, the part of the visual scene falling on the optic disk cannot be perceived. Under normal binocular conditions, however, the blind spot is not perceptually apparent: due to the lateral displacement of the eyes, a slightly different area of the visual scene will fall on the optic disk of each eye. Information about the part of the visual scene that falls on the optic disk of one eye is “filled in” by the other eye in the visual cortex, when information from the two eyes is integrated. As the temporal retina does not possess a “blind spot”, it is possible that during this “filling-in” process, information from the temporal retina is weighted more heavily, which might result in the temporal retina exerting more influence than the nasal retina over binocular perception.

Amblyopic Observer vs. Normal Observers

Due to uncorrected childhood strabismus, observer JO in the current study is amblyopic, a cortical visual deficit arising from abnormal binocular input during childhood that is associated with reduced visual acuity and disrupted binocular vision (Sloper, 2016). JO is classified as having intermittent left-eye esotropia, indicating that under some circumstances her left eye will deviate nasally during fixation. Although JO did perform normally on tests of color vision, her data were not included in the overall analysis due to the fact that it is not representative of normal binocular functioning. Nonetheless, her data were collected for comparison purposes to investigate whether there are differences in binocular color perception for amblyopes as

compared to healthy controls. Previous research (Bradley, Dahlman, Switkes, & De Valois, 1986; Davis et al., 2006; Mullen, Sankeralli, & Hess, 1996) has reported abnormal color perception in amblyopia, even when amblyopes exhibit normal color vision with traditional color vision tests (HRR Pseudoisochromatic Plates and D-15 Panel Test; Bradley et al., 1986).

Strabismic amblyopes with no detectable color deficiencies show diminished contrast sensitivity for both achromatic and isoluminant red-green sinusoidal gratings in the amblyopic eye as compared to both normal observers and their own non-amblyopic eyes (Bradley et al., 1986). In contrast, Hilz, Rentschler, and Baier (1989) found that strabismic amblyopes were better able to discriminate different wavelengths of light in their amblyopic than their normal eyes; although it is worth noting that Hilz et al. only compared across eyes for the amblyopes and did not include any normal observers in their study. That amblyopes have an advantage over normal observers in discriminating between wavelengths seems unlikely, since Davis et al. (2006) found that although amblyopes' unaffected eyes may appear to have normal color contrast sensitivity when compared to their fellow amblyopic eye, the color contrast sensitivity of the unaffected eye still exhibits deficits in color contrast sensitivity when compared to the performance of normal observers. This indicates that rather than amblyopes' binocular color vision being determined by one color-normal and one color-abnormal eye, it may, in fact, be governed by two color-abnormal eyes.

Bradley et al. (1986) and Hilz et al. (1989) both used only middle- and long-wavelength stimuli in their studies, and thus their results are difficult to generalize to short-wavelength perception. To address this gap in the literature, Mangelschots and colleagues (1996) tested color contrast thresholds modulated along a blue-yellow tritan axis for amblyopes and normal observers and found no statistically significant difference between the two groups. This may

imply that color vision disturbance in amblyopia affects only the L – M (R/G opponent), and not the S – (L + M) (B/Y opponent), channel. Amblyopes also show reduced sensitivity in luminance contrast (Bradley et al., 1986; Davis et al., 2006; Mullen et al., 1996); and the luminance channel, like the R/G opponent channel, results from a combination of signals from the L- and M-cones (although for the luminance channel, the L- and M-cone signals are summed, rather than subtracted). Thus, it is possible that L- and M-cone inputs combine abnormally in the visual pathways of amblyopes. Mullen et al. (1996) found that in amblyopes, perception of red appears suppressed in the amblyopic eye relative to the normal eye, as indicated by their findings that achieving isoluminance requires a different ratio of red to green for the normal vs. amblyopic eye in amblyopes, with the amblyopic eye requiring a greater red component.

In addition to chromatic perceptual abnormalities found monocularly in the amblyopic eye, there is evidence that chromatic signals do not combine normally between the two eyes in amblyopia. Lange-Malecki, Creutzfeldt, and Hinse (1985) found that although amblyopes were able to achieve dichoptic color mixing, the degree to which the amblyopic eye contributed to the color mixture varied considerably between individuals, with some amblyopic observers able to perceive dichoptic color mixtures comparable to those reported by normal observers, and others unable to perceive any dichoptic color mixture at all (i. e., the color perceived by the healthy eye was unaffected by the color presented to the amblyopic eye). These findings indicate that there is a range of dysfunction in the degree to which the two eyes can integrate information in amblyopia that may be related to the specific clinical features of the amblyopia in an individual (e. g., duration, cause, past treatment, degree of deviation of fixation of the strabismic eye in cases where strabismus is the cause, etc.).

Figure 4.1 presents hue-scaling functions for the amblyopic observer, comparing the binocular foveal condition (solid lines) with the binocular left fixation (left eye temporal, right eye nasal; dashed lines) and binocular right fixation (right eye temporal, left eye nasal; dotted lines) conditions. Note that for JO, the smallest stimulus size is 1.7° , rather than the 1.0° used for the normal observers, as she was not able to achieve binocular fusion for a 1.0° stimulus under these viewing conditions and as a result always perceived a double image of the stimulus rather than a single unified percept. Also important is that JO is strongly right eye dominant, as the left eye exhibits the deficits in visual function associated with amblyopia.

There are a number of differences in JO's binocular hue functions, shown in Figure 4.1, as compared to those of the observers with normal binocular vision (see Figure 3.4). Although JO shows the same narrowing of the blue response and expansion of the yellow across wavelengths, her binocular foveal blue function is more similar to the peripheral functions at all stimulus sizes than those of the normal observers; i. e., the range of wavelengths JO perceived as blue in the fovea is compressed compared to the binocular normal observers (top row of Figure 4.1 and Figure 3.4). JO's green function also differs from the normal observers': she does not show the same shift of the green response function toward shorter wavelengths relative to the foveal function as the normal observers do. She also perceives a *smaller* percentage of green in the periphery than the fovea (Figure 4.1, middle row, versus Figure 3.4, middle row). There appears to be little difference in the red function between JO and the normal observers. JO's percent saturation in the peripheral retina for wavelengths from approximately 450-590 nm is less than that reported in the fovea even for the largest stimulus size (bottom row, Figure 4.1). This result is not observed for the normal observers (bottom row of Figure 3.4).

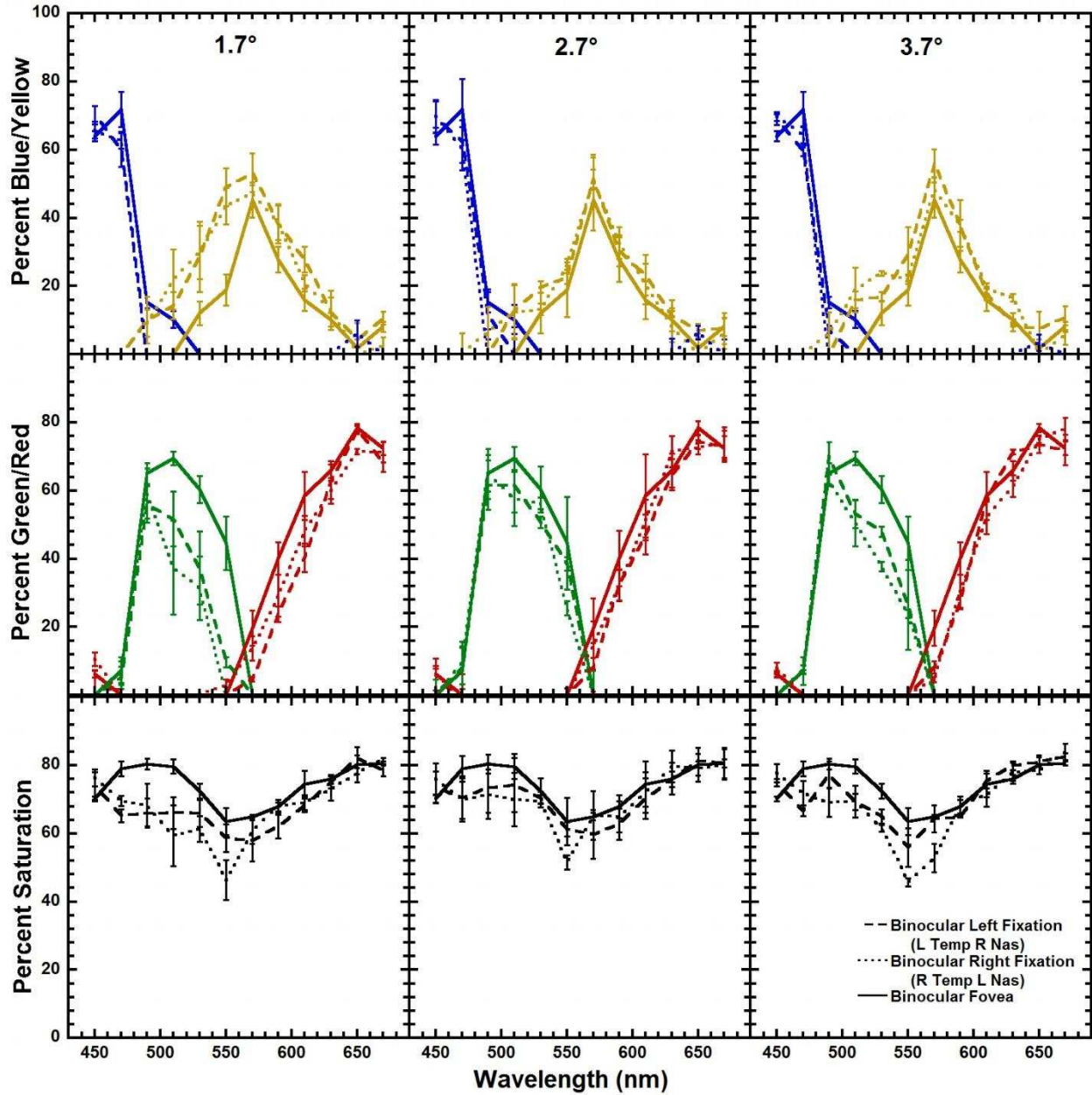


Figure 4.1. Hue-scaling data for the amblyopic observer for the binocular fovea (solid lines), binocular left fixation (left eye temporal, right eye nasal; dashed lines), and binocular right fixation (right eye temporal, left eye nasal; dotted lines). Compare to Figure 3.4, which shows the same data for the normal observers.

Figures 4.2 through 4.5 compare JO's hue-scaling data (left column) to the mean hue-scaling data of the normal observers (right column) for the 1.7° (Figures 4.2 and 4.4) and 3.7° (Figures 4.3 and 4.5) stimuli. In all these figures, binocular peripheral conditions are represented

with solid lines, monocular temporal conditions with dashed lines, and monocular nasal conditions with dotted lines. Figures 4.2 and 4.3 show results for the binocular left fixation (where the stimulus falls on the *left temporal* retina and the *right nasal* retina), the temporal retina of the left eye, and the nasal retina of the right eye. Figures 4.4 and 4.5 depict results for the binocular right fixation (where the stimulus falls on the *right temporal* and *left nasal* retina), the temporal retina of the right eye, and the nasal retina of the left eye. Although there are a number of differences between JO's hue and saturation functions and those of the binocular normal observers, the most consistent differences are seen in the yellow, red, and saturation functions. JO's yellow function extends into shorter wavelengths than does that of the binocular normal observers for both the monocular left (Figure 4.2, top row) and monocular right (Figure 4.4, top row) nasal 1.7° stimuli, and for the 3.7° stimulus presented to the left nasal retina (Figure 4.5, top row). This is seen whether the stimulus was presented to the amblyopic or non-amblyopic eye, which may indicate that it is the result of individual differences in hue perception between JO and the other observers, or may support previous findings regarding dysfunctional color vision in both the amblyopic and non-amblyopic eyes (Davis et al., 2006). It is difficult to conclude which is the case without a larger sample of amblyopes.

JO also perceived stimuli from 590-670 nm presented monocularly to the left nasal retina as having a lower percentage of red than did the binocular normal observers (Figures 4.4 and 4.5, middle row). The fact that this is only shown in the amblyopic eye appears consistent with previous research that found parvocellular (R/G pathway) abnormalities in amblyopia (Bradley et al., 1986; Hiltz et al., 1989; Mullen et al., 1996; Davis et al., 2006). Recall that JO's binocular red functions, however, do not appear to differ from those of normal observers (compare Figure 4.1, middle row, with Figure 3.4, middle row), indicating that under binocular viewing

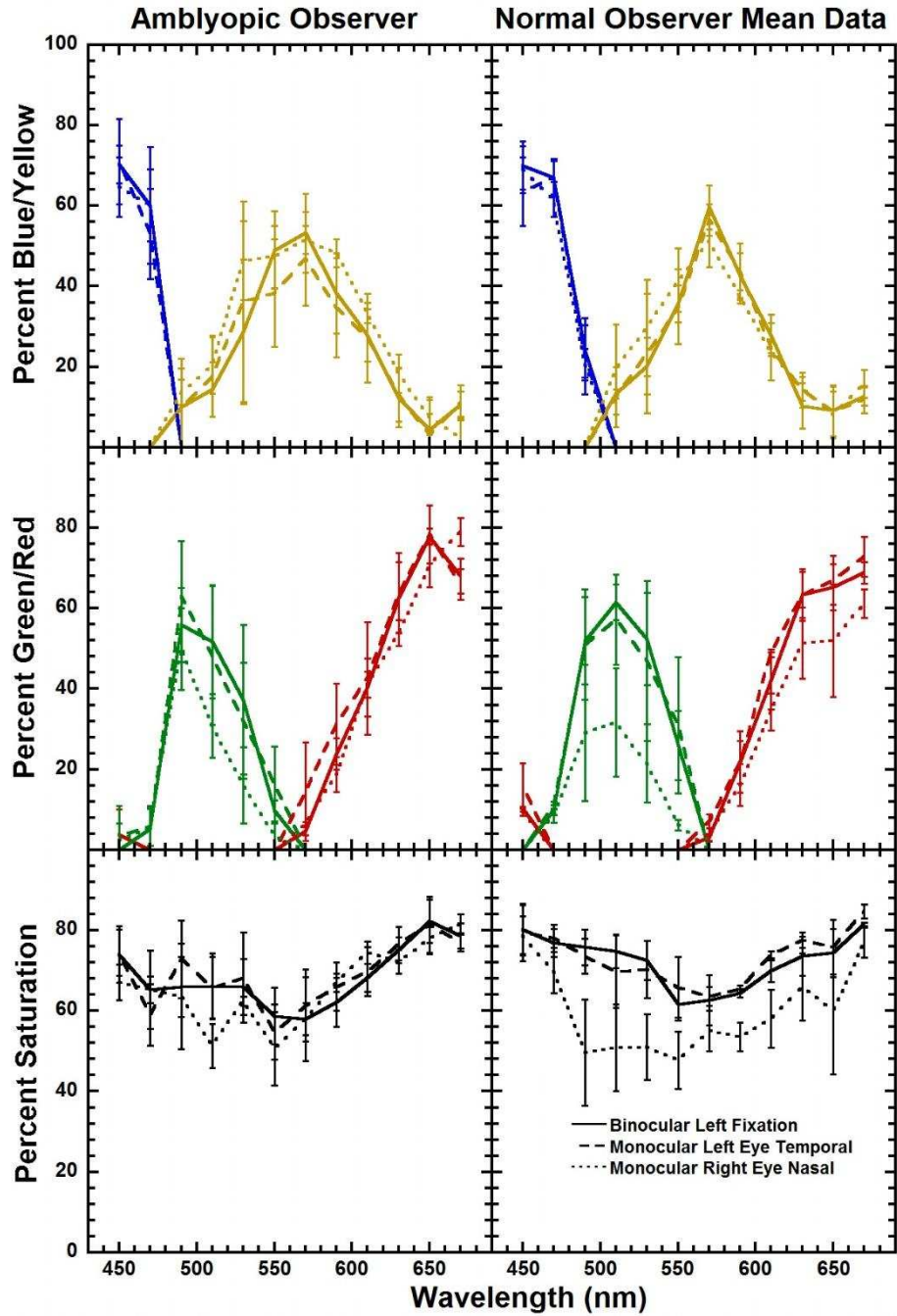


Figure 4.2. Comparison of 1.7° hue-scaling functions from the binocular left fixation (left eye temporal, right eye nasal; solid lines), monocular left eye temporal (dashed lines), and monocular right eye nasal (dotted lines) viewing conditions for the amblyopic observer (left column) with the mean data for the normal observers (right column).

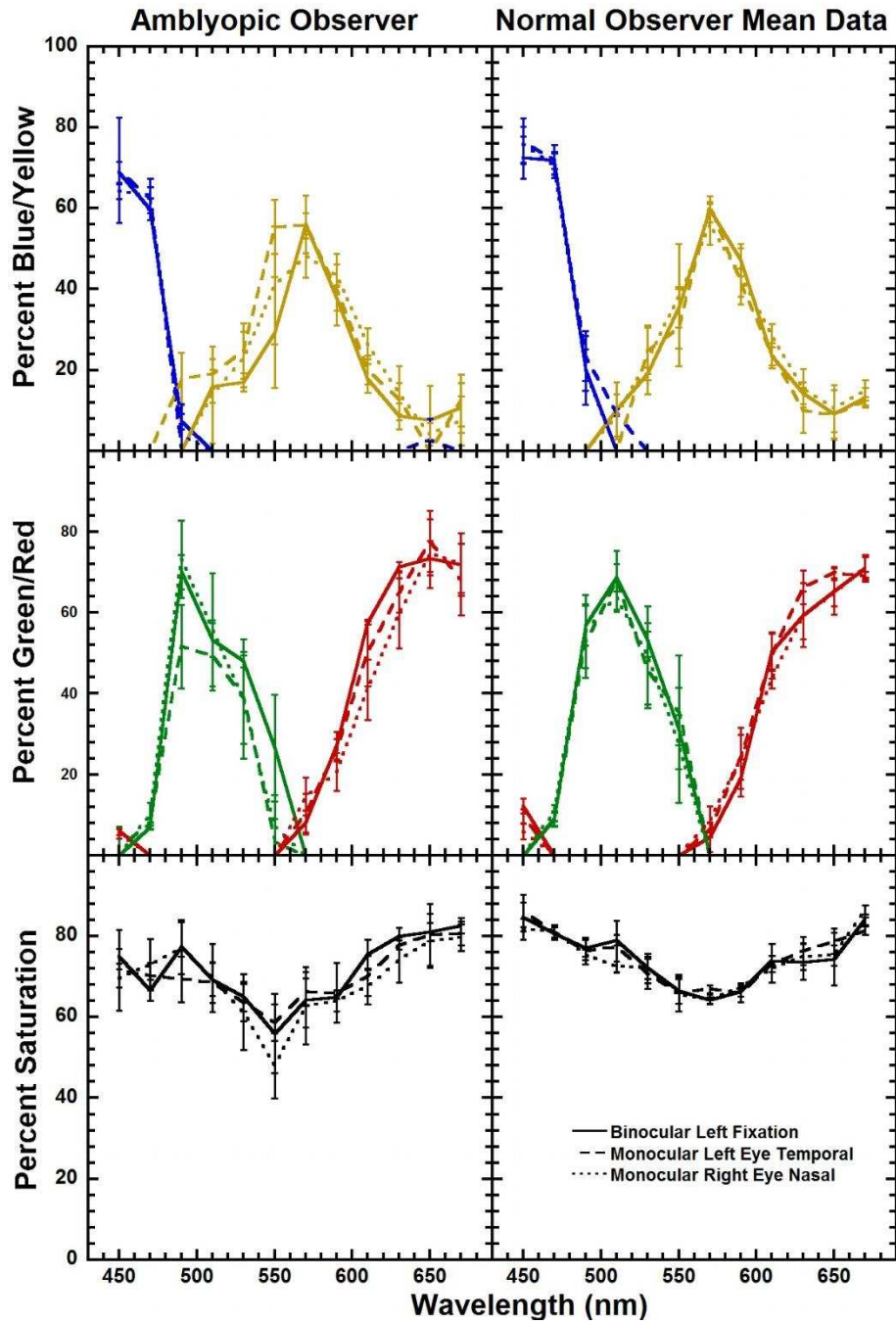


Figure 4.3. Comparison of 3.7° hue-scaling functions from the binocular left fixation (left eye temporal, right eye nasal; solid lines), monocular left eye temporal (dashed lines), and monocular right eye nasal (dotted lines) viewing conditions for the amblyopic observer (left column) with the mean data for the normal observers (right column).

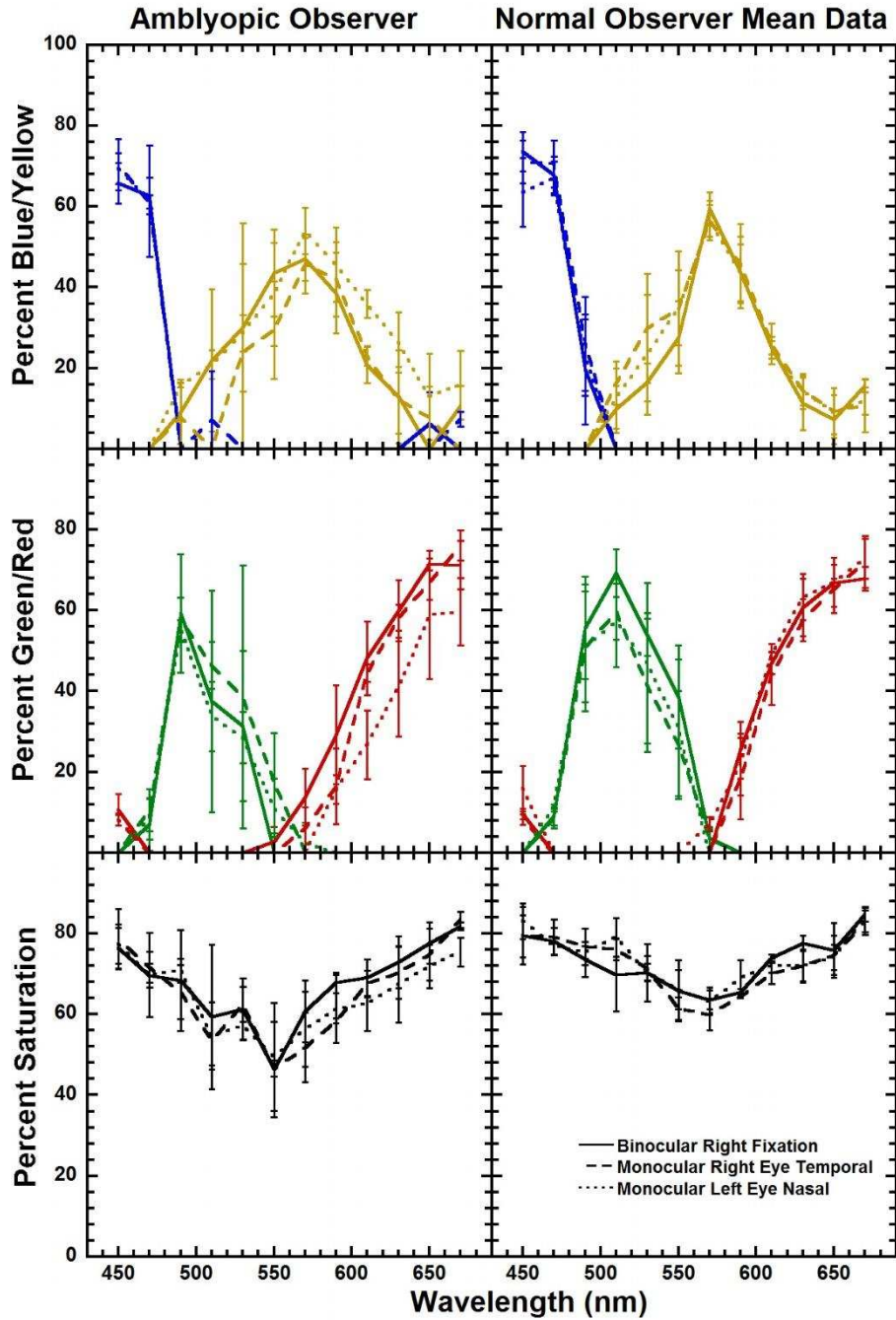


Figure 4.4. Comparison of 1.7° hue-scaling functions from the binocular right fixation (right eye temporal, left eye nasal; solid lines), monocular right eye temporal (dashed lines), and monocular left eye nasal (dotted lines) viewing conditions for the amblyopic observer (left column) with the mean data for the normal observers (right column).

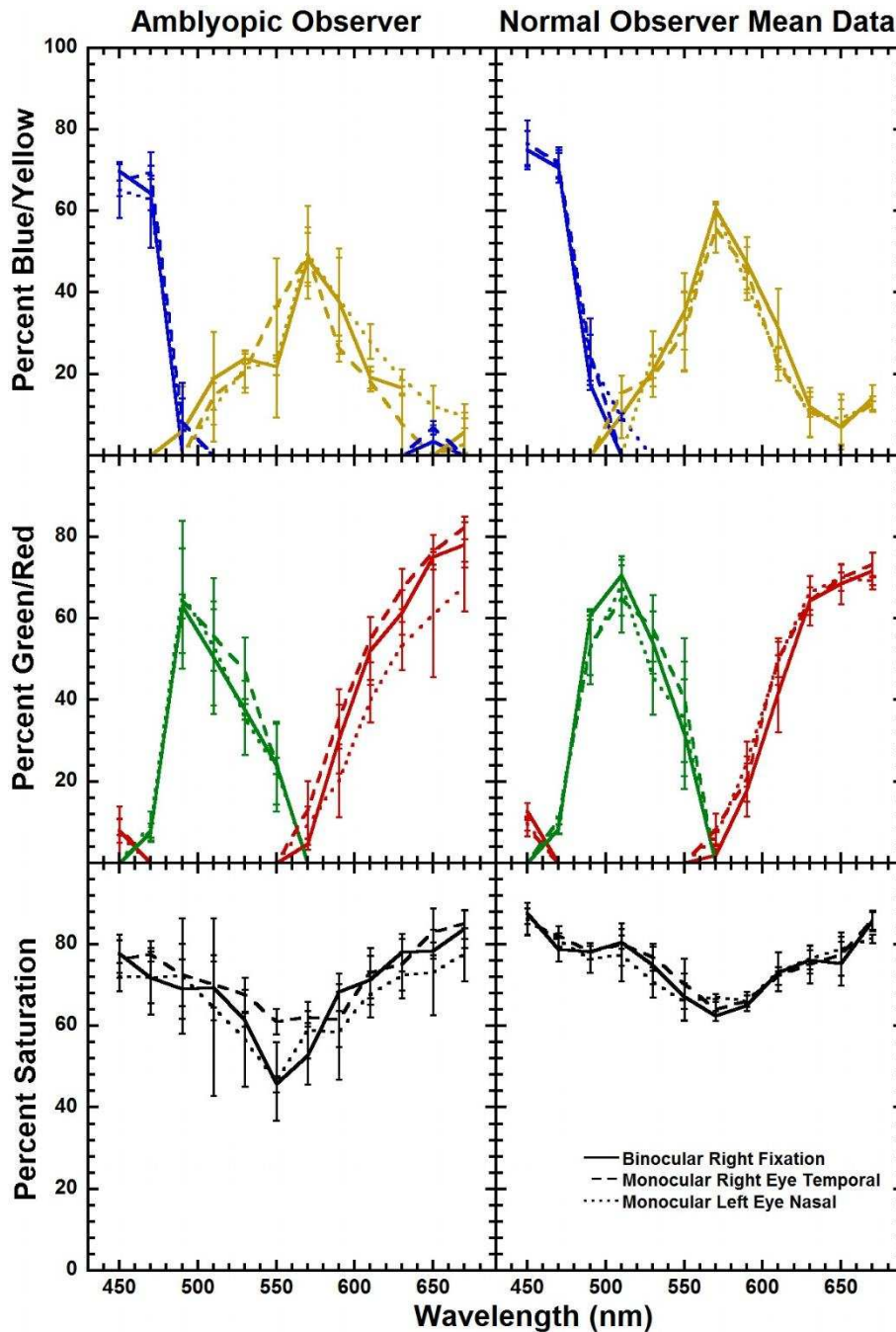


Figure 4.5. Comparison of 3.7° hue-scaling functions from the binocular right fixation (right eye temporal, left eye nasal; solid lines), monocular right eye temporal (dashed lines), and monocular left eye nasal (dotted lines) viewing conditions for the amblyopic observer (left column) with the mean data for the normal observers (right column).

conditions, the temporal retina of JO's non-amblyopic eye may be able to compensate for any deficiency in perception of red exhibited by the amblyopic eye.

The data further indicate that JO perceived stimuli between approximately 510 and 600 nm as less saturated than the binocular normal observers (Figures 4.2-4.5, bottom row). This appears to be fairly consistent across viewing conditions, with the possible exception of the 1.7° stimulus under left fixation viewing conditions, which makes it difficult to conclude whether it is the result of individual differences or a reflection of deficits due to amblyopia. Previous research on color vision in amblyopia does not appear to have investigated saturation separately from hue in the manner of the hue-scaling paradigm; more data is thus required regarding saturation perception in amblyopia before a hypothesis regarding a potential cause can be made.

As noted previously, because JO was the only amblyopic observer in the current study, it is difficult to generalize whether differences in her data from those of the normal observers reflect differences due to amblyopia, or simply normally-occurring differences in hue perception due to variation in cone distribution among individuals (Roorda & Williams, 1999). JO's reduced perception of red in the left nasal retina, however, is in keeping with previous research which has found shrinkage of cells in the parvocellular pathway, the pathway assumed to mediate perception of red and green, in amblyopia (Sloper, 2016). This may explain the selective long- and middle-wavelength contrast sensitivity abnormalities found in amblyopes (Bradley et al., 1986; Davis et al., 2006, 2008; Hilz et al., 1985; Mullen et al., 1996).

Conclusion

In keeping with previous hue-scaling research (Abramov et al., 1991; Gordon & Abramov, 1977; Parry et al., 2006; Volbrecht et al., 2009), peripheral hue perception approaches that of the fovea as stimulus size is increased, for both monocular and binocular viewing conditions. Peripheral binocular color vision for small stimuli in normal observers appears to be primarily influenced by information falling on the temporal retina, regardless of whether the

temporal retina is that of the observer's dominant or non-dominant eye, indicating that eye dominance may not play a role in binocular color vision. This is supported by findings regarding perceptive field size, as perceptive field sizes were quite similar for the binocular fixation and monocular temporal fixation conditions. Perceptive field sizes were largest for the monocular nasal retinal conditions, and particularly the right monocular nasal condition. In terms of hues, perceptive field sizes were largest for green, and relatively similar for all other hues.

The amblyopic observer was found to have a different pattern of results for yellow, red, and saturation. Notably, the amblyopic observer's perception of red and saturation were particularly reduced relative to those of the normal observers. The only result consistently associated only with the amblyopic eye, however, was that of reduced red perception in the left nasal retina, which supports previous research indicating dysfunctional parvocellular pathway functioning in amblyopia (Davis et al., 2008; Sloper, 2016).

Future research should incorporate a larger sample of amblyopic observers in order to ascertain whether the differences found between the amblyopic and normal observers in the current study are simply a consequence of individual differences in visual perception, or in fact due to amblyopia. Additionally, it would be beneficial to investigate why the temporal retina appears to dominate binocular color perception in observers with normal vision, and whether this might be related to perceptual "filling-in" of the blind spot, which is situated toward the nasal side of the retina. Both of these avenues may provide additional insight into how retinal signals from the two eyes combine further along the visual pathway, and how the brain manages to fuse two different monocular retinal images into a single, stable binocular percept.

REFERENCES

- Abramov, I., Gordon, J., & Chan, H. (1991). Color appearance in the peripheral retina: Effects of stimulus size. *Journal of the Optical Society of America A*, 8, 404-414.
- Aguilar, M., & Stiles, W. S. (1954). Saturation of the rod mechanism of the retina at high levels of stimulation. *Optica Acta*, 1, 59-65. doi: 10.1080/713818657
- Ahnelt, P. K., Kolb, H., & Pflug, R. (1987). Identification of a subtype of cone photoreceptor, likely to be blue sensitive, in the human retina. *Journal of Comparative Neurology*, 255, 18-34.
- Alpern, M., Rushton, W. A. H., & Torii, S. (1970a). The attenuation of rod signals by backgrounds. *Journal of Physiology*, 206, 209-227.
- Alpern, M., Rushton, W. A. H., & Torii, S. (1970b). The size of rod signals. *Journal of Physiology*, 206, 193-208.
- Bradley, A., Dahlman, C., Switkes, E., & De Valois, K. (1986). A comparison of color and luminance discrimination in amblyopia. *Investigative Ophthalmology & Visual Science*, 27, 1404-1409.
- Brainard, D., Roorda, A., Yamauchi, Y., Calderone, J. B., Metha, A., Neitz, M.,...Jacobs, G. H. (2000). Functional consequences of the relative numbers of L and M cones. *Journal of the Optical Society of America A*, 17, 607-614.
- Buck, S. L., Thomas, L. P., Hillyer, N., & Samuelson, E. M. (2006). Do rods influence the hue of foveal stimuli? *Visual Neuroscience*, 23, 519-523.
- Buck, S. L., Knight, R., Fowler, G., & Hunt, B. (1998). Rod influence on hue-scaling functions. *Vision Research*, 38, 3259-3263.

- Buck, S. L., Knight, R. F., & Bechtold, J. (2000). Opponent-color models and the influence of rod signals on the loci of unique hues. *Vision Research*, *40*, 3333-3344.
- Buck, S. L., & Pulos, E. (1987). Rod-cone interaction in monocular but not binocular pathways. *Vision Research*, *27*, 479-482.
- Ciganek, L. (1970). Binocular addition of the visually evoked response with different stimulus intensities in man. *Vision Research*, *10*, 479-487.
- Clavagnier, S., Dumoulin, S. O., & Hess, R. F. (2015). Is the cortical deficit in amblyopia due to reduced cortical magnification, loss of neural resolution, or neural disorganization? *Journal of Neuroscience*, *34*, 14740-14755. doi: 10.1523/jneurosci.1101-15.2015
- Costa, M. F., Ventura, D. F., Perazzolo, F., Murakoshi, M., & Silveira, L. C. D. (2006). Absence of binocular summation, eye dominance, and learning effects in color discrimination. *Visual Neuroscience*, *23*, 461-469. doi: 10.1017/S095252380623311X
- Crovitz, H. F., & Lipscomb, D. B. (1963). Binasal hemianopia as an early stage in binocular rivalry. *Science*, *139*, 596-597.
- Curcio, C. A., & Allen, K. A. (1990). Topography of ganglion cells in human retina. *Journal of Comparative Neurology*, *300*, 5-25.
- Curcio, C. A., Sloan, K. R., Kalina, R. E., & Hendrickson, A. E. (1990). Human photoreceptor topography. *Journal of Comparative Neurology*, *292*, 497-523.
- Curcio, C. A., Allen, K. A., Sloan, K. R., Lerea, C. L., Hurley, J. B., Klock, I. B., & Milam, A. H. (1991). Distribution and morphology of human cone photoreceptors stained with anti-blue opsin. *Journal of Comparative Neurology*, *312*, 610-624.
- Dacey, D. M. (1993). The mosaic of midget ganglion cells in the human retina. *Journal of*

- Neuroscience*, 13, 5334-5355.
- Dacey, D. M., & Peterson, M. R. (1992). Dendritic field size and morphology of midget and parasol ganglion cells of the human retina. *Proceedings of the National Academy of Sciences*, 89, 9666-9670.
- Davis, A. R., Sloper, J. J., Neveu, M. M., Hogg, C. R., Morgan, M. J., & Holder, G. E. (2006). Differential changes of magnocellular and parvocellular visual function in early- and late-onset strabismic amblyopia. *Investigative Ophthalmology & Visual Science*, 47, 4836-4841.
- Davis, A. R., Sloper, J. J., Neveu, M. M., Hogg, C. R., Morgan, M. J., & Holder, G. E. (2008). Differential changes in color and motion-onset visual evoked potentials from both eyes in early- and late-onset strabismic amblyopia. *Investigative Ophthalmology & Visual Science*, 49, 4418-4426.
- DeMonasterio, F. M., Gouras, P., & Tolhurst, D. J. (1975). Concealed colour opponency in ganglion cells of the rhesus monkey retina. *Journal of Physiology*, 251, 217-229.
- Derrington, A. M., Krauskopf, J., & Lennie, P. (1984). Chromatic mechanisms in lateral geniculate nucleus of macaque. *Journal of Physiology*, 357, 241-265.
- Erkelens, C. J., & van Ee, R. (2002). Multi-coloured stereograms unveil two binocular colour mechanisms in human vision. *Vision Research*, 42, 1103-1112.
- Frumkes, T. E., & Eysteinnsson, T. (1988). The cellular basis for suppressive rod-cone interaction. *Visual Neuroscience*, 1, 263-273.
- Gordon, J., & Abramov, I. (1977). Color vision in the peripheral retina. II. Hue and saturation. *Journal of the Optical Society of America*, 67, 202-207.
- Gordon, J., Abramov, I., & Chan, H. (1994). Describing color appearance: Hue and

- saturation scaling. *Perception & Psychophysics*, 56, 27-41.
- Hagstrom, S. A., Neitz, J., & Neitz, M. (1998). Variations in cone populations for red-green color vision examined by analysis of mRNA. *Neuroreport*, 9, 1963-1967.
- Hecht, S. (1928). On the binocular fusion of colors and its relation to theories of color vision. *Proceedings of the National Academy of Sciences*, 14, 237-241.
- Hilz, R., Rentschler, I., & Baier, M. (1989). Segregation of color and form: Intact spatial wavelength discrimination in strabismic amblyopia. *Naturwissenschaften*, 76, 479-480.
- Ikeda, M., & Sagawa, K. (1979). Binocular color fusion limit. *Journal of the Optical Society of America*, 69, 316-321.
- Johannsen, D. E. (1930). A quantitative study of binocular color vision. *Journal of General Psychology*, 4, 282-308.
- Kakizaki, S. (1960). Binocular rivalry and stimulus intensity. *Japanese Psychological Research*, 2, 94-105.
- Kaplan, I. T., & Metlay, W. (1964). Light intensity and binocular rivalry. *Journal of Experimental Psychology*, 67, 22-26.
- Kingdom, F. A. A., & Libenson, L. (2015). Dichoptic color saturation mixture: Binocular luminance contrast promotes perceptual averaging. *Journal of Vision*, 15, 1-15. doi: 10.1167/15.5.2
- Landisman, C. E., & Ts'o, D. Y. (2002). Color processing in macaque striate cortex: Electrophysiological properties. *Journal of Neurophysiology*, 87, 3138-3151. doi: 10.1152/jn.00957.1999
- Lange, G., Denny, N., & Frumkes, T. E. (1997). Suppressive rod-cone interactions:

- Evidence for separate retinal (temporal) and extraretinal (spatial) mechanisms in achromatic vision. *Journal of the Optical Society of America A*, *14*, 2487-2498.
- Lange-Malecki, B., Creutzfeldt, O. D., & Hinse, P. (1985). Haploscopic colour mixtures with and without contours in subjects with normal and disturbed binocular vision. *Perception*, *14*, 587-600.
- Leat, S. J., & Woodhouse, J. M. (1984). Rivalry with continuous and flashed stimuli as a measure of ocular dominance across the visual field. *Perception*, *13*, 351-357.
- Mangelschots, E., Beerlandt, N., Janssens, H., & Spileers, W. (1996). Colour contrast thresholds are normal in functional amblyopia. *Eye*, *10*, 479-484.
- Martin, P. R., Lee, B. B., White, A. J. R., Solomon, S. G., & Rüttiger, L. (2001). Chromatic sensitivity of ganglion cells in the peripheral primate retina. *Nature*, *410*, 933-936.
- McKeefry, D. J., Murray, I. J., & Parry, N. R. A. (2007). Perceived shifts in saturation and hue of chromatic stimuli in the near peripheral retina. *Journal of the Optical Society of America A*, *24*, 3168-3179.
- Miles, W. (1930). Ocular dominance in human adults. *Journal of General Psychology*, *3*, 412-430.
- Moreland, J. D., & Cruz, A. (1959). Colour perception with the peripheral retina. *Optica Acta*, *6*, 117-151.
- Mullen, K. T., & Kingdom, F. A. A. (1996). Losses in peripheral colour sensitivity predicted from “hit and miss” post-receptoral cone connections. *Vision Research*, *36*, 1995-2000.
- Mullen, K. T., & Kingdom, F. A. A. (2002). Differential distributions of red-green and blue-yellow cone opponency across the visual field. *Visual Neuroscience*, *19*, 109-118.

- Mullen, K. T., Sankeralli, M. J., & Hess, R. F. (1996). Color and luminance vision in human amblyopia: Shifts in isoluminance, contrast sensitivity losses, and positional deficits. *Vision Research*, *36*, 645-653.
- Murray, I. J., Parry, N. R. A., & McKeefry, D. J. (2006). Cone opponency in the near peripheral retina. *Visual Neuroscience*, *23*, 503-507.
- Nerger, J. L., & Cicerone, C. M. (1992). The ratio of L cones to M cones in the human parafoveal retina. *Vision Research*, *32*, 879-888.
- Nerger, J. L., Volbrecht, V. J., & Ayde, C. J. (1995). Unique hue judgments as a function of test size in the fovea and at 20-deg temporal eccentricity. *Journal of the Optical Society of America A*, *12*, 1225-1232.
- Nerger, J. L., Volbrecht, V. J., Ayde, C. J., & Imhoff, S. M. (1998). Effect of the S-cone mosaic and rods on red-green equilibria. *Journal of the Optical Society of America A*, *15*, 2816-2826.
- Newman, N. J., Wolfe, J. M., Stewart, M. I., & Lessell, S. (1991). Binocular visual function in patients with a history of monocular optic neuritis. *Clinical Vision Sciences*, *6*, 95-107.
- Opper, J. K., Douda, N. D., Volbrecht, V. J., & Nerger, J. L. (2014). Supersaturation in the peripheral retina. *Journal of the Optical Society of America A*, *31*, A148-A158. doi: dx.doi.org/10.1364/JOSA.A.31.001.148
- O'Shea, R. P., & Williams, D. R. (1996). Binocular rivalry with isoluminant stimuli visible only via short-wavelength-sensitive cones. *Vision Research*, *36*, 1561-1571.
- Østerberg, G. (1935). Topography of the layer of rods and cones in the human retina. *Acta Ophthalmologica (Suppl)*, *6*, 1-102.
- Parry, N. R. A., McKeefry, D. J., & Murray, I. J. (2006). Variant and invariant color

- perception in the near peripheral retina. *Journal of the Optical Society of America A*, 23, 1586-1597.
- Peirce, J. W., Solomon, S. G., Forte, J. D., & Lennie, P. (2008). Cortical representation of color is binocular. *Journal of Vision*, 8, 1-10. doi: 10.1167/8.3.6
- Perry, N. W., Childers, D. G., & Dawson, W. W. (1969). Human cortical correlates of color with monocular, binocular, and dichoptic vision. *Vision Research*, 9, 1357-1366.
- Pitts, M. A., Troup, L. J., Volbrecht, V. J., & Nerger, J. L. (2005). Chromatic perceptive field sizes change with retinal illuminance. *Journal of Vision*, 5, 435-443. doi: 10.1167/5.5.4
- Rogers, D. C., & Hollins, M. (1982). Is the binocular rivalry mechanism tritanopic? *Vision Research*, 22, 515-520.
- Roorda, A., & Williams, D. R. (1999). The arrangement of the three cone classes in the living human eye. *Nature*, 397, 520-522.
- Shapley, R., & Perry, V. H. (1986). Cat and monkey retinal ganglion cells and their visual functional roles. *Trends in Neurosciences*, 9, 229-235.
- Simmons, D. R., & Kingdom, F. A. A. (1994). Contrast thresholds for stereoscopic depth identification with isoluminant and isochromatic stimuli. *Vision Research*, 34, 2971-2982.
- Simmons, D. R., & Kingdom, F. A. A. (1997). On the independence of chromatic and achromatic stereopsis mechanisms. *Vision Research*, 37, 1271-1280.
- Sloper, J. (2016). The other side of amblyopia. *Journal of American Association for Pediatric Ophthalmology*, 20, 1.e1-1.e13. doi: dx.doi.org/10.1016/j.jaapos.2015.09.013

- Solomon, S. G., Lee, B. B., White, A. J. R., Rüttiger, L., & Martin, P. R. (2005). Chromatic organization of ganglion cell receptive fields in the peripheral retina. *Journal of Neuroscience*, *25*, 4527-4539. doi: 10.1523/jneurosci.3921-04.2005
- Solomon, S. G., & Lennie, P. (2007). The machinery of colour vision. *Nature Reviews Neuroscience*, *8*, 276-286. doi: 10.1038.nrn2094
- Stabell, B. & Stabell, U. (1976). Rod and cone contributions to peripheral colour vision. *Vision Research*, *16*, 1099-1104.
- Stabell, B., & Stabell, U. (1979). Rod and cone contributions to change in hue with eccentricity. *Vision Research*, *19*, 1121-1125.
- Stabell, U., & Stabell, B. (1999). Rod-cone color mixture: Effect of size and exposure time. *Journal of the Optical Society of America A*, *16*, 2638-2642.
- Stanley, J., Carter, O., & Forte, J. (2011). Color and luminance influence, but cannot explain, binocular rivalry onset bias. *PLoS One*, *6*, 1-9. doi: 10.1371/journal.pone.0018978
- Thomas, L. P., & Buck, S. L. (2006). Foveal and extra-foveal influences on rod hue biases. *Visual Neuroscience*, *23*, 539-542.
- Ts'o, D. Y., Roe, A. W., & Gilbert, C. D. (2001). A hierarchy of the functional organization for color, form and disparity in primate visual area V2. *Vision Research*, *41*, 1333-1349.
- Troup, L. J., Pitts, M. A., Volbrecht, V. J., & Nerger, J. L. (2005). Effect of stimulus intensity on the sizes of chromatic perceptual fields. *Journal of the Optical Society of America A*, *22*, 2137-2142.
- van Lier, R., & de Weert, C. M. M. (2003). Intra- and interocular colour-specific activation

- during dichoptic suppression. *Vision Research*, 43, 1111-1116. doi: 10.1016/S0042-6989(03)99975-0
- Verriest, G., Laethem, J. V., & Uvijls, A. (1982). A new assessment of the normal ranges of the Farnsworth-Munsell 100-Hue Test scores. *American Journal of Ophthalmology*, 93, 635-642.
- Volbrecht, V. J., Clark, C. J., Nerger, J. L., & Randall, C. E. (2009). Chromatic perceptive field sizes measured at 10° eccentricity along the horizontal and vertical meridians. *Journal of the Optical Society of America A*, 26, 1167-1177.
- Volbrecht, V. J., & Nerger, J. L. (2012). Color appearance at ±10° along the vertical and horizontal meridians. *Journal of the Optical Society of America A*, 29, A44-A51.
- Volbrecht, V. J., Nerger, J. L., Imhoff, S. M., & Ayde, C. J. (2000). Effect of the short-wavelength-sensitive-cone mosaic and rods on the locus of unique green. *Journal of the Optical Society of America A*, 17, 628-634.
- Volbrecht, V. J., Nerger, J. L., & Trujillo, A. R. (2011). Middle- and long-wavelength discrimination declines with rod photopigment regeneration. *Journal of the Optical Society of America A*, 28, 2600-2606.
- Wade, N. J. (2000). Jean Théophile Desaguliers (1683-1744) and eighteenth century vision research. *British Journal of Psychology*, 91, 275-285.
- Wade, N. J., & Ono, H. (2012). Early studies of binocular and stereoscopic vision. *Japanese Psychological Research*, 54, 54-70. doi: 10.1111/j.1468-5884.2011.00505.x
- Watson, A. B., & Yellott, J. I. (2012). A unified formula for light-adapted pupil size. *Journal of Vision*, 12, 1-16. doi: 1.1167/12.10.12
- Williams, D. R., MacLeod, D. I. A., & Hayhoe, M. M. (1981a). Foveal tritanopia. *Vision*

Research, 21, 1341-1356.

Williams, D. R., MacLeod, D. I. A., & Hayhoe, M. M. (1981b). Punctuate sensitivity of the blue-sensitive mechanism. *Vision Research, 21*, 1357-1375.

Wong, E. M., & Freeman, A. W. (1999). Colour but not form patterns combine between the eyes. *Australian and New Zealand Journal of Ophthalmology, 27*, 275-277.

Young, R. S. L., & Young, G. A. (1979). Do rod signals control stimulus field prevalence in binocular rivalry? *Investigative Ophthalmology & Visual Science, 18*, 194-199.

APPENDIX A.

Monocular Left Eye Left Fixation (Left Temporal)

1.0°						Standard Error of the Mean				
	Mean					Blue	Green	Yellow	Red	Sat
λ	Blue	Green	Yellow	Red	Sat	Blue	Green	Yellow	Red	Sat
450	69.98	0.00	0.00	9.86	79.83	8.16	0.00	0.00	1.33	7.07
470	65.65	5.64	0.00	0.00	71.29	3.70	3.54	0.00	0.00	4.66
490	25.87	42.47	0.00	0.00	68.34	5.07	14.35	0.00	0.00	9.61
510	0.00	50.90	14.65	0.00	65.55	0.00	15.39	11.83	0.00	11.25
530	0.00	42.49	22.88	0.00	65.37	0.00	15.65	7.78	0.00	8.49
550	0.00	30.17	29.98	0.00	60.15	0.00	17.32	8.98	0.00	8.60
570	0.00	0.00	54.34	6.59	60.93	0.00	0.00	6.92	4.68	4.91
590	0.00	0.00	44.16	19.80	63.96	0.00	0.00	4.98	5.39	1.49
610	0.00	0.00	25.30	46.33	71.64	0.00	0.00	5.67	5.99	1.19
630	0.00	0.00	13.55	60.39	73.94	0.00	0.00	8.09	5.01	1.29
650	0.00	0.00	11.06	63.12	74.18	0.00	0.00	6.81	3.02	2.71
670	0.00	0.00	15.61	68.18	83.79	0.00	0.00	1.98	3.93	2.46
1.7°						Standard Error of the Mean				
	Mean					Blue	Green	Yellow	Red	Sat
λ	Blue	Green	Yellow	Red	Sat	Blue	Green	Yellow	Red	Sat
450	63.55	0.00	0.00	15.87	79.43	8.56	0.00	0.00	5.62	7.09
470	66.99	11.06	0.00	0.00	78.05	4.10	0.85	0.00	0.00	3.38
490	22.60	50.99	0.00	0.00	73.59	9.48	13.75	0.00	0.00	4.29
510	0.00	57.22	12.49	0.00	69.71	0.00	11.19	7.53	0.00	9.05
530	0.00	46.99	23.28	0.00	70.26	0.00	19.89	14.87	0.00	7.14
550	0.00	30.91	34.93	0.00	65.84	0.00	16.90	9.32	0.00	7.58
570	0.00	0.00	56.52	7.05	63.57	0.00	0.00	3.88	1.76	2.33
590	0.00	0.00	43.65	21.81	65.46	0.00	0.00	7.08	7.67	0.92
610	0.00	0.00	25.06	48.87	73.93	0.00	0.00	1.59	1.02	0.85
630	0.00	0.00	14.23	63.36	77.59	0.00	0.00	4.34	5.72	1.85
650	0.00	0.00	8.92	66.92	75.84	0.00	0.00	6.10	6.07	6.82
670	0.00	0.00	11.88	72.84	84.72	0.00	0.00	3.47	5.00	1.69
2.25°						Standard Error of the Mean				
	Mean					Blue	Green	Yellow	Red	Sat
λ	Blue	Green	Yellow	Red	Sat	Blue	Green	Yellow	Red	Sat
450	72.20	0.00	0.00	10.17	82.38	5.59	0.00	0.00	0.97	4.92
470	66.04	11.17	0.00	0.78	77.99	3.70	1.87	0.00	0.78	2.02
490	30.46	44.61	0.00	0.00	75.07	10.19	7.61	0.00	0.00	4.31
510	0.00	67.47	9.57	0.00	77.03	0.00	7.52	5.12	0.00	5.11
530	0.00	42.90	21.18	0.00	64.08	0.00	7.39	6.35	0.00	1.06
550	0.00	34.87	31.21	0.00	66.08	0.00	14.22	9.59	0.00	4.82
570	0.00	0.00	55.00	5.59	60.59	0.00	0.00	2.67	0.82	2.71
590	0.00	0.00	44.20	19.82	64.02	0.00	0.00	7.88	7.82	0.83
610	0.00	0.00	20.69	49.23	69.92	0.00	0.00	2.26	0.92	1.86
630	0.00	0.00	10.61	66.75	77.36	0.00	0.00	6.05	3.20	0.50
650	0.00	0.00	8.20	71.04	79.24	0.00	0.00	5.20	1.89	1.24
670	0.00	0.00	13.15	67.51	80.66	0.00	0.00	1.99	3.01	1.06

Monocular Left Eye Left Fixation (Left Temporal)

2.7°					
	Mean				
λ	Blue	Green	Yellow	Red	Sat
450	75.53	0.00	0.00	6.96	82.48
470	71.53	7.33	0.00	0.00	78.86
490	21.90	53.62	0.00	0.00	75.52
510	0.00	69.19	8.18	0.00	77.37
530	0.00	50.95	19.84	0.00	70.79
550	0.00	33.44	28.01	0.00	61.45
570	0.00	0.00	59.19	5.60	64.79
590	0.00	0.00	38.68	28.95	67.63
610	0.00	0.00	21.59	50.24	71.83
630	0.00	0.00	9.88	66.78	76.66
650	0.00	0.00	6.84	69.02	75.86
670	0.00	0.00	12.39	72.07	84.46
3.7°					
	Mean				
λ	Blue	Green	Yellow	Red	Sat
450	76.61	0.00	0.00	9.68	86.29
470	72.03	9.05	0.00	0.00	81.08
490	23.49	52.86	0.00	0.00	76.36
510	9.50	67.98	0.00	0.00	77.48
530	0.00	45.92	24.86	0.00	70.78
550	0.00	35.38	30.54	0.00	65.92
570	0.00	0.00	60.59	6.38	66.97
590	0.00	0.00	41.66	24.32	65.98
610	0.00	0.00	23.87	49.41	73.28
630	0.00	0.00	9.96	66.36	76.32
650	0.00	0.00	8.98	69.88	78.86
670	0.00	0.00	12.29	69.14	81.43

Standard Error of the Mean				
Blue	Green	Yellow	Red	Sat
7.96	0.00	0.00	2.61	5.35
6.80	2.71	0.00	0.00	4.18
13.76	14.80	0.00	0.00	3.58
0.00	5.08	5.22	0.00	4.34
0.00	13.29	8.09	0.00	5.25
0.00	14.48	7.96	0.00	7.37
0.00	0.00	4.50	0.58	3.95
0.00	0.00	8.21	7.05	1.46
0.00	0.00	3.58	6.15	3.34
0.00	0.00	5.61	6.07	4.72
0.00	0.00	5.33	5.00	7.00
0.00	0.00	2.60	2.34	1.23
Standard Error of the Mean				
Blue	Green	Yellow	Red	Sat
5.63	0.00	0.00	1.67	4.01
3.61	1.84	0.00	0.00	1.78
6.09	8.99	0.00	0.00	3.25
0.90	7.27	0.00	0.00	6.43
0.00	9.42	5.71	0.00	3.72
0.00	14.09	9.57	0.00	4.54
0.00	0.00	0.93	1.74	0.94
0.00	0.00	3.42	5.52	2.34
0.00	0.00	2.76	5.77	4.77
0.00	0.00	5.56	4.14	3.51
0.00	0.00	6.16	1.38	3.12
0.00	0.00	1.08	0.90	1.04

Monocular Left Eye Right Fixation (Left Nasal)

1.0°					
	Mean				
λ	Blue	Green	Yellow	Red	Sat
450	54.12	0.00	0.00	7.73	61.84
470	52.98	7.07	0.00	0.00	60.05
490	9.16	53.36	0.00	0.00	62.51
510	0.00	22.40	17.19	0.00	39.58
530	0.00	10.30	18.34	0.00	28.63
550	0.00	11.67	25.67	0.00	37.34
570	0.00	1.79	40.26	0.00	42.04
590	0.00	0.00	25.27	7.99	34.91
610	0.00	0.00	19.61	25.30	44.91
630	0.00	0.00	10.35	39.51	49.86
650	0.00	0.00	4.87	44.26	49.13
670	0.00	0.00	10.01	43.12	53.13
1.7°					
	Mean				
λ	Blue	Green	Yellow	Red	Sat
450	66.21	0.00	0.00	8.97	75.18
470	54.55	13.01	0.00	0.00	67.57
490	21.72	40.30	0.00	0.00	62.01
510	0.00	40.23	17.25	0.00	57.48
530	0.00	24.54	22.97	0.00	47.51
550	0.00	16.51	30.13	0.00	46.64
570					
590	0.00	0.00	40.22	12.98	53.20
610	0.00	0.00	28.68	29.64	58.33
630	0.00	0.00	16.37	35.30	51.67
650	0.00	0.00	7.94	47.46	55.40
670	0.00	0.00	14.12	60.38	74.49
2.25°					
	Mean				
λ	Blue	Green	Yellow	Red	Sat
450	71.63	0.00	0.00	9.83	81.47
470	68.64	8.37	0.00	0.00	77.02
490	32.80	43.42	0.00	0.00	76.22
510	0.00	71.29	7.55	0.00	78.84
530	0.00	51.86	17.63	0.00	69.50
550	0.00	25.81	31.43	0.00	57.24
570	0.00	4.56	48.85	0.00	53.41
590	0.00	0.00	43.21	20.35	63.56
610	0.00	0.00	26.54	44.33	70.87
630	0.00	0.00	16.10	60.46	76.56
650	0.00	0.00	9.73	62.11	71.85
670	0.00	0.00	15.66	69.71	85.37

Standard Error of the Mean				
Blue	Green	Yellow	Red	Sat
10.99	0.00	0.00	2.07	12.92
7.89	4.07	0.00	0.00	10.35
6.93	18.32	0.00	0.00	20.84
0.00	13.39	9.34	0.00	13.73
0.00	1.79	7.91	0.00	7.19
0.00	4.15	14.14	0.00	10.17
0.00	1.57	14.40	0.00	13.62
0.00	0.00	13.23	4.37	14.68
0.00	0.00	16.37	16.37	21.73
0.00	0.00	5.34	20.17	25.08
0.00	0.00	5.69	20.88	24.70
0.00	0.00	6.06	22.03	26.59
Standard Error of the Mean				
Blue	Green	Yellow	Red	Sat
5.04	0.00	0.00	0.72	5.19
7.03	0.89	0.00	0.00	6.31
15.21	14.02	0.00	0.00	10.43
0.00	12.73	10.98	0.00	12.38
0.00	10.98	12.20	0.00	12.63
0.00	7.86	13.48	0.00	7.30
0.00	0.00	11.14	7.16	8.41
0.00	0.00	8.21	9.29	13.92
0.00	0.00	5.32	16.01	21.03
0.00	0.00	6.57	18.48	21.52
0.00	0.00	2.27	6.53	6.71
Standard Error of the Mean				
Blue	Green	Yellow	Red	Sat
6.04	0.00	0.00	0.81	5.48
4.07	2.53	0.00	0.00	1.84
12.39	13.19	0.00	0.00	0.99
0.00	4.96	5.56	0.00	2.83
0.00	6.04	12.06	0.00	1.47
0.00	10.26	9.17	0.00	3.59
0.00	4.65	7.70	0.00	4.69
0.00	0.00	7.71	10.64	3.46
0.00	0.00	5.64	6.71	1.95
0.00	0.00	5.17	7.52	2.43
0.00	0.00	6.18	5.79	6.06
0.00	0.00	3.33	5.29	2.61

Monocular Left Eye Right Fixation (Left Nasal)

2.7°					
	Mean				
λ	Blue	Green	Yellow	Red	Sat
450	74.94	0.00	0.00	6.77	81.71
470	70.43	8.38	0.00	0.00	78.81
490	23.03	51.03	0.00	0.00	74.06
510	7.61	69.15	0.00	0.00	76.76
530	0.00	54.91	15.84	0.00	70.75
550	0.00	28.25	30.11	0.00	58.36
570	0.00	0.00	52.08	2.81	54.89
590	0.00	0.00	45.28	15.76	61.04
610	0.00	0.00	25.06	41.44	66.51
630	0.00	0.00	16.14	58.60	74.74
650	0.00	0.00	8.93	66.55	75.48
670	0.00	0.00	14.34	69.67	84.02
3.7°					
	Mean				
λ	Blue	Green	Yellow	Red	Sat
450	76.43	0.00	0.00	7.90	84.33
470	70.88	9.45	0.00	0.00	80.33
490	25.02	53.90	0.00	0.00	78.92
510	0.00	68.97	9.20	0.00	78.17
530	0.00	52.02	20.93	0.00	72.95
550	0.00	25.41	28.38	0.00	53.79
570	0.00	2.80	42.31	0.00	45.11
590	0.00	0.00	44.30	17.31	61.61
610	0.00	0.00	24.13	46.15	70.28
630	0.00	0.00	17.58	55.70	73.28
650	0.00	0.00	9.89	67.10	76.98
670	0.00	0.00	15.91	69.42	85.33

Standard Error of the Mean				
Blue	Green	Yellow	Red	Sat
3.46	0.00	0.00	0.55	3.72
3.36	2.07	0.00	0.00	1.29
8.60	10.33	0.00	0.00	2.42
4.74	2.20	0.00	0.00	1.52
0.00	5.51	3.21	0.00	2.36
0.00	8.40	6.85	0.00	1.62
0.00	0.00	5.36	2.44	4.84
0.00	0.00	3.97	5.93	3.35
0.00	0.00	5.11	7.08	4.40
0.00	0.00	2.61	4.35	3.12
0.00	0.00	5.95	5.29	5.76
0.00	0.00	2.64	3.02	1.59
Standard Error of the Mean				
Blue	Green	Yellow	Red	Sat
3.22	0.00	0.00	1.43	3.55
2.28	0.92	0.00	0.00	2.02
4.26	4.25	0.00	0.00	0.46
0.00	1.55	5.52	0.00	2.02
0.00	2.91	1.97	0.00	3.06
0.00	8.84	5.34	0.00	8.90
0.00	1.67	9.40	0.00	9.56
0.00	0.00	4.54	2.82	3.43
0.00	0.00	2.95	4.53	1.85
0.00	0.00	2.35	2.81	1.31
0.00	0.00	5.34	3.65	1.26
0.00	0.00	1.22	1.77	2.51

Monocular Right Eye Left Fixation (Right Nasal)

1.0°					
	Mean				
λ	Blue	Green	Yellow	Red	Sat
450	65.88	0.00	0.00	6.13	72.01
470	54.70	5.87	0.00	0.00	60.57
490	0.00	32.28	10.81	0.00	43.09
510	20.58	29.56	0.00	0.00	50.14
530	0.00	16.86	21.48	0.00	38.34
550	0.00	11.16	29.65	0.00	40.82
570	0.00	3.69	25.04	0.00	28.73
590	0.00	0.00	38.98	7.31	46.29
610	0.00	0.00	23.12	30.83	53.94
630	0.00	0.00	16.50	46.61	63.12
650	0.00	0.00	9.69	56.82	66.51
670	0.00	0.00	13.37	54.00	67.37
1.7°					
	Mean				
λ	Blue	Green	Yellow	Red	Sat
450	69.05	0.00	0.00	9.54	78.59
470	61.58	8.41	0.00	0.00	69.99
490	20.54	29.05	0.00	0.00	49.59
510	0.00	31.59	19.30	0.00	50.89
530	0.00	21.46	29.61	0.00	51.08
550	0.00	6.15	41.56	0.00	47.71
570	0.00	0.00	51.25	3.78	55.03
590	0.00	0.00	37.42	16.10	53.52
610	0.00	0.00	23.79	34.27	58.05
630	0.00	0.00	14.58	51.35	65.93
650	0.00	0.00	8.08	51.93	60.02
670	0.00	0.00	15.79	61.18	76.98
2.25°					
	Mean				
λ	Blue	Green	Yellow	Red	Sat
450	71.20	0.00	0.00	6.77	77.97
470	66.01	7.82	0.00	0.00	73.83
490	28.99	39.35	0.00	0.00	68.35
510	0.00	53.42	16.21	0.00	69.64
530	0.00	34.43	22.94	0.00	57.36
550	0.00	11.93	43.70	0.00	55.63
570	0.00	0.00	53.73	2.91	56.64
590	0.00	0.00	37.20	18.83	56.02
610	0.00	0.00	27.00	35.82	62.82
630	0.00	0.00	17.79	54.84	72.63
650	0.00	0.00	10.24	59.67	69.91
670	0.00	0.00	15.74	63.25	78.99

Standard Error of the Mean					
Blue	Green	Yellow	Red	Sat	
4.89	0.00	0.00	3.46	4.56	
8.21	3.73	0.00	0.00	8.57	
0.00	9.18	7.35	0.00	10.24	
15.55	0.02	0.00	0.00	8.06	
0.00	9.46	9.58	0.00	3.60	
0.00	10.04	12.77	0.00	7.60	
0.00	3.51	1.32	0.00	1.86	
0.00	0.00	7.82	4.10	4.34	
0.00	0.00	11.05	9.91	7.92	
0.00	0.00	7.75	11.41	7.59	
0.00	0.00	7.24	5.72	6.89	
0.00	0.00	4.57	8.59	8.75	
Standard Error of the Mean					
Blue	Green	Yellow	Red	Sat	
5.81	0.00	0.00	1.02	4.89	
4.36	1.67	0.00	0.00	5.67	
3.85	16.93	0.00	0.00	13.17	
0.00	13.45	11.24	0.00	10.74	
0.00	9.70	11.97	0.00	8.13	
0.00	1.37	7.96	0.00	7.04	
0.00	0.00	6.51	1.53	4.98	
0.00	0.00	1.66	5.24	3.58	
0.00	0.00	7.09	4.64	7.15	
0.00	0.00	2.92	8.86	8.37	
0.00	0.00	5.78	14.02	15.81	
0.00	0.00	3.54	3.49	3.69	
Standard Error of the Mean					
Blue	Green	Yellow	Red	Sat	
5.01	0.00	0.00	0.76	4.49	
2.32	3.21	0.00	0.00	3.80	
7.98	12.78	0.00	0.00	5.98	
0.00	7.12	10.38	0.00	2.41	
0.00	5.00	4.74	0.00	6.84	
0.00	4.05	6.56	0.00	3.38	
0.00	0.00	3.53	3.14	2.54	
0.00	0.00	9.22	8.68	5.66	
0.00	0.00	8.23	11.39	3.74	
0.00	0.00	2.26	4.76	3.75	
0.00	0.00	6.37	6.32	6.46	
0.00	0.00	2.26	3.30	2.64	

Monocular Right Eye Left Fixation (Right Nasal)

2.7°					
	Mean				
λ	Blue	Green	Yellow	Red	Sat
450	69.95	0.00	0.00	9.54	79.48
470	68.69	8.90	0.00	0.00	77.59
490	22.19	47.48	0.00	0.00	69.67
510	0.00	58.85	16.53	0.00	75.38
530	0.00	44.30	21.75	0.00	66.06
550	0.00	12.78	47.23	0.00	60.02
570	0.00	0.00	55.50	4.22	59.72
590	0.00	0.00	43.99	12.72	56.72
610	0.00	0.00	27.35	44.60	71.96
630	0.00	0.00	15.02	58.80	73.82
650	0.00	0.00	7.93	65.86	73.79
670	0.00	0.00	12.47	73.44	85.91
3.7°					
	Mean				
λ	Blue	Green	Yellow	Red	Sat
450	75.79	0.00	0.00	5.95	81.74
470	70.52	10.46	0.00	0.00	80.97
490	20.00	55.41	0.00	0.00	75.41
510	0.00	63.97	8.48	0.00	72.46
530	0.00	49.51	22.54	0.00	72.05
550	0.00	27.30	38.20	0.00	65.50
570	0.00	0.00	56.04	8.32	64.37
590	0.00	0.00	43.23	24.05	67.28
610	0.00	0.00	28.57	43.48	72.05
630	0.00	0.00	15.49	59.43	74.92
650	0.00	0.00	10.50	64.77	75.27
670	0.00	0.00	14.99	71.25	86.23

Standard Error of the Mean				
Blue	Green	Yellow	Red	Sat
3.12	0.00	0.00	1.16	3.18
2.38	1.83	0.00	0.00	3.78
6.32	9.20	0.00	0.00	3.94
0.00	7.49	4.84	0.00	2.88
0.00	7.76	7.82	0.00	2.79
0.00	3.64	2.76	0.00	1.55
0.00	0.00	3.48	2.12	1.38
0.00	0.00	2.63	3.25	3.89
0.00	0.00	4.94	5.82	0.97
0.00	0.00	3.79	6.32	3.20
0.00	0.00	4.62	5.00	4.40
0.00	0.00	6.41	3.95	2.61
Standard Error of the Mean				
Blue	Green	Yellow	Red	Sat
4.48	0.00	0.00	1.91	2.57
3.09	2.03	0.00	0.00	1.30
8.53	9.02	0.00	0.00	1.29
0.00	3.81	5.50	0.00	1.27
0.00	12.13	8.46	0.00	3.68
0.00	14.24	12.94	0.00	4.02
0.00	0.00	4.98	3.80	1.23
0.00	0.00	6.92	7.49	0.70
0.00	0.00	2.91	2.21	0.86
0.00	0.00	4.81	7.86	3.32
0.00	0.00	5.88	3.25	2.56
0.00	0.00	2.53	2.44	1.46

Monocular Right Eye Right Fixation (Right Temporal)

1.0°					
	Mean				
λ	Blue	Green	Yellow	Red	Sat
450	68.42	0.00	0.00	9.91	78.33
470	63.55	9.36	0.00	0.00	72.90
490	17.91	60.76	0.00	0.00	78.67
510	0.00	48.62	17.69	0.00	66.31
530	0.00	36.84	27.72	0.00	64.56
550	0.00	19.49	34.85	0.00	55.02
570	0.00	13.55	42.70	0.00	60.25
590	0.00	0.00	42.28	19.75	62.03
610	0.00	0.00	26.66	44.39	71.05
630	0.00	0.00	13.94	61.71	75.64
650	0.00	0.00	10.56	63.95	74.51
670	0.00	0.00	10.66	72.03	82.70
1.7°					
	Mean				
λ	Blue	Green	Yellow	Red	Sat
450	71.03	0.00	0.00	8.24	79.28
470	70.62	8.55	0.00	0.00	79.16
490	25.97	50.76	0.00	0.00	76.73
510	0.00	59.70	16.28	0.00	75.99
530	0.00	41.48	29.88	0.00	71.36
550	0.00	26.66	34.75	0.00	61.42
570	0.00	3.27	56.54	0.00	59.81
590	0.00	0.00	45.89	18.42	64.31
610	0.00	0.00	26.02	44.14	70.16
630	0.00	0.00	14.42	57.57	71.99
650	0.00	0.00	9.31	65.32	74.63
670	0.00	0.00	10.69	72.04	82.74
2.25°					
	Mean				
λ	Blue	Green	Yellow	Red	Sat
450	72.21	0.00	0.00	10.11	82.32
470	72.66	9.69	0.00	0.00	82.35
490	16.75	60.87	0.00	0.00	77.62
510	0.00	66.12	12.68	0.00	78.80
530	0.00	53.76	20.26	0.00	74.01
550	0.00	27.58	38.25	0.00	65.84
570	0.00	0.00	57.58	5.17	62.75
590	0.00	0.00	46.85	17.69	64.54
610	0.00	0.00	30.87	41.98	72.85
630	0.00	0.00	14.07	60.73	74.80
650	0.00	0.00	9.42	64.94	74.36
670	0.00	0.00	14.54	70.45	84.99

Standard Error of the Mean				
Blue	Green	Yellow	Red	Sat
9.33	0.00	0.00	2.59	9.79
6.33	0.28	0.00	0.00	6.48
6.32	2.54	0.00	0.00	3.78
0.00	22.69	12.64	0.00	12.55
0.00	19.65	16.14	0.00	8.01
0.00	16.85	10.21	0.00	9.98
0.00	13.55	6.86	0.00	7.16
0.00	0.00	9.85	10.94	1.23
0.00	0.00	8.58	10.47	2.56
0.00	0.00	7.59	7.77	2.77
0.00	0.00	7.94	3.57	4.26
0.00	0.00	6.58	7.45	4.12
Standard Error of the Mean				
Blue	Green	Yellow	Red	Sat
5.31	0.00	0.00	1.25	5.21
5.82	2.43	0.00	0.00	4.29
11.64	15.79	0.00	0.00	4.50
0.00	6.97	5.39	0.00	2.56
0.00	16.54	13.52	0.00	3.10
0.00	13.37	14.18	0.00	2.83
0.00	3.10	4.88	0.00	3.73
0.00	0.00	9.81	10.02	0.24
0.00	0.00	5.10	7.53	2.56
0.00	0.00	3.63	5.24	3.81
0.00	0.00	5.73	6.04	4.87
0.00	0.00	6.49	6.36	3.04
Standard Error of the Mean				
Blue	Green	Yellow	Red	Sat
5.18	0.00	0.00	1.91	4.50
4.54	0.66	0.00	0.00	3.90
1.59	1.88	0.00	0.00	3.04
0.00	9.75	9.23	0.00	3.76
0.00	8.35	6.93	0.00	2.15
0.00	10.40	7.57	0.00	4.21
0.00	0.00	3.63	2.65	1.51
0.00	0.00	3.75	2.46	1.29
0.00	0.00	8.58	11.05	2.47
0.00	0.00	7.11	9.23	4.59
0.00	0.00	6.38	3.27	4.80
0.00	0.00	2.81	4.92	2.95

Monocular Right Eye Right Fixation (Right Temporal)

2.7°						Standard Error of the Mean				
	Mean					Blue	Green	Yellow	Red	Sat
λ	Blue	Green	Yellow	Red	Sat	Blue	Green	Yellow	Red	Sat
450	74.65	0.00	0.00	9.22	83.87	4.03	0.00	0.00	1.18	3.20
470	65.78	11.12	0.00	0.00	76.91	2.49	1.09	0.00	0.00	1.79
490	19.58	60.16	0.00	0.00	79.74	5.53	3.80	0.00	0.00	1.90
510	0.00	66.08	11.67	0.00	77.74	0.00	4.84	6.52	0.00	2.69
530	0.00	41.79	30.29	0.00	72.08	0.00	17.98	12.88	0.00	6.30
550	0.00	29.00	37.94	0.00	66.94	0.00	14.92	10.99	0.00	5.73
570	0.00	0.00	57.68	5.51	63.20	0.00	0.00	3.12	2.05	1.09
590	0.00	0.00	42.63	22.41	65.04	0.00	0.00	7.01	5.83	1.38
610	0.00	0.00	25.34	48.54	73.88	0.00	0.00	4.79	5.24	0.79
630	0.00	0.00	12.85	66.00	78.85	0.00	0.00	3.71	4.96	1.73
650	0.00	0.00	9.28	67.67	76.95	0.00	0.00	5.14	5.74	3.37
670	0.00	0.00	13.46	71.09	84.56	0.00	0.00	2.27	2.93	1.76
3.7°						Standard Error of the Mean				
	Mean					Blue	Green	Yellow	Red	Sat
λ	Blue	Green	Yellow	Red	Sat	Blue	Green	Yellow	Red	Sat
450	76.76	0.00	0.00	8.85	85.61	5.48	0.00	0.00	2.26	3.23
470	71.54	10.52	0.00	0.00	82.06	3.44	0.93	0.00	0.00	2.53
490	24.93	53.42	0.00	0.00	78.35	8.77	7.34	0.00	0.00	1.95
510	0.00	64.84	15.22	0.00	80.06	0.00	8.26	4.41	0.00	5.23
530	0.00	57.61	19.31	0.00	76.92	0.00	8.12	4.99	0.00	3.27
550	0.00	39.99	30.37	0.00	70.36	0.00	15.12	9.81	0.00	6.17
570	0.00	0.00	55.89	8.10	63.99	0.00	0.00	6.01	3.99	2.72
590	0.00	0.00	45.52	20.62	66.14	0.00	0.00	5.63	5.58	1.38
610	0.00	0.00	22.35	49.97	72.32	0.00	0.00	4.04	4.38	2.21
630	0.00	0.00	10.67	64.41	75.08	0.00	0.00	6.04	6.02	4.54
650	0.00	0.00	7.60	70.00	77.60	0.00	0.00	6.13	3.21	5.28
670	0.00	0.00	12.65	73.32	85.97	0.00	0.00	1.92	2.87	2.34

Binocular Left Fixation (Left Temporal, Right Nasal)

1.0°	Mean				
λ	Blue	Green	Yellow	Red	Sat
450	70.26	0.00	0.00	9.15	79.41
470	64.86	7.56	0.00	0.00	72.42
490	17.95	47.51	0.00	0.00	65.46
510	0.00	56.24	10.52	0.00	66.76
530	0.00	46.35	14.74	0.00	61.09
550	0.00	26.72	36.02	0.00	62.74
570	0.00	0.00	58.13	2.35	60.48
590	0.00	0.00	44.20	18.36	62.56
610	0.00	0.00	29.40	42.17	71.57
630	0.00	0.00	12.41	62.21	74.63
650	0.00	0.00	9.92	65.21	75.12
670	0.00	0.00	10.59	71.30	81.89
1.7°	Mean				
λ	Blue	Green	Yellow	Red	Sat
450	69.98	0.00	0.00	10.15	80.13
470	66.99	9.92	0.00	0.00	76.90
490	23.84	51.93	0.00	0.00	75.77
510	0.00	61.48	13.26	0.00	74.74
530	0.00	52.40	20.15	0.00	72.55
550	0.00	25.97	35.72	0.00	61.69
570	0.00	0.00	59.64	3.01	62.65
590	0.00	0.00	42.70	21.73	64.42
610	0.00	0.00	27.87	41.98	69.86
630	0.00	0.00	10.26	63.33	73.59
650	0.00	0.00	9.12	65.30	74.43
670	0.00	0.00	12.66	68.86	81.52
2.25°	Mean				
λ	Blue	Green	Yellow	Red	Sat
450	80.86	0.00	0.00	8.24	89.11
470	69.18	11.63	0.00	0.00	80.81
490	28.82	48.73	0.00	0.00	77.55
510	0.00	69.60	6.33	0.00	75.92
530	0.00	53.94	18.44	0.00	72.38
550	0.00	32.40	31.10	0.00	63.51
570	0.00	0.00	57.20	5.85	63.04
590	0.00	0.00	48.03	15.43	63.46
610	0.00	0.00	24.93	47.76	72.69
630	0.00	0.00	13.35	62.03	75.38
650	0.00	0.00	9.03	68.31	77.35
670	0.00	0.00	12.52	70.66	83.18

Standard Error of the Mean				
Blue	Green	Yellow	Red	Sat
8.14	0.00	0.00	1.93	6.51
6.49	0.92	0.00	0.00	6.64
2.95	14.85	0.00	0.00	14.24
0.00	14.93	7.25	0.00	11.78
0.00	15.07	1.24	0.00	14.31
0.00	9.90	5.15	0.00	5.93
0.00	0.00	1.77	2.43	0.31
0.00	0.00	5.08	3.44	4.41
0.00	0.00	3.87	4.76	1.00
0.00	0.00	6.71	6.65	3.23
0.00	0.00	7.39	3.81	5.21
0.00	0.00	6.04	3.92	1.46
Standard Error of the Mean				
Blue	Green	Yellow	Red	Sat
5.98	0.00	0.00	0.64	6.10
4.70	1.21	0.00	0.00	3.50
6.46	10.81	0.00	0.00	4.46
0.00	4.42	1.07	0.00	4.16
0.00	11.45	7.02	0.00	4.78
0.00	8.63	4.62	0.00	4.05
0.00	0.00	5.52	0.89	6.31
0.00	0.00	5.54	5.27	1.02
0.00	0.00	5.17	7.16	2.72
0.00	0.00	5.62	6.42	4.87
0.00	0.00	6.28	5.73	6.00
0.00	0.00	2.20	2.68	0.47
Standard Error of the Mean				
Blue	Green	Yellow	Red	Sat
2.59	0.00	0.00	2.45	0.14
4.58	1.22	0.00	0.00	4.08
9.17	9.74	0.00	0.00	2.08
0.00	2.32	4.04	0.00	1.70
0.00	7.81	4.53	0.00	4.25
0.00	13.02	7.41	0.00	5.98
0.00	0.00	5.77	2.25	4.54
0.00	0.00	8.03	4.90	3.21
0.00	0.00	3.38	2.25	1.40
0.00	0.00	4.55	4.01	2.30
0.00	0.00	6.32	4.42	5.55
0.00	0.00	2.18	3.05	1.05

Binocular Left Fixation (Left Temporal, Right Nasal)

2.7°						Standard Error of the Mean				
	Mean					Blue	Green	Yellow	Red	Sat
λ	Blue	Green	Yellow	Red	Sat	Blue	Green	Yellow	Red	Sat
450	73.02	0.00	0.00	10.40	83.42	5.39	0.00	0.00	1.50	4.39
470	69.42	9.24	0.00	0.00	78.66	2.25	1.48	0.00	0.00	2.69
490	27.32	48.43	0.00	0.00	75.76	4.48	4.73	0.00	0.00	1.19
510	5.99	71.68	0.00	0.00	77.68	5.27	4.72	0.00	0.00	3.26
530	0.00	50.57	21.05	0.00	71.62	0.00	7.41	5.22	0.00	2.66
550	0.00	35.09	30.97	0.00	66.07	0.00	12.00	9.64	0.00	3.13
570	0.00	0.00	56.95	6.74	63.69	0.00	0.00	4.99	3.26	1.84
590	0.00	0.00	46.59	18.67	65.26	0.00	0.00	7.47	5.03	2.63
610	0.00	0.00	28.34	42.56	70.90	0.00	0.00	5.93	7.77	3.48
630	0.00	0.00	13.18	61.12	74.29	0.00	0.00	2.70	3.08	3.46
650	0.00	0.00	7.97	67.55	75.52	0.00	0.00	5.05	3.39	3.86
670	0.00	0.00	12.60	72.80	85.39	0.00	0.00	2.97	2.59	2.13
3.7°						Standard Error of the Mean				
	Mean					Blue	Green	Yellow	Red	Sat
λ	Blue	Green	Yellow	Red	Sat	Blue	Green	Yellow	Red	Sat
450	72.54	0.00	0.00	12.21	84.74	5.23	0.00	0.00	1.77	3.59
470	71.90	8.84	0.00	0.00	80.74	2.09	1.75	0.00	0.00	1.52
490	20.03	57.00	0.00	0.00	77.03	5.08	5.14	0.00	0.00	2.05
510	0.00	68.73	10.27	0.00	79.00	0.00	3.39	6.73	0.00	1.28
530	0.00	53.20	19.08	0.00	72.28	0.00	4.17	1.50	0.00	2.77
550	0.00	31.01	35.55	0.00	66.56	0.00	3.70	5.01	0.00	3.29
570	0.00	0.00	59.77	4.43	64.20	0.00	0.00	3.23	3.56	0.79
590	0.00	0.00	47.20	19.12	66.33	0.00	0.00	3.98	4.57	1.22
610	0.00	0.00	23.58	50.36	73.94	0.00	0.00	3.19	4.43	1.26
630	0.00	0.00	14.27	59.37	73.65	0.00	0.00	2.68	5.92	4.46
650	0.00	0.00	9.11	65.22	74.33	0.00	0.00	6.05	5.71	6.51
670	0.00	0.00	13.19	70.92	84.10	0.00	0.00	2.36	3.30	1.30

Binocular Right Fixation (Right Temporal, Left Nasal)

1.0°					
	Mean				
λ	Blue	Green	Yellow	Red	Sat
450	66.10	0.00	0.00	10.32	76.42
470	68.46	4.07	0.00	0.00	72.53
490	14.45	49.69	0.00	0.00	64.13
510	0.00	49.98	17.50	0.00	67.48
530	0.00	44.38	19.04	0.00	63.41
550	0.00	31.63	28.72	0.00	60.36
570	0.00	4.07	58.49	0.00	62.55
590	0.00	0.00	43.58	18.16	61.73
610	0.00	0.00	31.36	35.98	67.34
630	0.00	0.00	14.05	56.68	70.74
650	0.00	0.00	9.84	61.62	71.45
670	0.00	0.00	13.72	69.69	83.41
1.7°					
	Mean				
λ	Blue	Green	Yellow	Red	Sat
450	73.53	0.00	0.00	9.55	83.09
470	67.88	9.05	0.00	0.00	76.93
490	19.62	55.72	0.00	0.00	75.34
510	0.00	69.25	9.82	0.00	79.07
530	0.00	54.05	16.44	0.00	70.49
550	0.00	38.57	27.61	0.00	66.18
570	0.00	3.58	59.62	0.00	63.21
590	0.00	0.00	43.69	25.42	69.11
610	0.00	0.00	25.08	46.92	72.00
630	0.00	0.00	11.19	60.76	71.96
650	0.00	0.00	7.27	66.85	74.11
670	0.00	0.00	15.67	67.83	83.50
2.25°					
	Mean				
λ	Blue	Green	Yellow	Red	Sat
450	77.28	0.00	0.00	7.25	84.53
470	69.08	10.14	0.00	0.00	79.23
490	14.72	63.47	0.00	0.00	78.19
510	0.00	73.94	7.59	0.00	81.53
530	0.00	57.44	16.14	0.00	73.58
550	0.00	36.29	29.76	0.00	66.05
570	0.00	0.00	56.87	3.80	60.67
590	0.00	0.00	49.78	14.20	63.98
610	0.00	0.00	22.20	48.26	70.45
630	0.00	0.00	9.18	64.85	74.03
650	0.00	0.00	7.83	69.07	76.89
670	0.00	0.00	14.92	69.71	84.63

Standard Error of the Mean				
Blue	Green	Yellow	Red	Sat
9.08	0.00	0.00	0.80	8.49
6.71	2.21	0.00	0.00	5.72
2.94	15.28	0.00	0.00	12.34
0.00	14.22	7.55	0.00	6.92
0.00	13.19	5.60	0.00	7.61
0.00	16.34	12.07	0.00	8.27
0.00	4.38	7.35	0.00	8.21
0.00	0.00	7.75	8.48	2.34
0.00	0.00	7.32	11.89	5.26
0.00	0.00	4.14	7.58	4.47
0.00	0.00	7.26	2.46	3.18
0.00	0.00	3.78	6.71	3.21
Standard Error of the Mean				
Blue	Green	Yellow	Red	Sat
4.89	0.00	0.00	1.30	4.42
4.46	2.22	0.00	0.00	2.24
13.66	12.64	0.00	0.00	1.53
0.00	5.90	5.86	0.00	4.73
0.00	5.30	4.72	0.00	2.08
0.00	12.80	8.91	0.00	4.85
0.00	2.21	3.83	0.00	3.36
0.00	0.00	8.83	7.07	4.29
0.00	0.00	2.64	2.73	1.69
0.00	0.00	6.54	7.14	4.13
0.00	0.00	6.01	1.06	3.08
0.00	0.00	1.62	2.96	3.08
Standard Error of the Mean				
Blue	Green	Yellow	Red	Sat
3.04	0.00	0.00	0.80	3.81
1.73	1.37	0.00	0.00	2.33
4.10	5.65	0.00	0.00	2.70
0.00	4.60	5.07	0.00	3.89
0.00	5.79	3.26	0.00	2.71
0.00	9.73	6.42	0.00	4.66
0.00	0.00	5.66	3.58	4.08
0.00	0.00	6.36	5.33	1.03
0.00	0.00	3.41	3.25	0.17
0.00	0.00	5.15	5.10	2.69
0.00	0.00	5.34	2.64	3.37
0.00	0.00	1.61	3.00	2.16

Binocular Right Fixation (Right Temporal, Left Nasal)

2.7°					
	Mean				
λ	Blue	Green	Yellow	Red	Sat
450	75.25	0.00	0.00	9.74	85.00
470	71.51	11.20	0.00	0.00	82.71
490	15.86	65.16	0.00	0.00	81.02
510	0.00	74.69	8.51	0.00	83.20
530	0.00	60.26	12.60	0.00	72.87
550	0.00	42.18	27.97	0.00	70.15
570	0.00	0.00	61.74	1.73	63.47
590	0.00	0.00	48.59	19.13	67.72
610	0.00	0.00	22.90	50.68	73.58
630	0.00	0.00	14.57	61.26	75.84
650	0.00	0.00	9.11	63.42	72.53
670	0.00	0.00	13.44	74.66	88.11
3.7°					
	Mean				
λ	Blue	Green	Yellow	Red	Sat
450	75.04	0.00	0.00	12.67	87.71
470	70.57	8.31	0.00	0.00	78.87
490	17.31	60.96	0.00	0.00	78.27
510	0.00	70.71	9.90	0.00	80.61
530	0.00	54.10	20.79	0.00	74.90
550	0.00	31.64	35.44	0.00	67.08
570	0.00	0.00	60.63	1.81	62.45
590	0.00	0.00	47.19	17.91	65.10
610	0.00	0.00	31.43	41.60	73.03
630	0.00	0.00	11.94	64.30	76.24
650	0.00	0.00	6.89	68.47	75.36
670	0.00	0.00	14.02	71.64	85.66

Standard Error of the Mean				
Blue	Green	Yellow	Red	Sat
4.91	0.00	0.00	2.51	2.41
4.11	2.87	0.00	0.00	3.00
2.05	3.64	0.00	0.00	2.30
0.00	4.99	5.66	0.00	4.15
0.00	4.55	6.55	0.00	1.66
0.00	10.72	9.03	0.00	2.50
0.00	0.00	3.32	2.16	2.44
0.00	0.00	5.61	6.50	0.90
0.00	0.00	5.00	5.64	0.77
0.00	0.00	3.99	4.81	1.10
0.00	0.00	6.56	7.00	8.21
0.00	0.00	2.35	3.73	2.51
Standard Error of the Mean				
Blue	Green	Yellow	Red	Sat
4.67	0.00	0.00	2.10	2.61
3.63	1.26	0.00	0.00	3.06
1.14	1.28	0.00	0.00	0.21
0.00	3.69	5.56	0.00	1.59
0.00	7.61	3.78	0.00	4.59
0.00	13.41	9.37	0.00	5.88
0.00	0.00	1.75	1.68	1.24
0.00	0.00	6.35	6.57	0.40
0.00	0.00	9.54	9.51	0.42
0.00	0.00	2.42	3.33	2.36
0.00	0.00	4.47	4.91	5.38
0.00	0.00	3.25	4.49	2.40

Monocular Left Fovea

1.0°	Mean				
λ	Blue	Green	Yellow	Red	Sat
450	72.35	0.00	0.00	13.99	86.33
470	73.56	6.33	0.00	0.00	79.89
490	47.29	28.87	0.00	0.00	76.16
510	36.61	37.85	0.00	0.00	74.46
530	9.63	61.20	0.00	0.00	70.83
550	0.00	47.17	20.39	0.00	67.57
570	0.00	0.00	56.66	4.87	61.53
590	0.00	0.00	38.13	30.04	68.17
610	0.00	0.00	21.19	55.90	77.09
630	0.00	0.00	10.04	68.52	78.56
650	0.00	0.00	10.85	69.09	79.94
670	0.00	0.00	14.15	71.80	85.95

Standard Error of the Mean				
Blue	Green	Yellow	Red	Sat
5.30	0.00	0.00	1.21	4.16
0.80	0.82	0.00	0.00	0.92
8.91	10.20	0.00	0.00	1.37
8.64	9.36	0.00	0.00	2.87
9.32	7.44	0.00	0.00	2.55
0.00	6.36	2.94	0.00	3.42
0.00	0.00	2.00	3.68	1.35
0.00	0.00	9.27	11.28	2.15
0.00	0.00	6.86	7.54	1.24
0.00	0.00	5.39	4.46	1.97
0.00	0.00	6.33	3.68	2.38
0.00	0.00	1.11	3.11	3.11

Monocular Right Fovea

1.0°	Mean				
λ	Blue	Green	Yellow	Red	Sat
450	74.06	0.00	0.00	12.86	86.92
470	73.53	8.57	0.00	0.00	82.09
490	49.82	27.77	0.00	0.00	77.59
510	33.50	43.83	0.00	0.00	77.33
530	14.78	57.60	0.00	0.00	72.38
550	0.00	36.83	30.19	0.00	67.01
570	0.00	0.00	55.26	9.88	65.14
590	0.00	0.00	35.78	31.91	67.69
610	0.00	0.00	18.67	57.00	75.67
630	0.00	0.00	14.04	66.60	80.65
650	0.00	0.00	9.01	70.47	79.48
670	0.00	0.00	13.17	74.02	87.19

Standard Error of the Mean				
Blue	Green	Yellow	Red	Sat
4.30	0.00	0.00	0.40	4.32
1.72	0.64	0.00	0.00	1.38
7.62	8.63	0.00	0.00	1.05
12.30	11.75	0.00	0.00	0.84
8.06	4.64	0.00	0.00	2.12
0.00	9.65	8.23	0.00	1.69
0.00	0.00	5.19	6.64	0.44
0.00	0.00	6.90	7.30	0.65
0.00	0.00	2.68	3.48	1.32
0.00	0.00	1.62	2.43	1.22
0.00	0.00	2.34	5.00	5.27
0.00	0.00	1.43	4.65	3.89

Binocular Fovea

1.0°	Mean				
λ	Blue	Green	Yellow	Red	Sat
450	75.41	0.00	0.00	12.61	88.02
470	75.73	5.14	0.00	0.00	80.88
490	52.57	24.97	0.00	0.00	77.54
510	35.02	42.93	0.00	0.00	77.95
530	18.46	51.34	0.00	0.00	69.80
550	0.00	42.25	26.16	0.00	68.41
570	0.00	0.00	61.18	6.48	67.65
590	0.00	0.00	40.04	31.21	71.25
610	0.00	0.00	19.85	57.11	76.95
630	0.00	0.00	13.87	64.75	78.62
650	0.00	0.00	8.63	72.08	80.71
670	0.00	0.00	14.30	70.68	84.98

Standard Error of the Mean				
Blue	Green	Yellow	Red	Sat
2.83	0.00	0.00	1.60	3.62
1.02	2.82	0.00	0.00	1.74
7.54	9.29	0.00	0.00	3.22
3.82	4.36	0.00	0.00	0.54
10.68	4.68	0.00	0.00	1.78
0.00	11.90	9.86	0.00	3.15
0.00	0.00	3.02	2.94	1.07
0.00	0.00	9.48	10.55	1.70
0.00	0.00	3.73	5.11	1.46
0.00	0.00	3.85	5.70	1.93
0.00	0.00	5.35	3.89	3.43
0.00	0.00	1.26	2.49	3.75

APPENDIX B.

Monocular Left Eye Left Fixation (Left Temporal)

1.7°					
	Mean				
λ	Blue	Green	Yellow	Red	Sat
450	71.01	3.40	0.00	0.00	74.41
470	53.07	5.95	0.00	0.00	59.02
490	0.00	63.03	9.80	0.00	72.84
510	0.00	48.29	17.51	0.00	65.80
530	0.00	32.05	36.21	0.00	68.26
550	0.00	16.32	38.42	0.00	54.74
570	0.00	0.00	46.85	14.48	61.33
590	0.00	0.00	34.72	31.29	66.01
610	0.00	0.00	27.19	42.61	69.79
630	0.00	0.00	12.97	63.77	76.74
650	0.00	0.00	3.06	78.36	81.42
670	0.00	0.00	11.10	65.96	77.06
2.7°					
	Mean				
λ	Blue	Green	Yellow	Red	Sat
450	69.29	0.00	0.00	2.12	71.41
470	55.49	9.76	0.00	0.00	65.25
490	0.00	59.56	11.78	0.00	71.34
510	0.00	56.87	12.78	0.00	69.65
530	0.00	36.89	24.43	0.00	61.32
550	0.00	25.47	28.66	0.00	54.13
570	0.00	0.00	51.41	5.59	57.00
590	0.00	0.00	31.84	31.13	62.96
610	0.00	0.00	22.52	46.58	69.10
630	0.00	0.00	11.64	68.00	79.64
650	0.00	0.00	4.19	77.58	81.77
670	0.00	0.00	12.20	65.95	78.15
3.7°					
	Mean				
λ	Blue	Green	Yellow	Red	Sat
450	69.38	2.20	0.00	0.00	71.58
470	62.50	7.79	0.00	0.00	70.29
490	0.00	51.64	17.78	0.00	69.42
510	0.00	49.45	19.14	0.00	68.59
530	0.00	38.97	24.70	0.00	63.67
550	0.00	3.23	55.42	0.00	58.66
570	0.00	0.00	55.69	10.56	66.24
590	0.00	0.00	39.98	26.04	66.02
610	0.00	0.00	20.04	50.11	70.15
630	0.00	0.00	12.85	64.98	77.82
650	2.68	0.00	0.00	77.67	80.34
670	0.00	0.00	12.55	68.17	80.73

Standard Error of the Mean				
Blue	Green	Yellow	Red	Sat
5.28	3.75	0.00	1.87	2.85
5.60	2.44	0.00	0.00	3.79
2.72	6.81	4.87	0.00	4.83
0.00	8.61	4.94	0.00	3.84
0.00	7.19	12.48	0.00	5.57
0.00	4.68	6.68	0.00	3.40
0.00	0.00	5.81	6.08	4.45
0.00	0.00	6.18	5.03	2.99
0.00	0.00	5.53	6.99	3.02
0.00	0.00	3.30	5.01	2.06
1.95	0.00	2.59	3.61	3.49
0.00	0.00	2.20	1.88	1.11
Standard Error of the Mean				
Blue	Green	Yellow	Red	Sat
3.36	0.00	0.00	2.12	2.19
2.31	1.32	0.00	0.00	1.45
0.00	3.91	2.57	0.00	1.41
0.00	6.74	2.32	0.00	4.49
0.00	5.44	4.95	0.00	2.22
0.00	8.80	9.98	0.00	6.30
0.00	0.00	4.15	1.33	5.47
0.00	0.00	2.64	2.99	2.70
0.00	0.00	2.19	5.05	2.86
0.00	0.00	3.23	1.57	1.68
0.00	0.00	2.17	2.43	0.68
0.00	0.00	1.23	1.28	0.33
Standard Error of the Mean				
Blue	Green	Yellow	Red	Sat
7.51	2.84	0.00	1.86	5.78
1.57	0.20	0.00	0.00	1.77
0.00	5.94	3.79	0.00	3.26
0.00	4.97	2.11	0.00	2.90
0.00	6.53	3.93	0.00	2.65
0.00	3.29	3.86	2.89	2.63
0.00	0.00	1.77	2.76	1.97
0.00	0.00	5.11	1.62	4.28
0.00	0.00	2.02	4.77	2.85
0.00	0.00	2.26	2.81	0.65
3.04	0.00	1.53	4.40	4.41
0.00	0.00	3.70	5.13	1.66

Monocular Left Eye Right Fixation (Left Nasal)

1.7°					
	Mean				
λ	Blue	Green	Yellow	Red	Sat
450	69.37	0.00	0.00	8.08	77.45
470	61.33	8.45	0.00	0.00	69.78
490	0.00	55.11	15.71	0.00	70.82
510	0.00	33.77	20.83	0.00	54.60
530	0.00	28.50	28.59	0.00	57.09
550	0.00	11.17	38.27	0.00	49.45
570	0.00	2.36	53.97	0.00	56.32
590	0.00	0.00	45.62	15.67	61.29
610	0.00	0.00	35.89	26.71	62.59
630	0.00	0.00	26.39	41.08	67.46
650	0.00	0.00	12.91	58.89	71.80
670	0.00	0.00	15.73	59.69	75.42
2.7°					
	Mean				
λ	Blue	Green	Yellow	Red	Sat
450	69.20	0.00	0.00	6.69	75.90
470	65.49	8.06	0.00	0.00	73.55
490	0.00	62.41	9.58	0.00	71.99
510	0.00	53.29	16.82	0.00	70.11
530	0.00	32.48	27.69	0.00	60.17
550	0.00	10.40	36.81	0.00	47.21
570	0.00	3.88	56.85	0.00	60.73
590	0.00	0.00	45.08	20.34	65.41
610	0.00	0.00	25.41	40.88	66.29
630	0.00	0.00	19.24	54.63	73.87
650	0.00	0.00	8.54	69.80	78.34
670	0.00	0.00	14.15	66.57	80.71
3.7°					
	Mean				
λ	Blue	Green	Yellow	Red	Sat
450	65.12	0.00	0.00	6.89	72.01
470	62.76	9.08	0.00	0.00	71.84
490	6.35	65.90	0.00	0.00	72.24
510	0.00	53.31	11.31	0.00	64.62
530	0.00	35.68	21.31	0.00	57.00
550	0.00	23.39	23.01	0.00	46.40
570	0.00	0.00	49.85	9.14	58.99
590	0.00	0.00	38.35	20.17	58.52
610	0.00	0.00	28.01	39.76	67.77
630	0.00	0.00	19.12	53.30	72.42
650	0.00	0.00	12.13	61.01	73.14
670	0.00	0.00	9.71	67.84	77.55

Standard Error of the Mean				
Blue	Green	Yellow	Red	Sat
2.20	0.00	0.00	0.74	2.80
8.00	2.96	0.00	0.00	5.98
0.00	1.50	0.31	0.00	1.72
0.00	4.96	2.05	0.00	4.83
0.00	3.64	2.64	0.00	1.98
0.00	4.16	7.38	0.00	7.72
0.00	2.94	3.35	1.86	5.40
0.00	0.00	5.36	2.06	4.85
0.00	0.00	2.03	4.87	3.88
0.00	0.00	4.30	7.07	5.44
0.00	0.00	6.16	9.14	3.11
0.00	0.00	4.93	4.83	2.06
Standard Error of the Mean				
Blue	Green	Yellow	Red	Sat
1.30	0.00	0.00	1.01	0.31
1.64	0.73	0.00	0.00	1.05
0.00	1.12	1.32	0.00	2.44
0.00	5.71	2.19	0.00	5.28
0.00	2.82	2.32	0.00	1.55
0.00	10.18	3.71	1.46	6.29
0.00	2.86	3.96	1.96	3.77
0.00	0.00	4.53	4.85	3.35
0.00	0.00	1.36	3.85	2.50
0.00	0.00	2.05	3.51	1.51
2.43	0.00	5.20	4.88	2.27
0.00	0.00	5.60	8.34	3.23
Standard Error of the Mean				
Blue	Green	Yellow	Red	Sat
3.42	0.00	0.00	3.48	1.70
5.87	1.79	0.00	0.00	4.55
3.88	9.08	2.48	0.00	7.05
0.90	8.35	3.92	0.00	10.91
0.00	4.58	2.29	0.00	5.95
0.00	5.37	6.79	0.00	4.84
0.00	0.00	5.69	2.33	3.46
0.00	0.00	5.15	4.45	5.86
0.00	0.00	2.15	2.61	2.82
0.00	0.00	1.03	2.95	2.80
0.00	0.00	2.49	7.64	5.27
0.00	0.00	1.44	3.03	3.26

Monocular Right Eye Left Fixation (Right Nasal)

1.7°					
	Mean				
λ	Blue	Green	Yellow	Red	Sat
450	64.65	2.38	0.00	0.00	67.04
470	60.13	5.17	0.00	0.00	65.31
490	0.00	49.87	13.69	0.00	63.56
510	0.00	30.74	20.55	0.00	51.29
530	0.00	16.05	46.37	0.00	62.41
550	0.00	3.36	47.31	0.00	50.67
570	0.00	0.00	51.55	6.43	57.97
590	0.00	0.00	48.24	18.70	66.94
610	0.00	0.00	33.40	41.07	74.46
630	0.00	0.00	18.33	53.85	72.18
650	0.00	0.00	7.43	70.58	78.01
670	0.00	0.00	2.48	78.97	81.46
2.7°					
	Mean				
λ	Blue	Green	Yellow	Red	Sat
450	77.13	0.00	0.00	2.59	79.73
470	61.25	7.60	0.00	0.00	68.85
490	0.00	62.15	13.23	0.00	75.38
510	0.00	53.74	17.38	0.00	71.12
530	0.00	34.44	31.34	0.00	65.78
550	0.00	7.90	48.12	0.00	56.02
570	0.00	0.00	59.02	8.96	67.97
590	0.00	0.00	40.91	21.77	62.68
610	0.00	0.00	24.82	44.73	69.55
630	0.00	0.00	16.80	58.82	75.62
650	0.00	0.00	7.76	69.65	77.40
670	0.00	0.00	8.68	72.93	81.61
3.7°					
	Mean				
λ	Blue	Green	Yellow	Red	Sat
450	64.17	0.00	0.00	5.37	69.54
470	63.12	9.81	0.00	0.00	72.93
490	3.80	73.24	0.00	0.00	77.05
510	0.00	55.83	13.85	0.00	69.68
530	0.00	38.66	22.63	0.00	61.30
550	0.00	7.04	40.97	0.00	48.00
570	0.00	0.00	48.32	14.55	62.87
590	0.00	0.00	43.37	20.64	64.01
610	0.00	0.00	26.55	41.01	67.56
630	0.00	0.00	14.27	59.89	74.16
650	0.00	0.00	4.16	74.68	78.84
670	0.00	0.00	7.41	72.28	79.69

Standard Error of the Mean				
Blue	Green	Yellow	Red	Sat
4.26	2.38	0.00	0.00	2.53
8.37	2.91	0.00	0.00	5.62
0.00	5.88	1.78	0.00	7.59
0.00	4.57	4.13	0.00	3.16
0.00	5.49	5.68	0.00	0.69
0.00	1.90	4.49	0.90	5.26
0.00	0.00	2.03	0.25	2.29
0.00	0.00	2.05	2.48	1.30
0.00	0.00	1.44	1.84	1.59
0.00	0.00	2.72	1.85	1.71
0.00	0.00	2.47	3.10	2.30
1.79	0.00	3.02	1.97	1.43
Standard Error of the Mean				
Blue	Green	Yellow	Red	Sat
1.60	0.00	0.00	1.50	1.82
1.52	0.66	0.00	0.00	1.96
0.00	7.42	3.67	0.00	3.94
0.00	5.53	3.98	0.00	2.59
0.00	9.79	11.04	0.00	7.24
0.00	1.48	5.59	0.00	5.03
0.00	0.00	3.08	0.88	2.56
0.00	0.00	5.22	4.62	2.23
0.00	0.00	1.34	2.07	1.19
0.00	0.00	1.40	4.46	3.29
0.00	0.00	2.23	2.66	1.74
0.00	0.00	2.71	4.15	1.47
Standard Error of the Mean				
Blue	Green	Yellow	Red	Sat
0.90	0.00	0.00	0.58	1.15
2.12	1.64	0.00	0.00	3.16
3.93	4.76	1.63	0.00	3.18
3.09	6.97	5.98	0.00	4.21
0.00	7.39	3.42	0.00	4.69
0.00	4.11	7.27	1.24	4.03
0.00	0.00	2.70	2.34	4.77
0.00	0.00	1.42	2.36	1.31
0.00	0.00	1.91	3.73	2.21
0.00	0.00	3.33	4.32	2.79
0.00	0.00	1.41	4.27	3.32
0.00	0.00	3.04	3.73	1.66

Monocular Right Eye Right Fixation (Right Temporal)

1.7°	Mean				
λ	Blue	Green	Yellow	Red	Sat
450	70.36	0.00	0.00	8.20	78.55
470	61.16	10.52	0.00	0.00	71.68
490	0.00	57.67	7.77	0.00	65.44
510	7.10	46.35	0.00	0.00	53.46
530	0.00	38.58	23.90	0.00	62.48
550	0.00	17.19	29.41	0.00	46.59
570	0.00	0.00	45.73	6.05	51.78
590	0.00	0.00	41.93	16.45	58.37
610	0.00	0.00	22.98	44.50	67.48
630	0.00	0.00	12.05	58.22	70.27
650	0.00	0.00	7.80	67.00	74.80
670	7.34	0.00	0.00	76.11	83.45
2.7°	Mean				
λ	Blue	Green	Yellow	Red	Sat
450	63.55	0.00	0.00	9.68	73.23
470	63.76	10.11	0.00	0.00	73.87
490	9.83	63.26	0.00	0.00	73.09
510	0.00	49.16	20.02	0.00	69.18
530	0.00	39.01	22.98	0.00	61.99
550	0.00	17.09	31.20	0.00	48.30
570	0.00	0.00	47.21	6.85	54.05
590	0.00	0.00	30.53	35.44	65.97
610	0.00	0.00	22.59	52.41	75.01
630	0.00	0.00	8.26	70.32	78.58
650	5.98	0.00	0.00	76.62	82.60
670	0.00	0.00	6.05	76.42	82.47
3.7°	Mean				
λ	Blue	Green	Yellow	Red	Sat
450	67.60	0.00	0.00	8.86	76.46
470	69.52	7.99	0.00	0.00	77.51
490	8.20	64.40	0.00	0.00	72.60
510	0.00	55.65	14.56	0.00	70.20
530	0.00	47.23	20.54	0.00	67.77
550	0.00	24.54	36.54	0.00	61.08
570	0.00	0.00	49.22	12.97	62.19
590	0.00	0.00	26.32	35.34	61.66
610	0.00	0.00	18.17	54.83	73.00
630	0.00	0.00	7.78	67.31	75.09
650	6.82	0.00	0.00	76.29	83.12
670	0.00	0.00	2.76	82.21	84.97

Standard Error of the Mean				
Blue	Green	Yellow	Red	Sat
3.64	0.00	0.00	0.84	4.32
0.92	3.00	0.00	0.00	2.15
2.55	3.19	5.02	0.00	3.87
6.98	3.36	5.44	0.00	3.53
0.00	18.71	18.54	1.99	2.46
0.00	7.16	6.92	0.00	1.13
0.00	0.00	4.20	3.05	4.98
0.00	0.00	5.32	5.39	0.38
0.00	0.00	1.39	1.23	1.92
0.00	0.00	4.74	1.81	3.67
1.43	0.00	4.37	2.49	3.74
1.04	0.00	0.00	2.19	1.15
Standard Error of the Mean				
Blue	Green	Yellow	Red	Sat
1.81	0.00	0.00	1.86	3.21
2.33	3.56	0.00	0.00	1.51
7.96	3.37	5.00	0.00	2.30
0.00	3.25	3.42	0.00	0.26
0.00	1.82	2.31	0.00	1.79
0.00	8.55	6.85	0.00	1.86
0.00	0.00	2.97	2.69	1.67
0.00	0.00	7.26	8.21	1.47
0.00	0.00	0.44	4.96	4.58
4.02	0.00	5.90	1.28	1.61
0.65	0.00	0.00	1.69	1.07
3.22	0.00	4.41	2.67	2.54
Standard Error of the Mean				
Blue	Green	Yellow	Red	Sat
2.22	0.00	0.00	1.11	2.69
0.94	1.04	0.00	0.00	0.96
5.63	7.39	2.86	0.00	4.41
0.00	4.90	1.95	0.00	3.22
0.00	4.71	2.97	0.00	2.41
0.00	5.85	6.83	0.00	1.79
0.00	0.00	3.91	4.10	0.83
0.00	0.00	1.86	4.21	3.92
0.00	0.00	1.43	3.19	3.57
1.45	0.00	4.33	2.85	3.66
0.95	0.00	0.00	2.45	3.30
2.54	0.00	3.69	1.58	2.10

Binocular Left Fixation (Left Temporal, Right Nasal)

1.7°					
	Mean				
λ	Blue	Green	Yellow	Red	Sat
450	70.23	0.00	0.00	3.77	74.00
470	60.11	5.16	0.00	0.00	65.27
490	0.00	55.94	10.05	0.00	65.99
510	0.00	51.71	14.35	0.00	66.05
530	0.00	37.29	28.69	0.00	65.97
550	0.00	9.72	49.00	0.00	58.72
570	0.00	0.00	53.26	4.69	57.94
590	0.00	0.00	38.27	23.82	62.09
610	0.00	0.00	27.90	40.34	68.24
630	0.00	0.00	12.39	62.70	75.09
650	0.00	0.00	4.39	77.82	82.22
670	0.00	0.00	10.59	68.02	78.60
2.7°					
	Mean				
λ	Blue	Green	Yellow	Red	Sat
450	69.66	0.00	0.00	3.94	73.60
470	62.47	8.08	0.00	0.00	70.55
490	11.72	61.64	0.00	0.00	73.36
510	0.00	61.54	12.72	0.00	74.26
530	0.00	50.80	19.75	0.00	70.55
550	0.00	38.55	22.72	0.00	61.27
570	0.00	0.00	51.47	8.24	59.71
590	0.00	0.00	30.37	32.37	62.74
610	0.00	0.00	23.20	47.17	70.37
630	0.00	0.00	11.33	64.80	76.13
650	0.00	0.00	6.97	74.41	81.38
670	0.00	0.00	7.54	73.11	80.66
3.7°					
	Mean				
λ	Blue	Green	Yellow	Red	Sat
450	68.92	0.00	0.00	6.10	75.02
470	59.78	6.93	0.00	0.00	66.71
490	7.29	70.06	0.00	0.00	77.35
510	0.00	53.27	16.03	0.00	69.30
530	0.00	48.02	17.02	0.00	65.05
550	0.00	26.54	29.37	0.00	55.91
570	0.00	0.00	56.09	8.20	64.29
590	0.00	0.00	37.82	27.16	64.98
610	0.00	0.00	17.92	57.51	75.43
630	0.00	0.00	8.58	71.36	79.94
650	0.00	0.00	7.57	73.49	81.06
670	0.00	0.00	10.66	71.94	82.60

Standard Error of the Mean				
Blue	Green	Yellow	Red	Sat
2.71	0.00	0.00	3.58	4.04
5.17	3.29	0.00	0.00	1.89
0.00	5.33	6.88	0.00	4.29
0.00	8.08	3.89	0.00	4.70
0.00	10.70	10.34	0.00	4.02
0.00	1.53	5.53	0.00	4.09
0.00	0.00	5.66	0.64	6.01
0.00	0.00	5.73	2.25	3.49
0.00	0.00	3.76	4.20	1.99
0.00	0.00	4.27	5.06	1.85
2.20	0.00	4.71	1.16	3.10
0.00	0.00	1.88	2.50	1.78
Standard Error of the Mean				
Blue	Green	Yellow	Red	Sat
1.94	0.00	0.00	2.12	3.57
2.97	2.07	0.00	0.00	1.68
3.56	5.74	0.00	0.00	2.22
0.00	8.02	4.21	0.00	3.86
0.00	3.37	2.28	0.00	1.64
0.00	3.07	3.29	0.00	0.45
0.00	0.00	2.32	1.55	1.02
0.00	0.00	2.32	1.06	2.77
0.00	0.00	0.16	2.57	2.63
3.35	0.00	6.37	5.26	4.09
2.63	0.00	5.19	4.69	2.90
4.29	0.00	5.66	1.91	1.09
Standard Error of the Mean				
Blue	Green	Yellow	Red	Sat
1.53	0.00	0.00	0.61	1.07
1.52	0.45	0.00	0.00	1.52
1.10	4.28	0.00	0.00	3.84
0.00	4.11	2.40	0.00	2.34
0.00	1.46	1.27	0.00	2.10
0.00	13.27	7.93	0.00	5.68
0.00	0.00	4.12	1.72	3.99
0.00	0.00	1.77	2.00	0.24
0.00	0.00	2.07	0.22	2.15
0.00	0.00	1.82	0.66	1.27
2.50	0.00	4.98	2.50	1.34
0.00	0.00	3.54	4.42	1.07

Binocular Right Fixation (Right Temporal, Left Nasal)

1.7°					
	Mean				
λ	Blue	Green	Yellow	Red	Sat
450	65.78	0.00	0.00	10.58	76.36
470	62.71	6.87	0.00	0.00	69.57
490	0.00	59.22	9.12	0.00	68.34
510	0.00	37.44	21.93	0.00	59.37
530	0.00	31.37	29.96	0.00	61.33
550	0.00	0.00	43.53	2.82	46.36
570	0.00	0.00	46.97	13.75	60.72
590	0.00	0.00	38.61	29.22	67.83
610	0.00	0.00	20.90	48.18	69.08
630	0.00	0.00	12.98	59.94	72.92
650	6.14	0.00	0.00	71.46	77.60
670	0.00	0.00	10.54	71.22	81.76
2.7°					
	Mean				
λ	Blue	Green	Yellow	Red	Sat
450	69.90	0.00	0.00	6.08	75.98
470	60.39	9.51	0.00	0.00	69.89
490	0.00	64.90	6.66	0.00	71.57
510	0.00	57.64	12.34	0.00	69.99
530	0.00	56.24	13.25	0.00	69.49
550	0.00	25.57	26.02	0.00	51.59
570	0.00	0.00	50.70	14.64	65.34
590	0.00	0.00	32.71	32.27	64.98
610	0.00	0.00	20.67	51.44	72.11
630	0.00	0.00	8.27	71.45	79.71
650	6.40	0.00	0.00	72.73	79.14
670	0.00	0.00	6.12	74.15	80.28
3.7°					
	Mean				
λ	Blue	Green	Yellow	Red	Sat
450	69.82	0.00	0.00	7.94	77.76
470	64.42	7.49	0.00	0.00	71.90
490	0.00	63.04	6.03	0.00	69.07
510	0.00	50.44	18.97	0.00	69.40
530	0.00	37.72	23.78	0.00	61.51
550	0.00	23.84	21.89	0.00	45.74
570	0.00	0.00	48.16	4.67	52.83
590	0.00	0.00	37.86	30.44	68.30
610	0.00	0.00	19.24	52.05	71.30
630	0.00	0.00	16.64	61.43	78.07
650	3.45	0.00	0.00	75.08	78.53
670	0.00	0.00	5.66	78.10	83.75

Standard Error of the Mean				
Blue	Green	Yellow	Red	Sat
2.49	0.00	0.00	1.95	2.49
2.25	3.20	0.00	0.00	1.44
0.00	7.32	4.00	0.00	6.22
0.00	13.72	8.81	0.00	8.93
0.00	9.31	7.89	0.00	3.80
0.00	0.00	5.39	1.82	5.87
0.00	0.00	2.62	3.50	3.80
0.00	0.00	5.03	6.16	1.27
0.00	0.00	2.31	4.53	2.25
0.00	0.00	5.77	3.79	3.19
3.93	0.00	0.00	0.73	2.57
0.00	0.00	2.52	2.99	0.48
Standard Error of the Mean				
Blue	Green	Yellow	Red	Sat
0.97	0.00	0.00	1.31	1.62
4.93	1.84	0.00	0.00	4.42
0.00	7.22	4.35	0.00	4.56
0.00	6.48	2.87	0.00	5.15
0.00	1.93	1.85	0.00	3.73
0.00	10.49	10.29	0.00	7.20
0.00	0.00	0.21	2.66	2.86
0.00	0.00	4.03	4.35	0.63
0.00	0.00	1.28	0.88	0.48
0.00	0.00	0.42	2.38	2.17
0.65	0.00	0.00	5.06	5.11
1.67	0.00	3.43	0.52	0.96
Standard Error of the Mean				
Blue	Green	Yellow	Red	Sat
1.29	0.00	0.00	1.73	2.71
2.45	1.29	0.00	0.00	3.63
0.00	1.71	6.30	0.00	4.21
0.00	6.81	6.54	0.00	4.58
0.00	1.44	0.75	0.00	0.99
0.00	1.16	1.18	0.00	1.19
0.00	0.00	3.74	0.78	4.11
0.00	0.00	7.48	4.86	2.64
0.00	0.00	1.55	4.77	3.44
0.00	0.00	1.06	3.16	2.64
2.35	0.00	0.00	1.10	1.18
0.00	0.00	2.84	3.22	2.60

Monocular Left Fovea

1.0°	Mean				
λ	Blue	Green	Yellow	Red	Sat
450	69.02	0.00	0.00	7.44	76.46
470	70.02	3.66	0.00	0.00	73.68
490	12.97	61.21	0.00	0.00	74.19
510	9.36	71.70	0.00	0.00	81.06
530	0.00	50.58	18.91	0.00	69.49
550	0.00	31.33	29.52	0.00	60.85
570	0.00	0.00	45.25	22.50	67.75
590	0.00	0.00	23.36	42.11	65.47
610	0.00	0.00	18.28	51.77	70.04
630	0.00	0.00	6.45	72.74	79.19
650	3.60	0.00	0.00	78.97	82.58
670	0.00	0.00	4.86	76.70	81.56

Standard Error of the Mean				
Blue	Green	Yellow	Red	Sat
2.45	0.00	0.00	0.62	2.74
4.26	1.91	0.00	0.00	2.40
1.65	5.23	0.00	0.00	3.60
4.25	3.42	0.00	0.00	1.34
0.00	7.63	6.22	0.00	1.57
0.00	14.74	7.98	0.00	6.76
0.00	0.00	3.84	4.29	2.19
0.00	0.00	2.85	2.84	0.97
0.00	0.00	1.85	1.64	1.93
2.43	0.00	3.98	1.46	0.71
2.48	0.00	1.74	0.78	0.83
0.00	0.00	2.67	1.53	2.07

Monocular Right Fovea

1.0°	Mean				
λ	Blue	Green	Yellow	Red	Sat
450	69.18	0.00	0.00	6.16	75.34
470	76.44	4.65	0.00	0.00	81.09
490	20.54	58.34	0.00	0.00	78.88
510	9.94	70.71	0.00	0.00	80.65
530	0.00	60.18	10.91	0.00	71.08
550	0.00	52.55	12.48	0.00	65.02
570	0.00	0.00	49.12	7.93	57.05
590	0.00	0.00	27.88	39.40	67.27
610	0.00	0.00	19.35	53.16	72.52
630	0.00	0.00	13.08	64.73	77.81
650	0.00	0.00	5.30	77.51	82.81
670	0.00	0.00	1.74	80.03	81.77

Standard Error of the Mean				
Blue	Green	Yellow	Red	Sat
0.67	0.00	0.00	0.76	1.32
4.73	2.65	0.00	0.00	3.30
3.75	2.97	0.00	0.00	1.22
1.77	4.53	0.00	0.00	4.13
0.00	4.38	2.87	0.00	1.63
0.00	1.89	3.59	0.00	1.70
0.00	0.00	6.68	1.03	5.79
0.00	0.00	2.60	4.37	2.42
0.00	0.00	0.64	2.31	2.24
0.00	0.00	1.53	1.86	0.33
1.85	0.00	3.55	3.06	2.28
0.00	0.00	1.74	1.88	0.68

Binocular Fovea

1.0°	Mean				
λ	Blue	Green	Yellow	Red	Sat
450	64.04	0.00	0.00	6.19	70.23
470	71.91	7.10	0.00	0.00	79.01
490	15.31	65.03	0.00	0.00	80.35
510	10.27	69.45	0.00	0.00	79.71
530	0.00	60.40	12.11	0.00	72.51
550	0.00	44.66	18.92	0.00	63.57
570	0.00	0.00	45.28	19.70	64.98
590	0.00	0.00	27.84	40.14	67.98
610	0.00	0.00	16.02	58.51	74.53
630	0.00	0.00	10.12	65.84	75.96
650	0.00	0.00	1.83	78.39	80.22
670	0.00	0.00	8.12	72.50	80.62

Standard Error of the Mean				
Blue	Green	Yellow	Red	Sat
1.42	0.00	0.00	0.92	0.69
5.14	3.99	0.00	0.00	2.14
1.71	3.09	0.00	0.00	1.59
2.46	1.95	0.00	0.00	2.17
0.00	3.92	3.45	0.00	2.20
0.00	7.84	4.64	0.00	4.03
0.00	0.00	5.20	5.07	0.63
0.00	0.00	3.76	4.71	1.96
0.00	0.00	3.22	7.03	3.85
0.00	0.00	1.96	2.87	1.36
0.00	0.00	2.50	1.21	2.86
0.00	0.00	1.52	2.02	0.64